TRITIUM EFFLUENT REMOVAL SYSTEM

P. H. Lamberger and G. E. Gibbs
Monsanto Research Corporation
Mound Facility*
Miamisburg, Ohio 45342

Abstract

An air detritiation system has been developed and is in routine use for removing tritium and tritiated compounds from glovebox effluent streams before they are released to the atmosphere. The system is also used, in combination with temporary enclosures, to contain and decontaminate airborne releases resulting from the opening of tritium containment systems during maintenance and repair operations. This detritiation system, which services all the tritium handling areas at Mound Facility, has played an important role in reducing effluents and maintaining them at 2% of the level of 8 yr ago.

The system has a capacity of 1.7 m^3/min (60 cfm) and has operated around the clock for several years. A refrigerated in-line filtration system removes water, mercury, or pump oil and other organics from gaseous waste streams. The filtered waste stream is then heated and passed through two different types of oxidizing beds; the resulting tritiated water is collected on molecular sieve dryer beds. Liquids obtained from regenerating the dryers and from the refrigerated filtration system are collected and transferred to a waste solidification and packaging station. Component redundancy and by-pass capabilities ensure uninterrupted system operation during maintenance. When processing capacity is exceeded, an evacuated storage tank of 45 m^3 (1600 ft^3) is automatically opened to the inlet side of the system.

The gaseous effluent from the system is monitored for tritium content and recycled or released directly to the stack. The average release is <1 Ci/day. The tritium effluent can be reduced by isotopically swamping the tritium; this is accomplished by adding hydrogen prior to the oxidizer beds, or by adding water to the stream between the two final dryer beds.

Introduction

One of the principal goals of Mound Facility is to keep tritium discharges as low as practicable. To achieve this goal, concentrated gaseous effluents from any application or process involving tritium must be discharged to a tritium removal system. Mound conducts a variety of operations involving tritium, including the recovery of tritium from many kinds of wastes generated by U. S. Department of Energy contractors. This recovered tritium is put into gaseous form and separated from other hydrogen isotopes in thermal diffusion columns. Tritium effluents from Mound to the atmosphere have been reduced to about 2% of the level of 8 yr ago.

*Mound Facility is operated by Monsanto Research Corporation for the U.S. Department of Energy under Contract No. EY-76-C-04-0053.

The major operating system in use at Mound for tritium removal from concentrated gaseous effluents is the Effluent Removal System (ERS). The ERS has a 1.7 m^3/min processing capability for tritium removal from gaseous effluents prior to their release to the atmosphere. This tritium removal is accomplished by the oxidation of tritium and tritium-containing compounds to water, followed by the collection of the water on drying beds. Effluents contaminated with tritium come to the ERS from such sources as flushing of passboxes, purges of glovebox atmospheres, regeneration of glovebox inert atmosphere purification systems, vacuum pump exhausts, relief of glovebox overpressures, solvent vapors from boxline decontamination operations, purges of space between double layer drybox gloves, discharges of unrecoverable tritium in contaminated waste gases, and a variety of maintenance operations.

The wide spectrum of gases processed by the ERS includes argon, nitrogen, air, helium, hydrogen, water vapor, and various organic compounds such as several types of solvent and vacuum pump oil vapors. The introduction of halogen-containing compounds is forbidden because of the corrosion that would result from the formation of various corrosive agents within the system.

Use in Maintenance Operations

The capability of the ERS to move substantial amounts of gas is used at Mound to greatly reduce or eliminate tritium releases to the atmosphere. Various maintenance operations require the opening of tritium-contaminated lines or equipment and exposing the interior to the laboratory air. During these operations, the release of tritium to the atmosphere is inevitable without some type of containment and decontamination of effluents. At Mound, the item to be opened is enclosed in flexible plastic sheet supported on a metal frame. The enclosure is exhausted to the ERS through plastic tubing connected to one of the ERS inlet lines. Sufficient air flow is maintained through the enclosure to prevent tritium migration to the room air. All the tools and equipment needed to perform the operation are placed inside the enclosure prior to the start of the maintenance work.

There are two types of temporary enclosures used at Mound. In situations where high concentrations of tritium could be present, an enclosure with built-in gloves is erected. The repair work is performed through these gloves by the operating and maintenance personnel. For low tritium levels where the volume to be contained is large an enclosure large enough to allow operating and maintenance personnel to work inside is used. While inside the enclosure, a worker wears a plastic bubblesuit with supplied breathing air so that all physical contact with tritium is avoided.

Several methods are used to decontaminate or reduce the quantities of tritum in lines and equipment if they must be opened for maintenance. If liquid could be present, the item is fitted with a specially designed piercing valve. This valve makes a small hole and the liquid drains into a container without any release of tritium. If welding is involved in the maintenance operation, external heat is applied to the area while a small flow (0.05 m^3/min) of air is flushed through the line. This vaporizes moisture and liberates sorbed tritium in the vicinity of the repair and carries it to the ERS. For general decontamination of lines, equipment or enclosures, moist air is more effective than dry gases.

During the maintenance operation, air flow from the enclosure to the ERS is limited to only that necessary for tritium containment. At times, this type of operation requires the maximum capacity (1.7 m^3/min) of the ERS for several hours. Not only is the enclosure ventilated, but, whenever possible, open contaminated lines are directly purged to the ERS. The intent is to move air from the room, through the enclosure, into the open equipment and process lines, and then into the ERS.

These simple but very effective methods have helped considerably in reducing tritium releases to the atmosphere and have contributed to reducing personnel exposures to tritium by a factor of 16 over the past several years.

System Description

The tritium handling operations are connected to the ERS through an inlet collection system consisting of 2, 3 and 4-inch copper trunklines (see Figure 1). This inlet system is maintained at a pressure of 600 torr. In the event that the capacity of the compressors is temporarily exceeded causing trunkline pressure to exceed 700 torr, the system influent is automatically diverted to a 45 m^3 evacuated storage tank. The tank inlet valve, which is controlled by a pressure switch, opens and closes when necessary to maintain the trunkline pressure. This pressure control is very important as a pressure above atmospheric could seriously harm certain operations and equipment serviced by the ERS, resulting in a possible release of tritium to the atmosphere.

A pressure of 100 torr is automatically maintained inside the storage tank by a vacuum pump. If influent flow contines at a high rate for an extended period and fills the tank, it is isolated from the ERS trunkline when the pressure reaches 720 torr. Any additional flow to the ERS in excess of its processing capacity is then released directly to the stack. This has occurred only once in the past 6 yr.

Each branch of the inlet collection system is equipped with a gas flowmeter whose output is displayed and recorded on a strip chart. Each branch is periodically sampled for tritium concentration which is also recorded. This branch monitoring permits administrative control by operating personnel in case of system overloads and also provides an historical record.

Downstream of the point where the various branch trunklines merge into a single process line, a series of two filters (30 μm and 10 μm) remove particulate material and liquid droplets from the incoming gases. The purpose of this filtration is to protect the Teflon piston rings of the compressors against abrasive materials. The collected liquid and solids from the filters are held in storage tanks while awaiting disposal [1].

The next processing step is the cooling of the incoming gas by refrigerated heat exchangers. Here the contaminated gas is dried to a dew point of -50°C. Two shell and tube heat exchangers are used alternately, one cooling the gas while the other is being heated to defrost the collected condensate which is then stored in a stainless steel tank and later packaged for burial[1]. The heat transfer fluid

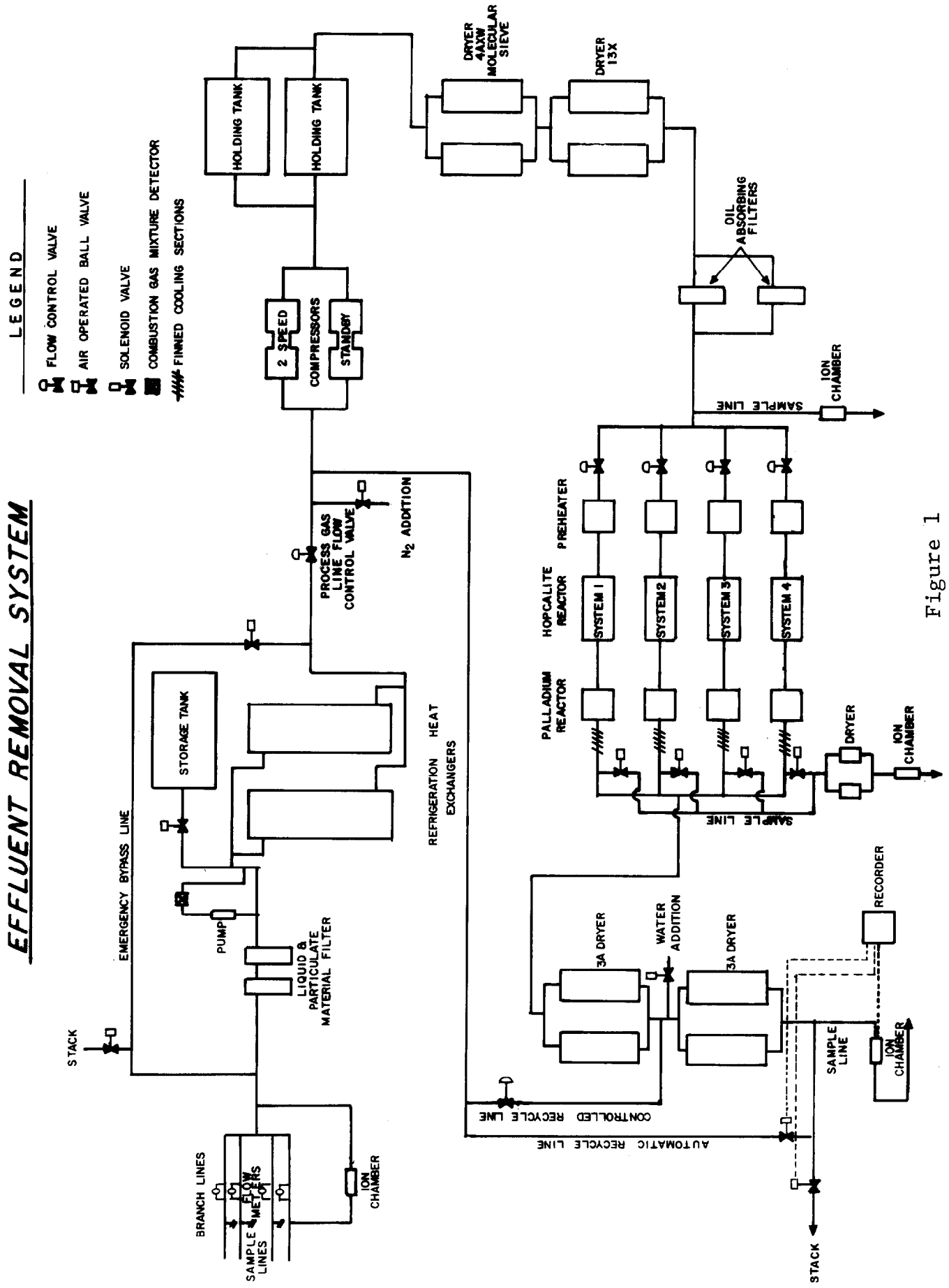
EFFLUENT REMOVAL SYSTEM
LEGEND
FLOW CONTROL VALVE
AIR OPERATED BALL VALVE
SOLENOID VALVE
COMBUSTION GAS MIXTURE DETECTOR
FINNED COOLING SECTIONS
HOLDING TANK
HOLDING TANK
DRYER 4AXW MOLECULAR SIEVE
DRYER 13X
OIL ABSORBING FILTERS
2 SPEED
COMPRESSORS
STANDBY
ION CHAMBER
SAMPLE LINE
PROCESS GAS LINE FLOW CONTROL VALVE
N2 ADDITION
PREHEATER
HOPCALITE REACTOR
PALLADIUM REACTOR
SYSTEM 1
SYSTEM 2
SYSTEM 3
SYSTEM 4
STORAGE TANK
REFRIGERATION HEAT EXCHANGERS
DRYER
ION CHAMBER
SAMPLE LINE
EMERGENCY BYPASS LINE
PUMP
LIQUID & PARTICULATE MATERIAL FILTER
3A DRYER
WATER ADDITION
3A DRYER
RECORDER
SAMPLE LINE
ION CHAMBER
STACK
CONTROLLED RECYCLE LINE
AUTOMATIC RECYCLE LINE
BRANCH LINES
SAMPLE LINES
FLOW METERS
ION CHAMBER
STACK

Figure 1

is cooled to -55°C by a cascade refrigeration compressor system. Steam is used to supply heat for the defrost cycle.

The flow of contaminated gas and heat transfer fluid through the heat exchangers is automatically governed by a programmable step selector. A cycle timer with adjustable settings is used to advance the selector. This allows for variation in time intervals between the defrost and gas cooling cycles.

Prior to the heat exchanger switching from the defrost cycle to the gas cooling cycle, a three-step time interval is devoted to pre-cooling the hot heat exchanger. This provides for constant cooling of the gas during the switching process. The system has built-in failsafe features to ensure uninterrupted operation. In the event of a valve failure, gas will automatically bypass the refrigeration system.

A combustible gas detector is installed on the gas line; its purpose is to warn of the presence of a combustible mixture of hydrogen and oxygen. The detector will alarm when the mixture of hydrogen and oxygen reaches 25% of the lower explosive limit. When the mixture reaches the 75% level, nitrogen gas is added automatically for dilution purposes.

An automatic flow control valve is located in the process line for the purpose of regulating gas flow to maintain the gas inlet header at a pressure of 600 torr. The pressure downstream of the control valve normally is maintained at 510 torr by the addition of recycled gas from within the system. A pressure controller is used to operate this recycle flow control valve which is similar to the process line control valve. The purpose of this controlled recycle gas is to provide the positive displacement compressors with sufficient gas to maintain the inlet pressure at 510 torr. The compressors have the capability of reducing the inlet pressure to 310 torr which could cause damage to the diaphragms in the compressor inlet valves.

Gas is moved through the ERS by either of two oil-less-head compressors connected in parallel. This type of compressor was chosen because the introduction of oil into the system would require additional filtration to protect the Hopcalite oxidizing reactors. Oil vapor has a tendency to coat the Hopcalite and seriously reduce its effectiveness. One compressor of 0.85 m^3/min capacity is maintained in standby condition. Should the normally operating compressor become inoperative the standby unit is automatically activated. The active compressor has a capacity of either 0.85 or 1.7 m^3/min and is equipped with a two-speed motor, which changes to high speed automatically when the gas flow rate exceeds the low speed capacity or the gas line pressure increases to 670 torr.

The gas discharged by the compressor is fed to two 4.25 m^3 holding tanks which are normally held at 2000-2300 torr. This pressure provides the driving force for gas flow through the remainder of the system. Following the holding tanks are two dual-tower, automatic, self-regenerating dryers using molecular sieve as the desiccant. The first dryer is filled with 4AXW molecular sieve to remove trace amounts of water vapor. The second dryer is filled with type 13X molecular sieve for hydrocarbon removal. It is important that halogenated hydrocarbons be removed from the gas stream prior to its entry into the hot oxidizing

reactors since decomposition of the halogen compounds leads to the formation of corrosive agents.

After the gas exits the 13X dryer, it is passed through an oil absorbing filter. The gas is now considered completely free of any vapor which will harm the oxidizing reactors or produce corrosive agents at the high temperatures of the reactors. At this point, a 28 liter/min sample is fed through an ion chamber which measures the tritium concentration of the gas prior to entering the reactor system.

The ERS is equipped with four identical parallel reactor systems, which have the function of oxidizing hydrogen isotopes and compounds into water. Each reactor system consists of a preheater, a Hopcalite reactor and a palladium reactor. An automatic ball-valve switching mechanism is used to select any two reactor systems for processing gas contaminated with tritium. The other two reactors are held in a hot standby condition. A gas flow control valve is located on each reactor system and the gas flow can be regulated from 0.17 to 0.43 m^3/min as desired. A pressure switch, located on the holding tanks, will automatically introduce gas to the two standby reactors when the tank pressure reaches 2400 torr. This switch will also return the two reactors to standby status upon the reduction in tank pressure to 1950 torr.

An electric preheater raises the temperature of the incoming gas to 400°C prior to entering the Hopcalite (15% CuO and 85% MnO_2) reactors. Here the hydrogen is oxidized by the CuO, and the MnO_2 acts as a catalyst for the reaction. The CuO provides an oxygen supply if the incoming gas stream does not contain any air. There is normally sufficient oxygen in the gas to maintain the copper in the oxidized state; but as a precaution, air is routinely introduced into the system to avoid oxygen depletion. A second reactor downstream of each Hopcalite reactor contains a palladium catalyst held at 600°C. The purpose of this palladium reactor is for oxidizing tritiated organic compounds, such as radiolytically generated methane, for which the Hopcalite is ineffective.

The efficiency of each reactor can be determined by automatically sampling the gas leaving each reactor, drying the gas and measuring the tritium content with an ionization chamber.

The gas is passed through air-cooled, finned, copper heat exchangers before entering another pair of dual-tower dryers. These two dryers use type 3A molecular sieve. The water collected in these dryers was produced in the oxidation process of the reactors. Upon regneration of the dryers, the accumulated water is collected and packaged for burial.

Additional removal of tritiated water from the gas is achieved by the use of isotopic swamping. This is accomplished by periodically loading the final dryer with several kilograms of natural water. Since there is rapid exchange between water in the adsorbed and vapor phases, the HTO is adsorbed and H_2O is released resulting in the virtual elimination of HTO from the discharge of the second dryer. Periodically, the dryer is regenerated and, after cooling, is again loaded with clean water.

A hydrometer is used to measure the trace amounts of water vapor in the gas entering and leaving the third dryer, and leaving the final dryer. This information is useful for troubleshooting during brief and rare periods of system inefficiency. By combining the information from the tritium concentration monitors, the explosive mixture monitor, and the hydrometer, the cause of most problems can be determined and corrective action taken.

As the decontaminated gas exits the final dryer, the tritium concentration is measured with an ion chamber whose output is fed to a recorder equipped with an alarm set point. If the tritium concentration reaches the set point, a series of valves will automatically divert the contaminated gas back into the compressor inlet line for recycle. This recycling continues until the tritium concentration is less than the set point. When this point is reached, the valves automatically reverse to the normal position and the gas is discharged to the atmosphere.

Detritiation factors of 10^5 can be attained by use of the ERS. In tests with tritium concentrations of 10 ppm (25 Ci/m^3) in the influent, tritium concentrations in the output or discharge were less than 250 $\mu Ci/m^3$.

Engineering Data

The system is relatively large and complex because of its capacity, redundancy of critical components and safety features. Current replacement cost is $1.5 million. The ERS was designed for, and is operating on, a continuous 24-hr/day basis with almost no downtime. Normal maintenance of the system can be performed without seriously reducing its capacity or efficiency.

Containment of tritium, operating life and ease of maintenance are the main design criteria when selecting materials and equipment for the ERS. The lines not subjected to elevated temperatures are copper tubing joined with silver solder. The lines exposed to high temperatures are 316 stainless steel, and the reactors and preheaters are constructed from 304H rerolled stainless steel. Heliarc welding in an argon atmosphere is used for fixed stainless steel joints. Flexible bellows connections, which allow for thermal expansion, are used between the Hopcalite reactors and the preheaters. The stainless steel bellows are welded to stainless steel flanges and when assembled are in a state of stress. Upon thermal expansion of the reactors during operation, the stress in the bellows is relieved. A special gold-plated, K-shaped gasket is used between these flanges. Flanges were selected for use in these locations to allow the reactor or preheater to be removed easily.

The finned cooling sections are fabricated from oxygen-free copper (OFC) tubing to resist corrosion. Viton, which has high resistance to tritium, is used as gasket material for flanges where temperatures are not greater than 100°C.

Many different thermal insulating materials are used in the ERS. In the refrigeration system, the holding tank containing the heat-transfer fluid is insulated with foam glass. The refrigerant transfer lines are insulated with foam rubber and fiberglass. The Hopcalite reactors

and preheaters are enclosed with rigid, 23-cm thick, pressed fiber insulation. The palladium reactors are insulated with high-temperature, evacuated glass beads contained within a stainless steel enclosure.

Several of the significant improvements of the present system, built in 1972, compared to the original system, are the following: The capacity has been increased by a factor of 10. The addition of the refrigerated heat exchangers has provided for an essentially dry system resulting in more reliable operation and less hazard to maintenance personnel from tritiated condensates. The absence of tritiated liquids requires less preparation before maintenance work can start, resulting in decreased system downtime. The use of effective filters and condensers and proper control of the cooling water has extended the operating time of the compressors between overhauls from ∿600 hr to ∿15,000 hr. Improved tritiated liquid handling equipment has reduced losses to the atmosphere. The addition of the palladium reactors has given the system the capability to oxidize tritiated organic compounds which otherwise would be released to the environment; this has resulted in reduced effluents and in increased flexibility in choosing decontaminating solvents. Improved pressure, temperature, and gas flow instrumentation has improved the control and efficiency of the system.

Conclusion

There are two methods of disposing of tritiated effluents -- releasing them to the environment or exhausting them to an effluent decontamination system. Mound has shown, through use of the ERS, that most effluents need not be discharged to the environment and that an effluent goal of "as low as practicable" can truly be achieved.

Acknowledgement

The authors thank T. B. Rhinehammer for many helpful discussions and comments.

Reference

1. E. A. Mershad, W. W. Thomasson, and J. J. Dauby, "Packaging of Tritium Contaminated Liquid Waste," Nuc. Tech., 32:1, 53-59 (1977).

DISCUSSION

O'BRIEN: First, is the output of the ERS linearly related to the input or is the output concentration the same no matter what the input concentration? Second, what becomes of the water absorbed on the drying beds?

LAMBERGER: The output is constant over a wide range of inputs but does increase when the input concentration reaches very high levels. The answer to your second question is that the dryers are regenerated and the water moved to storage tanks. Ultimately, the water is solidified, using Portland cement, and packaged in a series of three drums with a very low release rate.

PARISH: Why are you using a Hopcalite catalyst in series with a precious metal?

LAMBERGER: The oxygen in CuO is available to oxidize hydrogen in case insufficient oxygen is present in the incoming gas stream.

CARTER: In what form is the tritium released from the stack? Is the input to the cleanup system all tritium gas rather than tritiated water vapor? Finally, what is the effective decontamination factor for plastic suits?

LAMBERGER: Tritium is released from the stack both as elemental hydrogen and as the oxide. The input to the cleanup system contains tritium gas and oxide in varying amounts. I don't know what decontamination factor applies to plastic suits. We have a publication on the subject that contains the data you are seeking.

MODIFICATION AND TESTING OF THE SANDIA LABORATORIES LIVERMORE TRITIUM DECONTAMINATION SYSTEMS*

P. D. Gildea, H. G. Birnbaum and W. R. Wall
Sandia Laboratories
Livermore, California 94550

Abstract

Sandia Laboratories, Livermore, has put into operation a new facility, the Tritium Research Laboratory. The laboratory incorporates containment and cleanup facilities such that any tritium accidentally released is captured rather than vented to the atmosphere. This containment is achieved with hermetically sealed glove boxes that are connected on demand by manifolds to two central decontamination systems called the Gas Purification System (GPS) and the Vacuum Effluent Recovery System (VERS). The primary function of the GPS is to remove tritium and tritiated water vapor from the glove box atmosphere. The primary function of the VERS is to decontaminate the gas exhausted from the glove box pressure control systems and vacuum pumps in the building before venting the gas to the stack. Both of these systems are designed to remove tritium to the few parts per billion range.

Acceptance tests at the manufacturer's plant and preoperational testing at Livermore demonstrated that the systems met their design specifications. After preoperational testing the Gas Purification System was modified to enhance the safety of maintanance operations. Both the Gas Purification System and the Vacuum Effluent Recovery System were performance tested with tritium. Results show that concentration reduction factors (ratio of inlet to exhaust concentrations) much in excess of 1000 per pass have been achieved for both systems at inlet concentrations of 1 ppm or less.

Introduction

Sandia Laboratories, Livermore, has put into operation a new facility, the Tritium Research Laboratory (TRL). The laboratory (Figure 1), designed for a wide range of experiments using multi-gram amounts of tritiu, entered its start-up phase on October 1, 1977. In addition to the usual pressure-gradient-controlled once-through ventilation system, the Tritium Research Laboratory provides for both personnel safety and environmental protection by employing a glove box secondary containment system connected to the two central decontamination systems, the Gas Purification System (GPS) and the Vacuum Effluent Recovery System (VERS).

This paper describes the glove boxes and operating principles of the GPS and VERS. It gives their performance specifications, and details Sandia's modifications to the manufacturer's design to enhance the safety of maintenance operations. Performance tests, preoperational and with tritium, are also discussed.

*Work supported by the Department of Energy under Contract AT(29-1)-789.

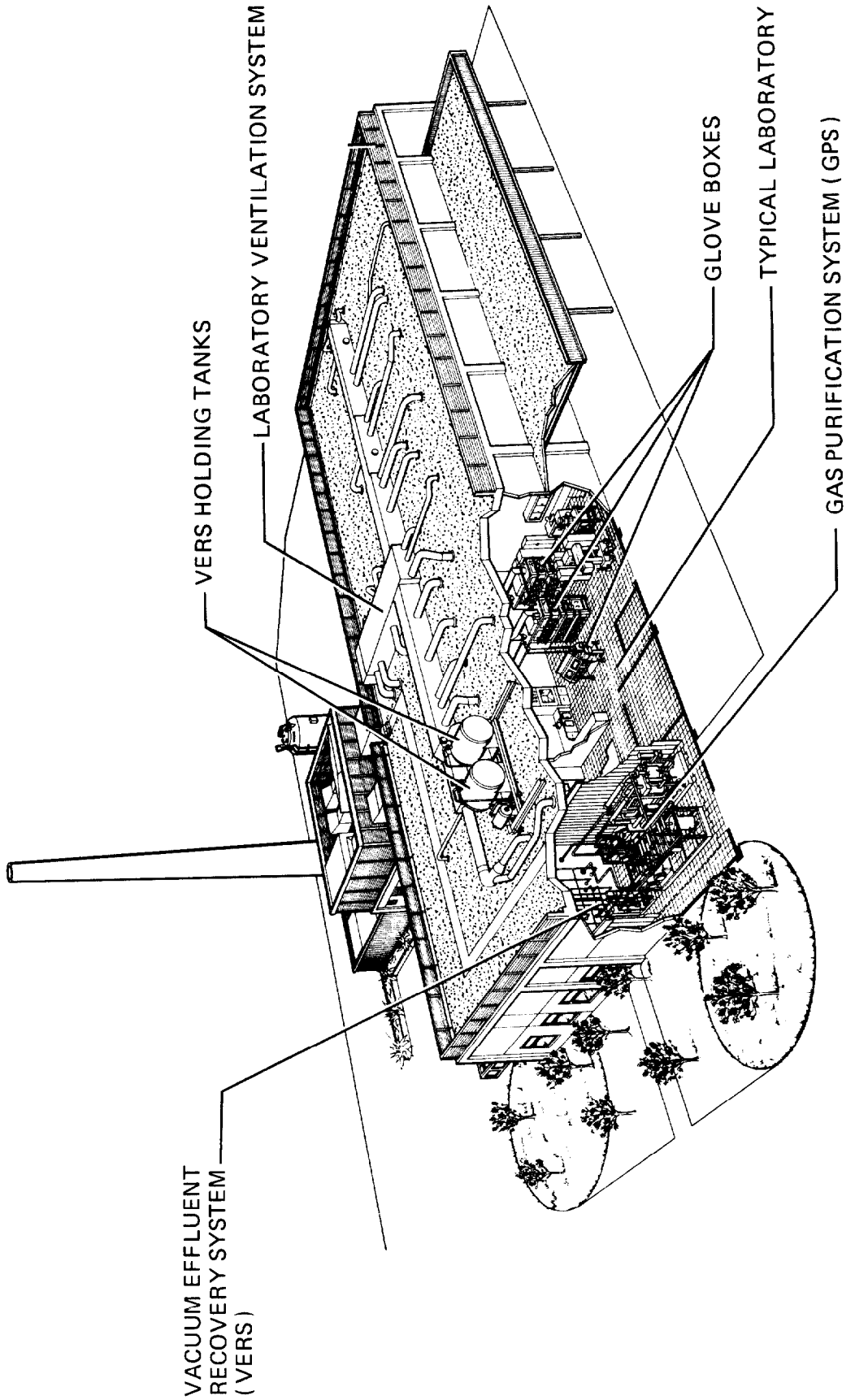

Figure 1 The TRL building at Livermore, showing the arrangement of some of the major systems and a typical experiment station.

Containment

All experiments are secondarily contained in sealed stainless steel glove boxes of welded construction (Figure 2). Each box is equipped with glove ports, viewing windows, and an air lock pass-through; and on each end there are removable panels for the installation of large items. Both regular utility and emergency electrical power are provided to the box. Also, there are feed-through provisions for instrumentation and inert gas pressure connections, and a cooling system to remove the heat generated by experiments. Both tritium concentration and humidity control are maintained by processing the glove box atmosphere through the GPS. Normally, the glove boxes are operated with dry nitrogen maintained by the box pressure control system at a pressure of -0.25 to -1.0 kPa with respect to the room. However, the box can be operated with an argon or air atmosphere if desired.

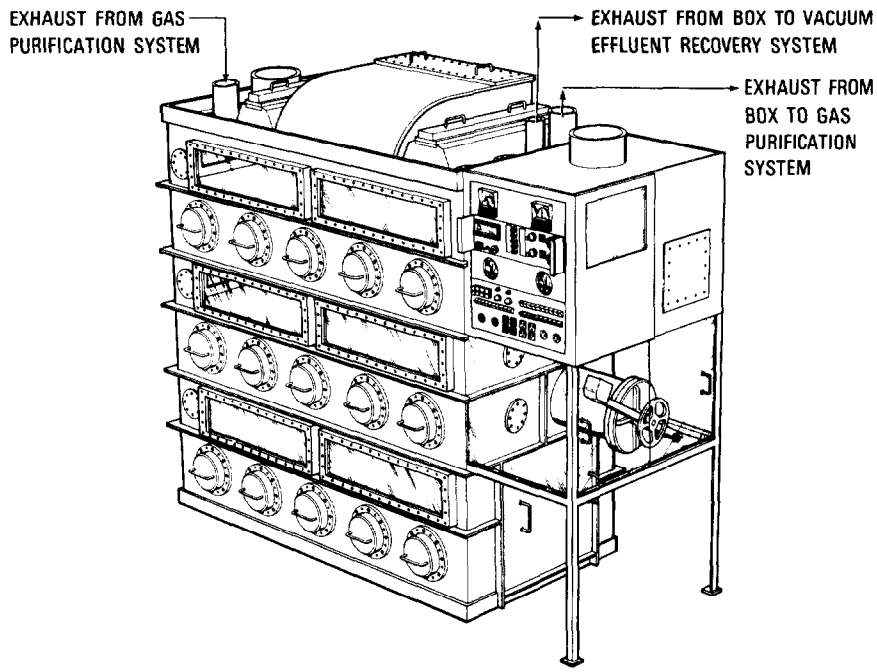

Figure 2 Sealed glove box.

Decontamination

Decontamination is accomplished by two centralized systems.[1] The first of these, the Gas Purification System (GPS), removes tritium and tritiated water vapor from the glove box atmospheres. The second, the Vacuum Effluent Recovery System (VERS), removes tritium, tritiated water vapor, and tritiated hydrocarbons from gases exhausted from the glove box pressure control systems and laboratory vacuum systems before the decontaminated residue gases are vented to the stack. The original systems were manufactured to a Sandia performance specification by Engelhard Industries Systems Department, Union, New Jersey. Both systems were designed to reduce tritium concentrations to a few parts per billion. The tritium removed by the decontamination systems is contained, either for recovery or for disposal, as solid waste on Type 4A molecular sieves.

Gas Purification System

Design and Operation

The Gas Purification System (GPS), conceptually illustrated in Figure 3, removes tritium from the glove box atmosphere in the event of either an accidental release or a slow buildup of background concentration.

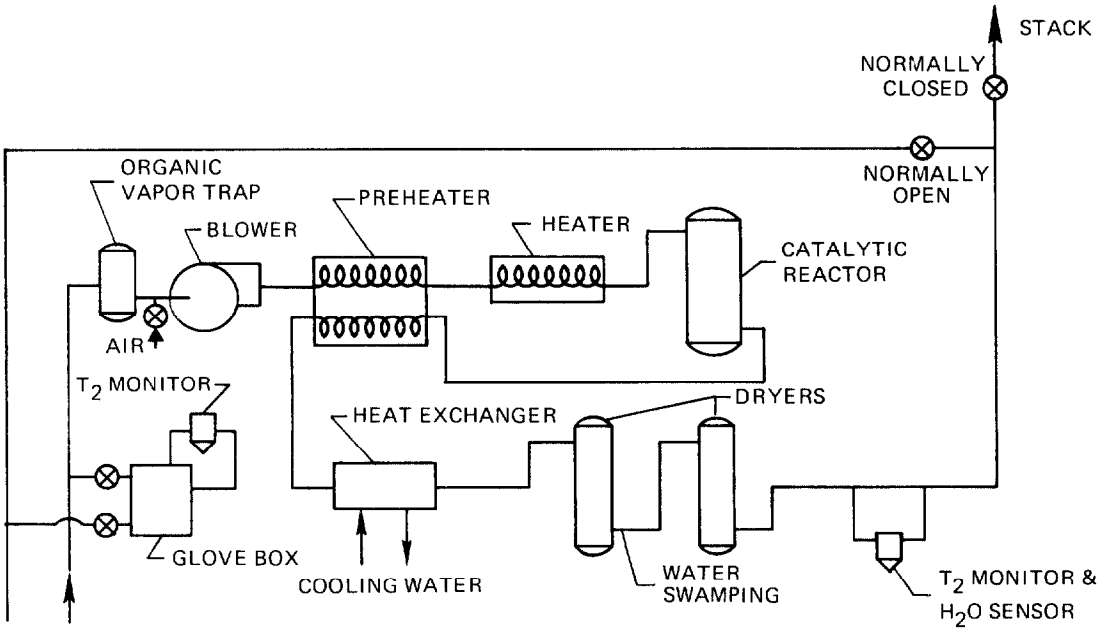

Figure 3 Gas purification system schematic.

The GPS consists of a central manifold connected to each of the laboratory glove boxes, a catalytic reactor to oxidize the tritium, two molecular sieve dryers in series to collect the tritiated water, a blower to circulate the glove box atmosphere through the system, and a control and diagnostics system to provide both automatic and manual control and to assess operational status. Redundant prime function components, i.e., blowers, heaters, and catalyst and dryer beds are provided for reliability. A dryer regeneration system provides for removal of water from a loaded dryer while the GPS is operating with the use of the other two dryers. Entry and exit nozzles allow safe removal and replacement of both catalyst and sieve material while the system remains operational by the use of a redundant flow path. Major system performance criteria are summarized in Table I.

The GPS can be operated either in a recirculation mode or in a stacking mode. In the recirculation mode, the normal method of operation, the glove box gases are pumped from the box, through the GPS, and back to the box until tritium contamination is reduced to an acceptable level. The stacking mode is similar to the recirculation mode with the exception that the glove box atmosphere is not recirculated but stacked after passing through the GPS. This is accomplished by drawing clean box atmosphere gas into the manifold ahead of the glove box and venting the GPS effluent to the ventilation exhaust. This mode of operation may

Table I GPS performance criteria.

Processing Capacity	340 m^3 hr^{-1}
Catalytic Reactor	
Operating Temperature	783 K
Standby Temperature	783 K
Catalyst	Engelhard Minerals and Chemicals No. A-16648
Tritium Concentration Reduction Factor*	1000 per pass for concentrations from 20,000 ppm to 1 ppm.
Molecular Sieve Dryer	
Capacity	37 moles of water while maintaining less than 1 ppm water at exit
Regeneration Time	6 hours
Regeneration Temperature	589 K
Molecular Sieve	Type 4A
Startup Operating Time	30 s
Glove Box Pressure Control	-0.25 to -1.0 kPa relative to the laboratory
System Leak Rate	1×10^{-10} m^3 (STP)s^{-1} maximum helium at 98 kPa differential

*Ratio of inlet to outlet tritium concentrations.

be used to backfill the glove box with dry nitrogen or argon when an inert atmosphere is required. It can also be used to drive the glove box concentration to low levels when it is necessary to clean up a box for reentry.

GPS Modifications

The GPS as originally received from the manufacturer is shown in Figures 4 and 5.

As a result of experience gained during preoperational testing of the GPS in the TRL, it became apparent that system changes were required primarily to increase the safety of maintenance operations. Modifications were necessary to reduce to a minimum the volume of the GPS opened up to the room during such operations as valve seat, heater, catalyst, and sieve removal and replacement. The diagnostics and control systems were also modified at this time. To achieve

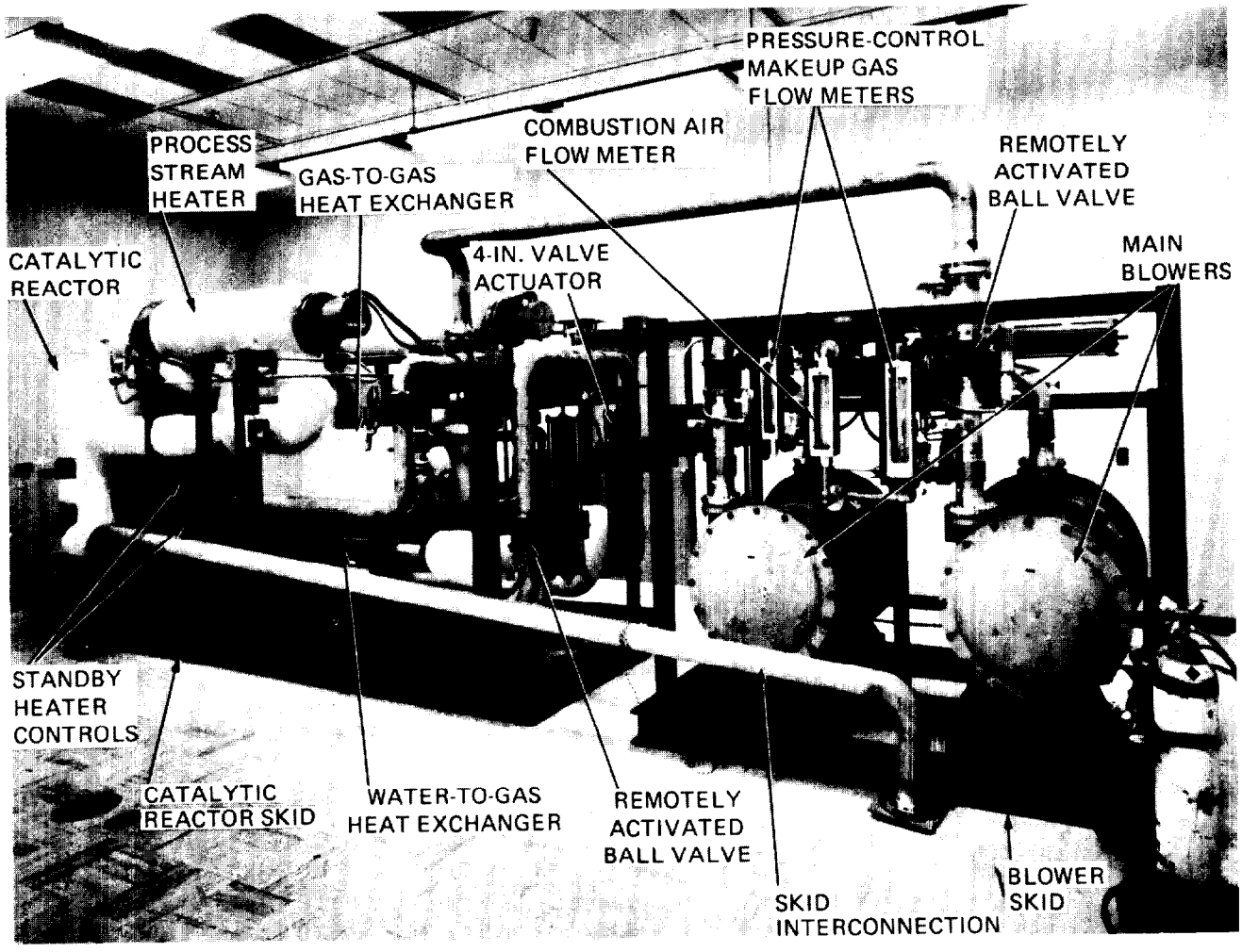

Figure 4 GPS blower and catalytic reactor skids, as received from manufacturer.

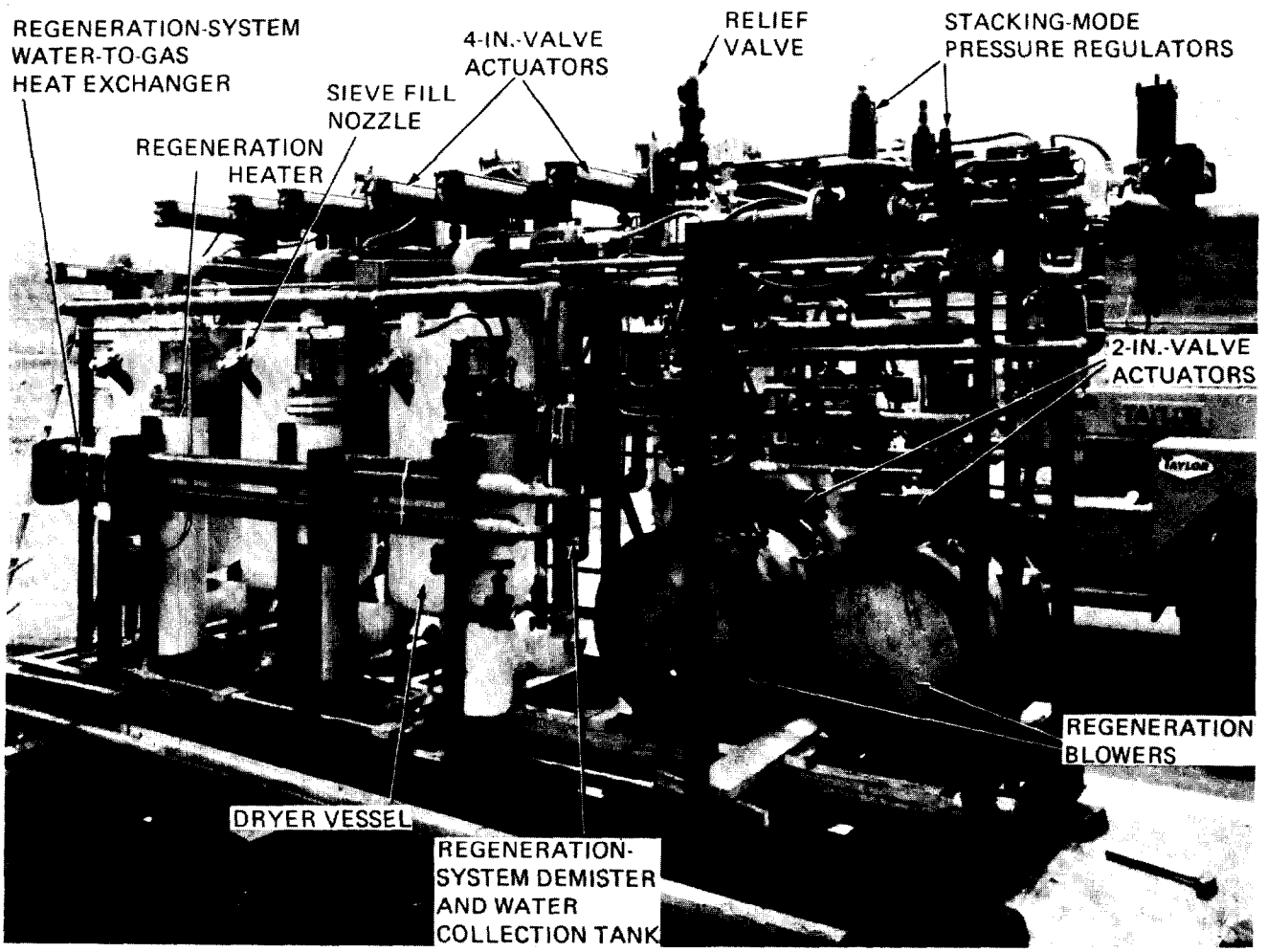

Figure 5 GPS dryer skid as received from manufacturer.

this end the GPS was removed from the laboratory and modified after completion of preoperational testing but prior to tritium testing. The major modification problem encountered was finding a suitable arrangement of the dryer skid that would allow space for placement of isolation valves on both sides of the eleven 4-in. and thirteen 2-in. remotely actuated ball valves on the skid.

Mechanical Modifications. The three skids were disassembled and modified as follows:

1. Isolation valves and purge ports were added on either side of all remotely actuated valves and on the catalyst and sieve vessel entry and exit nozzles.

2. A sealing surface was added to the main heater vessel to allow for installation of a glove box for heater removal.

3. Raceways were installed on the outside of the main heater and catalyst vessels for ease of replacement of standby heating elements.

4. The catalytic reactor skid was split into two separable independent skids to allow replacement of one complete flow path without major interruption of system operation.

5. A bypass was added to the catalytic reactor skid to allow system operation without flow through the catalyst and to allow isolation of the catalyst when the system is not operating.

Figures 6, 7, and 8 show the three skids after completion of the mechanical modifications. The purge port arrangement used on the dryer vessel sieve fill nozzle is shown in Figure 9.

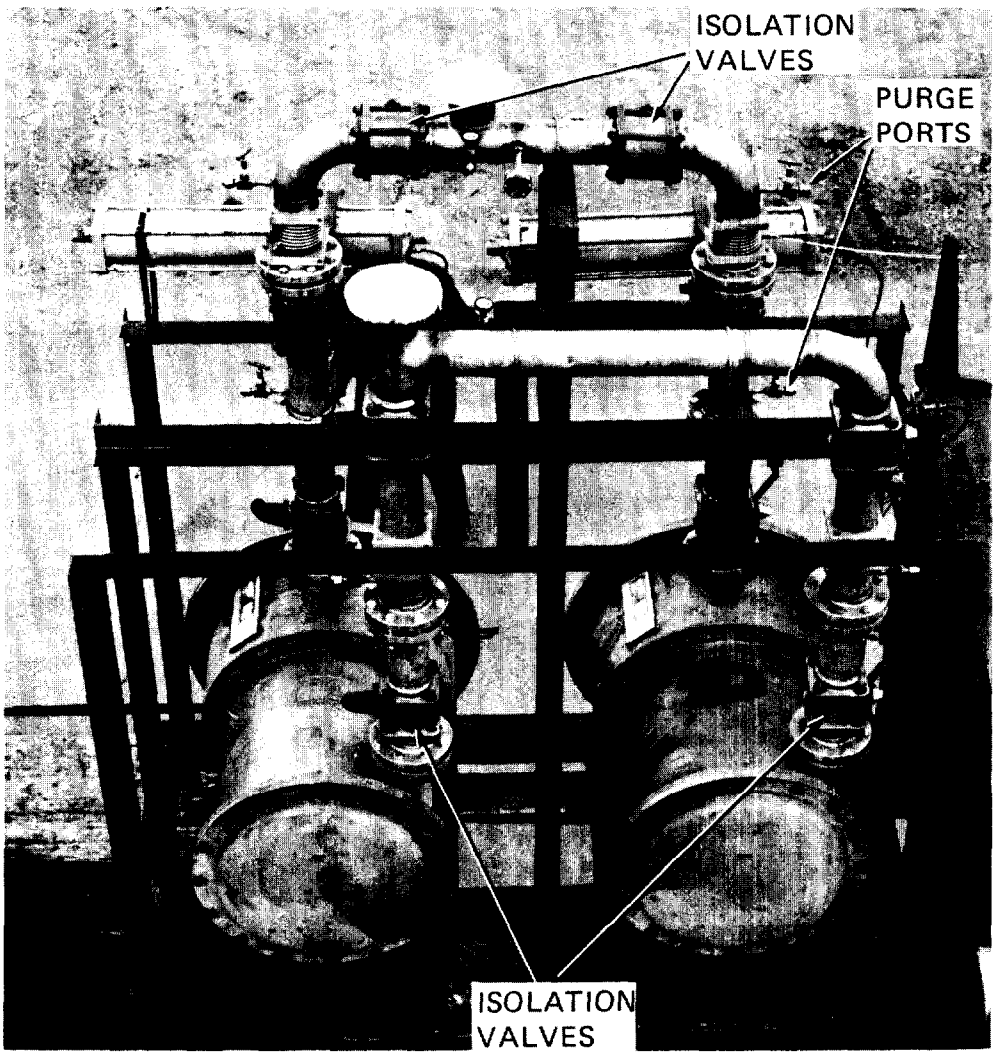

Figure 6 Modified GPS blower skid.

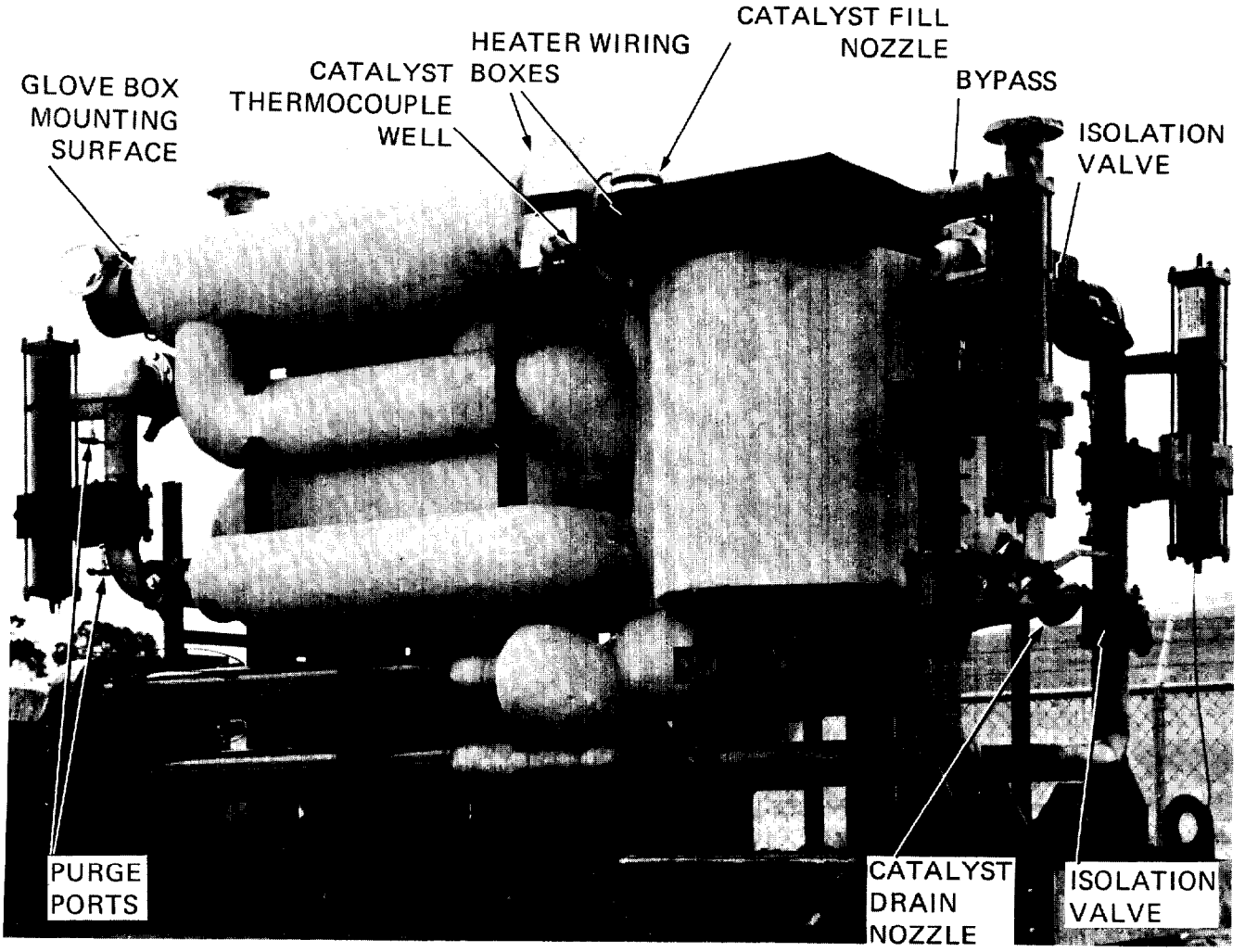

Figure 7 Modified GPS catalytic reactor skid.

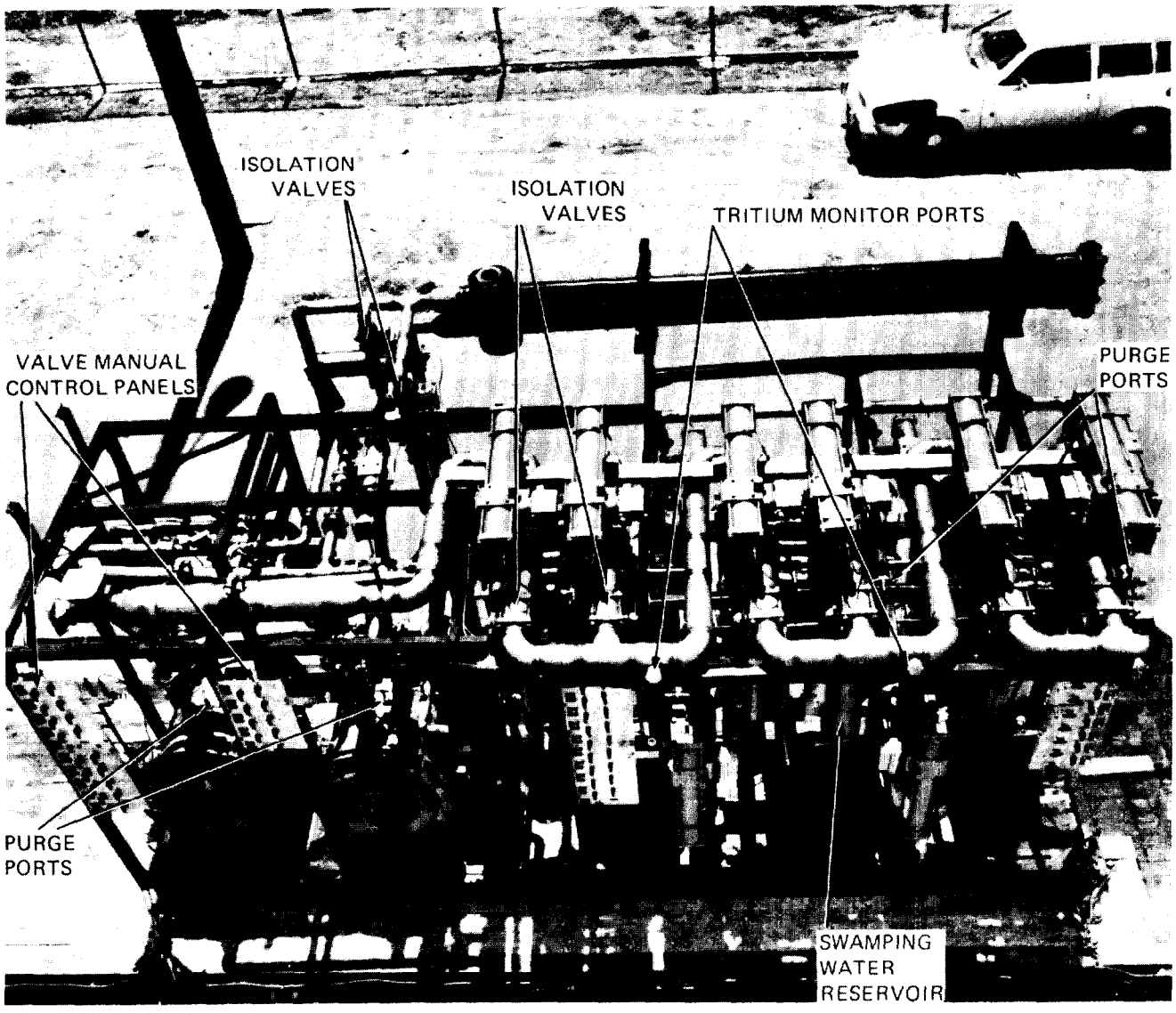

Figure 8 Modified GPS dryer skid.

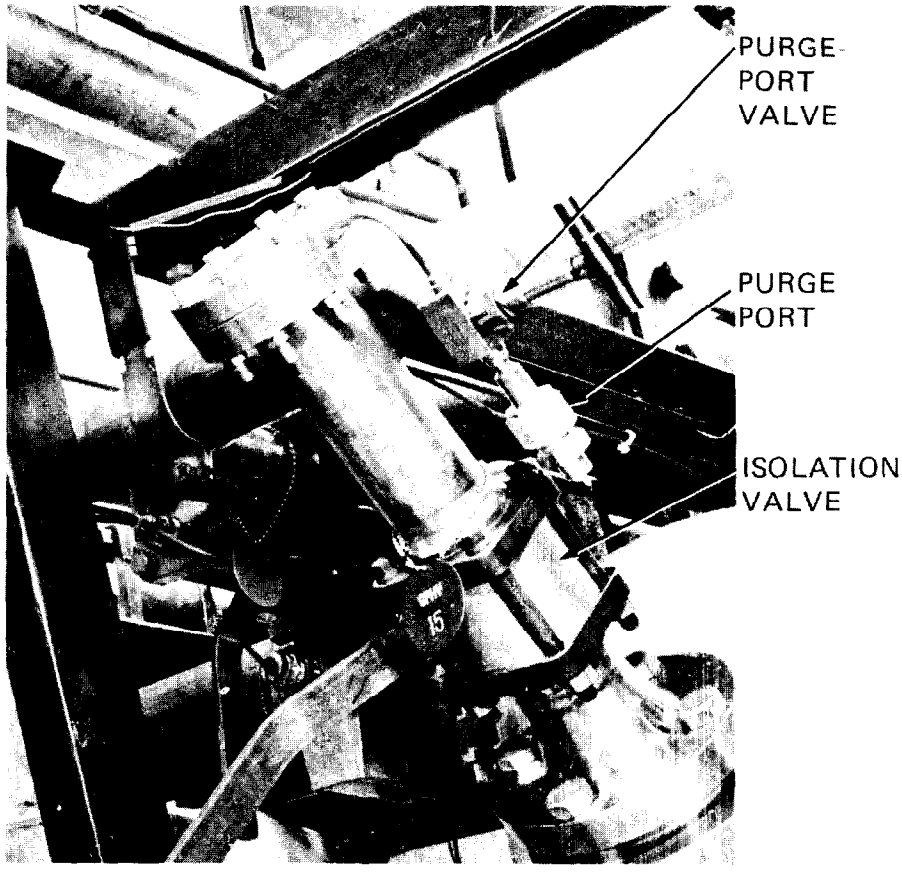

Figure 9 Dryer fill nozzle purge port configuration.

Instrument and Control System Modifications. To enhance both reliability and ease of maintenance, the diagnostics and control systems were changed as follows:

1. The mechanical relay control system was replaced by a microprocessor controlled solid state system to provide increased flexibility and reliability.

2. All heater, motor, and valve control elements except disconnects were removed from the skids and placed outside the hood surrounding the GPS to allow ease of maintenance.

3. The Variac standby heater controls were replaced with silicone controlled rectifier units to achieve better temperature control.

4. Thermocouples were placed in the catalyst bed to provide more accurate temperature control and allow assessment of catalyst performance. Thermocouples were also added at the dryer inlet to provide more accurate determination of regeneration completion.

The GPS control panel in the TRL control room is shown in Figure 10; the wall mounted GPS combustion air and makeup gas flow instrumentation and control valves are shown in Figure 11. The catalytic reactor standby heater and thermocouple mounting arrangements are presented in Figure 12.

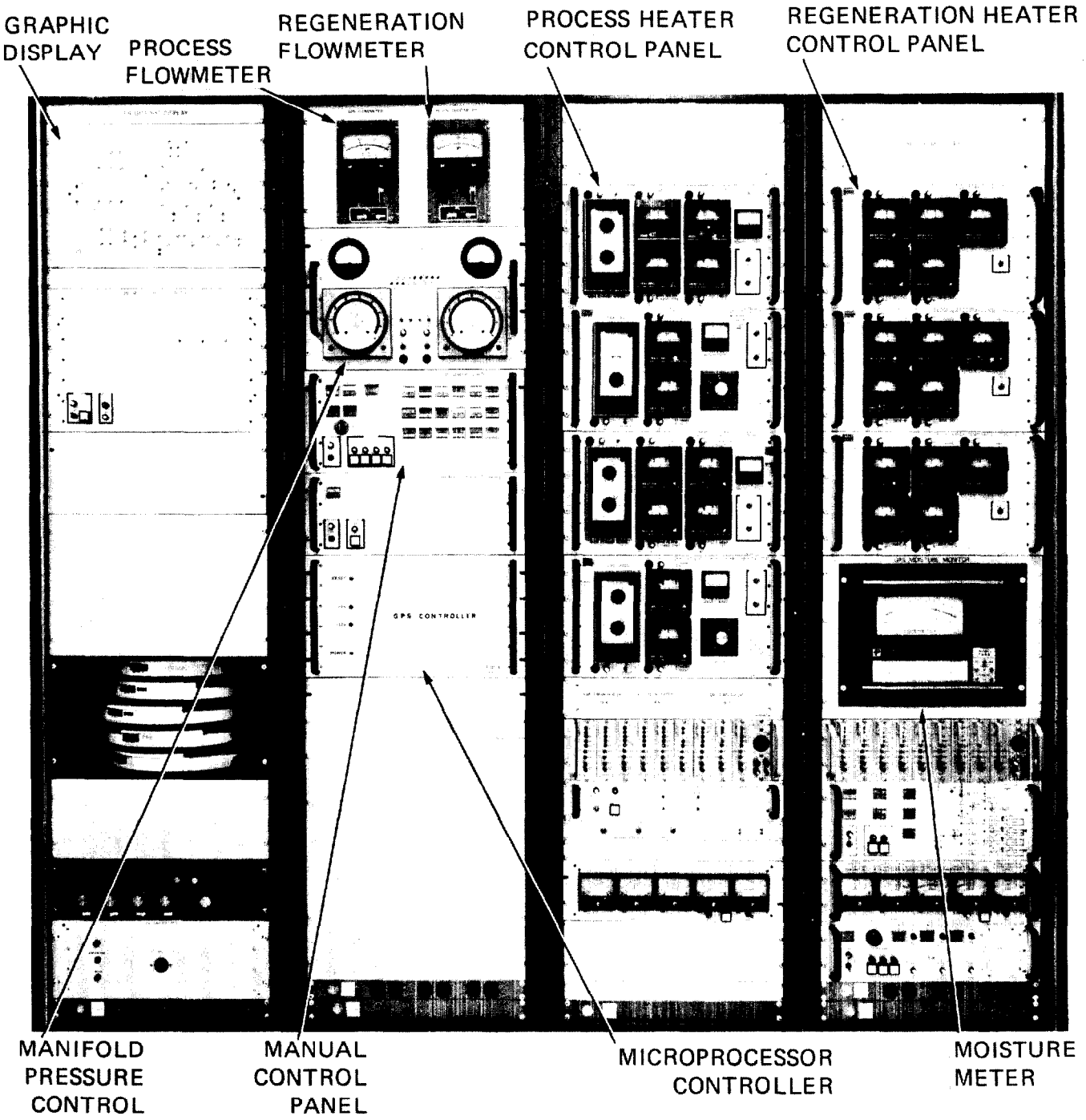

Figure 10 GPS control panel.

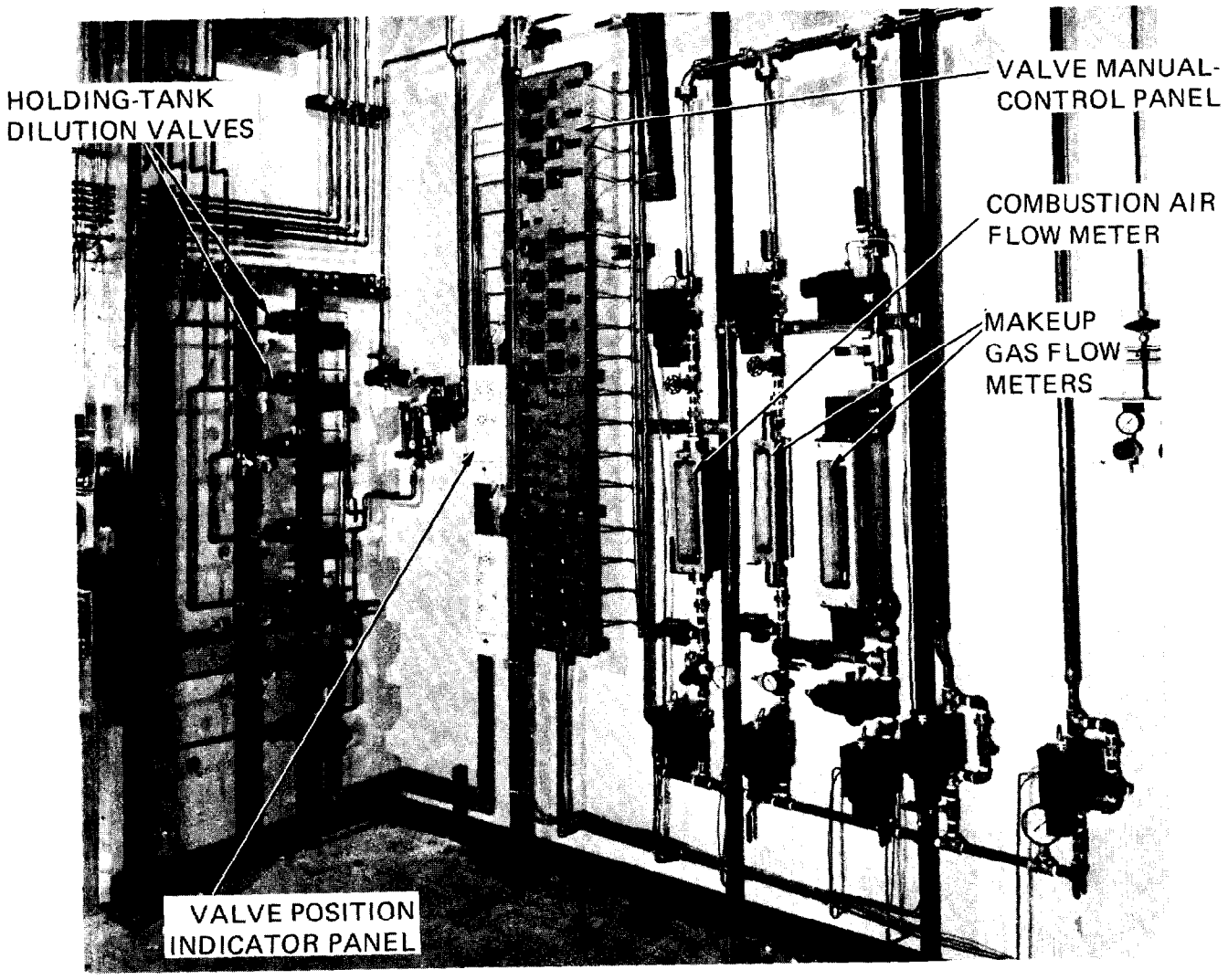

Figure 11 GPS gas flow instrumentation and control valves.

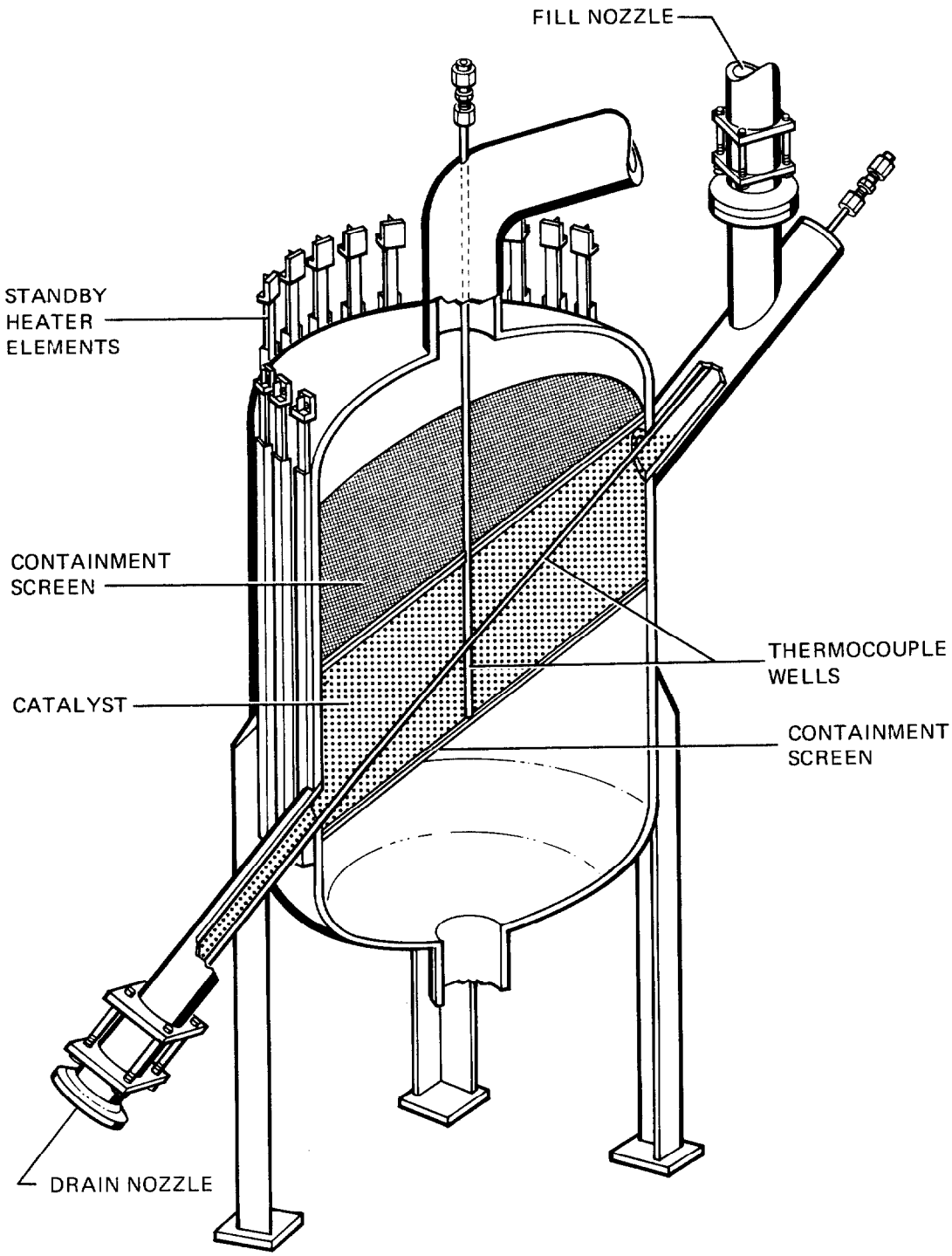

Figure 12 GPS catalytic reactor.

Vacuum Effluent Recovery System

Design and Operation

The VERS, conceptually shown in Figure 13, is used to remove tritium from the exhaust gases of the laboratory vacuum systems before venting to the stack. The VERS removes tritium in the same manner as the GPS and uses the same precious metal catalyst. The system consists primarily of a laboratory vacuum manifold and two holding tanks to collect the contaminated waste gases, a catalytic reactor to oxidize the tritium, two molecular sieve dryers connected in series to collect the tritiated water, the necessary pumps to evacuate the laboratory manifold and transfer the waste gas through the system, and a control and diagnostics section to provide both automatic and manual operation and to assess operational status. That portion of the VERS containing the heater, catalytic reactor, heat exchanger, dryers, and transfer pump is referred to as the "decontamination section."

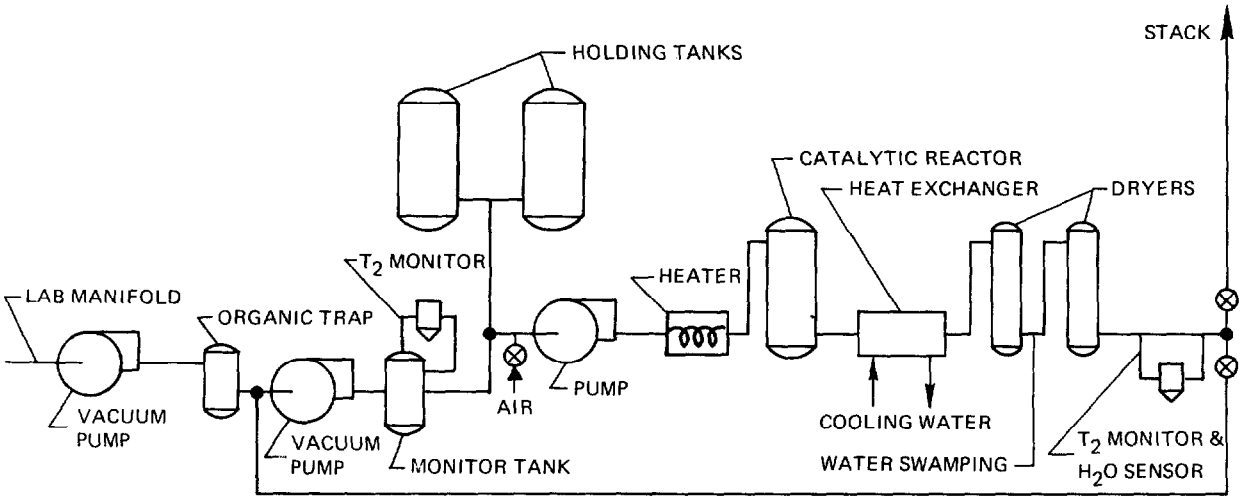

Figure 13 Vacuum effluent recovery system schematic.

The VERS catalytic reactor like that of the GPS is maintained at an elevated temperature (783 K) in standby condition to ensure combustion of tritiated hydrocarbons and readiness to begin processing upon receipt of a start signal. Because holding tank capacity provides adequate time for most maintenance operations, redundant components are limited to the vacuum and gas transfer pumps. Major system performance criteria are summarized in Table II.

The VERS is normally operated in a batch processing mode. The laboratory vacuum manifold is maintained at an average pressure of approximately 3.3 kPa. The effluent exhausted to the manifold is pumped into a 0.3 m^3 tank, where its contamination level is monitored. To minimize VERS operating time, the effluent of the 0.3 m^3 tank is divided into two levels of tritium concentration which are collected in separate 5.7 m^3 holding tanks. The lower concentration is selected such that effluent can be vented directly to the stack while the effluent with the higher tritium concentration is decontaminated before stacking.

Effluent is collected until the holding tank pressure reaches 86 kPa. The decision to stack the holding tank contents is made by control room personnel and

Table II VERS performance criteria.

Processing Capacity	18 m^3 hr^{-1}
Holding Capacity	9.5 m^3 at 86 kPa
Catalytic Reactor	
Operating Temperature	783 K
Standby Temperature	783 K
Catalyst	Engelhard Minerals and Chemicals No. A-16648
Tritium Concentration Reduction Factor*	1000 per pass for concentration from 20,000 ppm to 1 ppm
Molecular Sieve Dryer	Will use GPS dryers
Molecular Sieve	Type 4A
System Operating Pressure	13 to 86 kPa
System Leak Rate	1×10^{-10} m^3 (STP)s^{-1} maximum helium at 98 kPa differential

*Ratio of inlet to outlet tritium concentrations.

must be initiated manually. The decision to process the holding tank contents through the decontamination section is automatically made by the VERS control system. The tritium monitor at the exit of the decontamination section generates a signal, depending upon the tritium concentration, either to recirculate the effluent through the VERS or to direct it to the stack.

When a holding tank is to be processed through the decontamination section, the VERS control system alerts the control room by means of an alarm light and begins circulation of the holding tank contents through the decontamination section. When the holding tank pressure is reduced below 13 kPa, the system shuts down. The VERS has the capability for being operated in a continuous stacking and processing mode. However, the decision to use this mode will depend upon operational experience still to be gained.

VERS Modifications

The decontamination section of the VERS is shown in Figure 14 as originally received from the manufacturer.

With the exception of the decontamination section, the VERS was designed and fabricated by Sandia. A major task was to integrate the decontamination section into the rest of the system. Because of space limitations, the manufacturer's skid was disassembled and the major components, with the exception of the catalytic reactor, were mounted on the Sandia skid. A new catalytic reactor was built to provide a larger flow capacity and catalyst entry, and exit nozzles

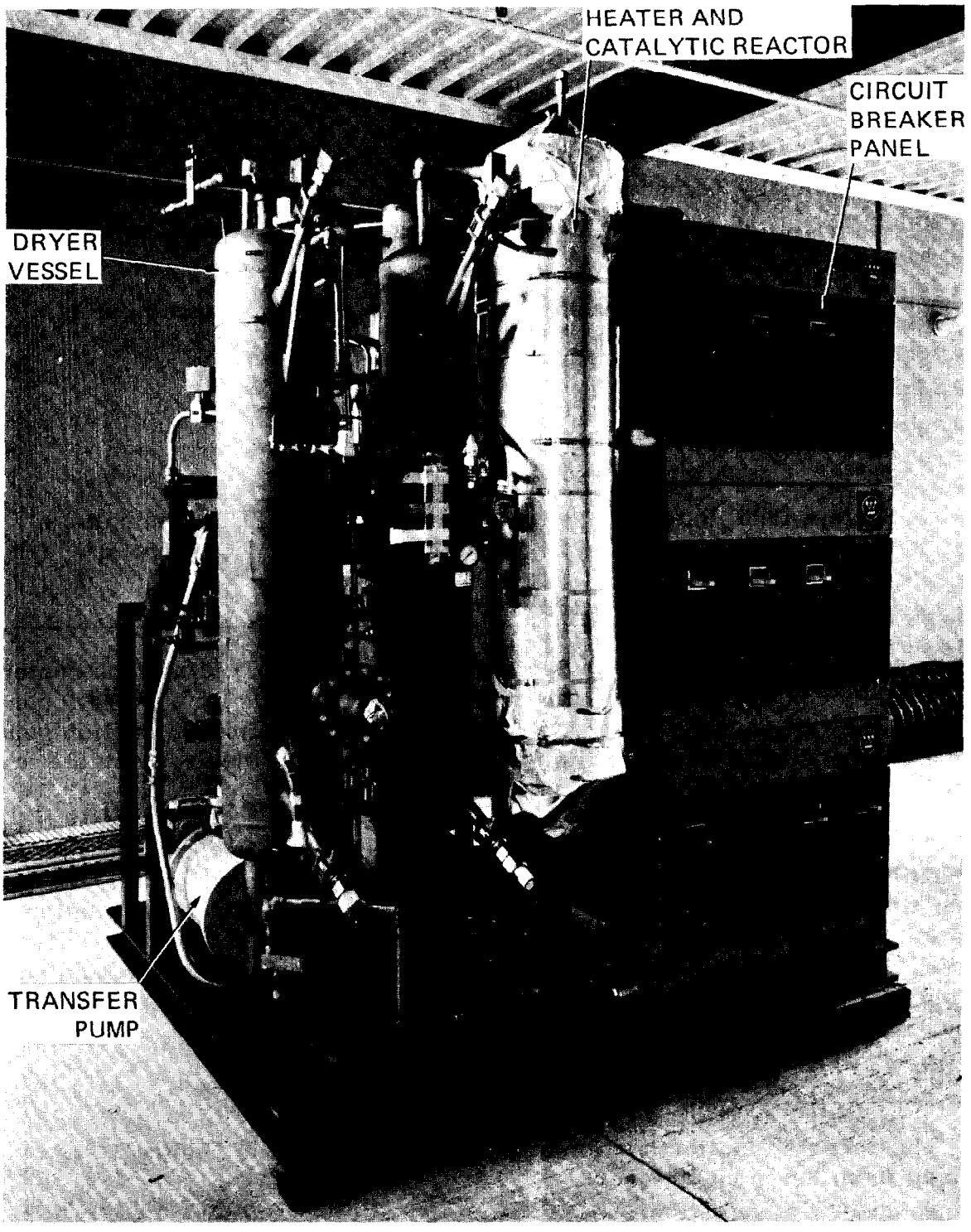

Figure 14 VERS decontamination section as received from manufacturer.

were relocated to facilitate catalyst addition and removal. The VERS exhaust was interconnected to the GPS so that GPS dryers could be used for water collection.

Where possible the control system elements used for acceptance testing of the skid were integrated with the microprocessor controlled solid state system designed by Sandia. As with the GPS, all of the control elements except disconnects were removed from the skid and mounted outside the air hood. The heater control was changed to a silicone controlled rectifier unit, and thermocouples were placed in the catalytic reactor to allow for more accurate temperature control and to provide a means for monitoring catalyst performance. The final VERS skid configuration is shown in Figure 15, and the control panel located in the TRL control room is shown in Figure 16.

Test Program

The GPS and VERS were subjected to acceptance tests at the manufacturer's plant, and preoperational and tritium tests in the TRL. Acceptance testing at the manufacturer's plant verified the ability of the two systems to meet the performance criteria required by the specification (Tables I and II), with the exception of the concentration reduction factors, which required tritium testing for verification. Hydrogen was combusted as part of the acceptance testing to demonstrate that the catalyst was operating and to provide a source of moisture for loading the first dryer. The swamping system was used to load the second and third dryers.

Preoperational testing of the systems in the TRL included essentially a repeat of the manufacturer's acceptance tests. These tests demonstrated that the systems installed in the TRL met the processing capacity, pressure control, and startup operating time, etc., specifications in the actual laboratory operating configuration. The preoperational testing also included a series of catalyst performance tests with hydrogen and methane.[2] These tests were run to provide confidence that the catalytic reactors in both systems were operating properly before tritium was introduced and also to determine the appropriate catalyst operating temperature.

The final series of tests was made with tritium and tritiated methane[2] to determine that the systems were capable of achieving the design requirement of a single-pass concentration reduction factor (ratio of inlet to exhaust concentration) of 1000 per pass for inlet concentrations of 1 part per million. Sensitivity limitations of gas chromatography required that this confirmation be made with tritium as the test gas. Tests were run with methane and tritiated methane because tritiated hydrocarbons are expected to be present in both systems,[3] particularly in the VERS.

GPS and VERS Hydrogen and Methane Tests

The GPS tests were performed first. Approximately ten runs were made to assess the system operation before the parameters were selected for tests measuring temperature effects upon catalyst performance. The VERS test parameters were selected as a result of this experience. The test parameters used are

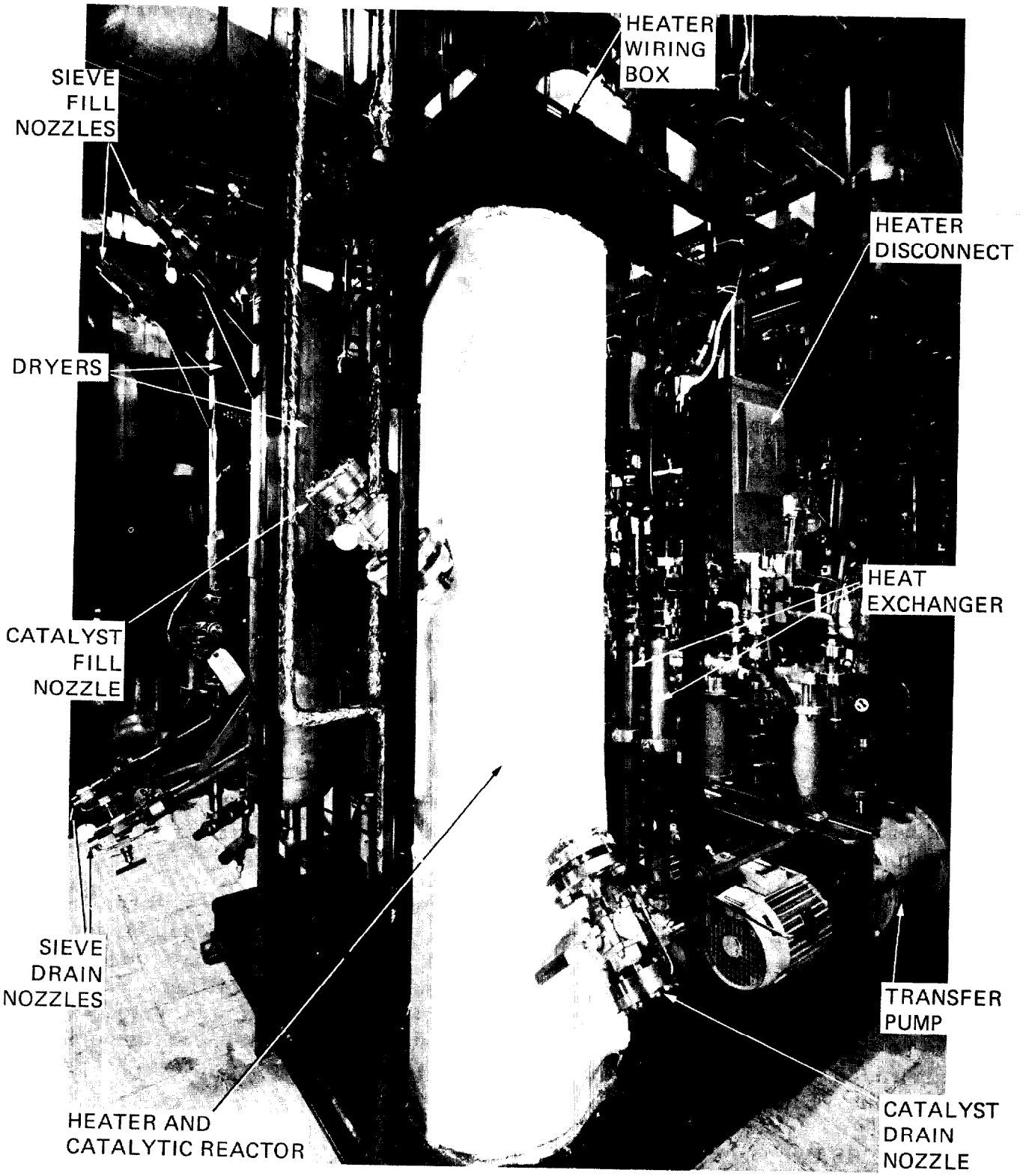

Figure 15 VERS skid final configuration.

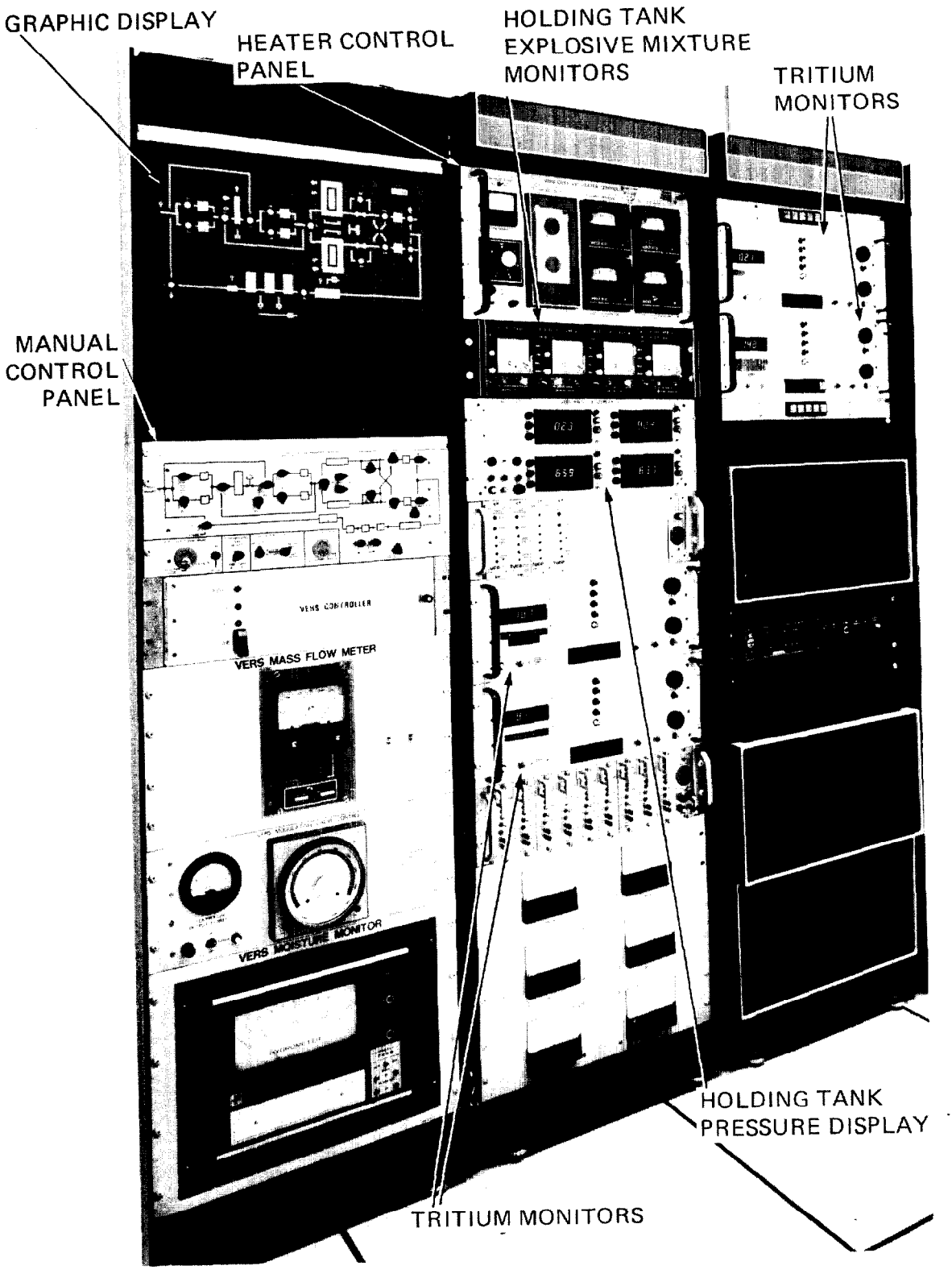

Figure 16 VERS control panel.

summarized in Table III. Inlet concentrations were chosen to provide a reasonable range of detection for the gas chromatograph.

Table III Hydrogen and methane test parameters.

System	Test Gas	Flow Rate (std m^3 hr^{-1})	Inlet Concentration (ppm)	Catalyst Temperature (°K)
GPS	Hydrogen	340	120	316-743
GPS	Methane	261	700	316-810
VERS	Hydrogen	16.4	100	302
VERS	Methane	13.3	2000	302-810

The test gases along with nitrogen and combustion air were injected upstream of the catalytic reactor, and inlet and exhaust concentrations were measured with a gas chromatograph upstream and downstream of the catalytic reactor, respectively. Combustion air was injected in excess of stoichiometric requirements. The results of the GPS catalyst temperature tests are displayed in Figure 17 for both hydrogen and methane. Temperatures below 316 K were not achievable because of the heat of compression generated by the circulation blowers.

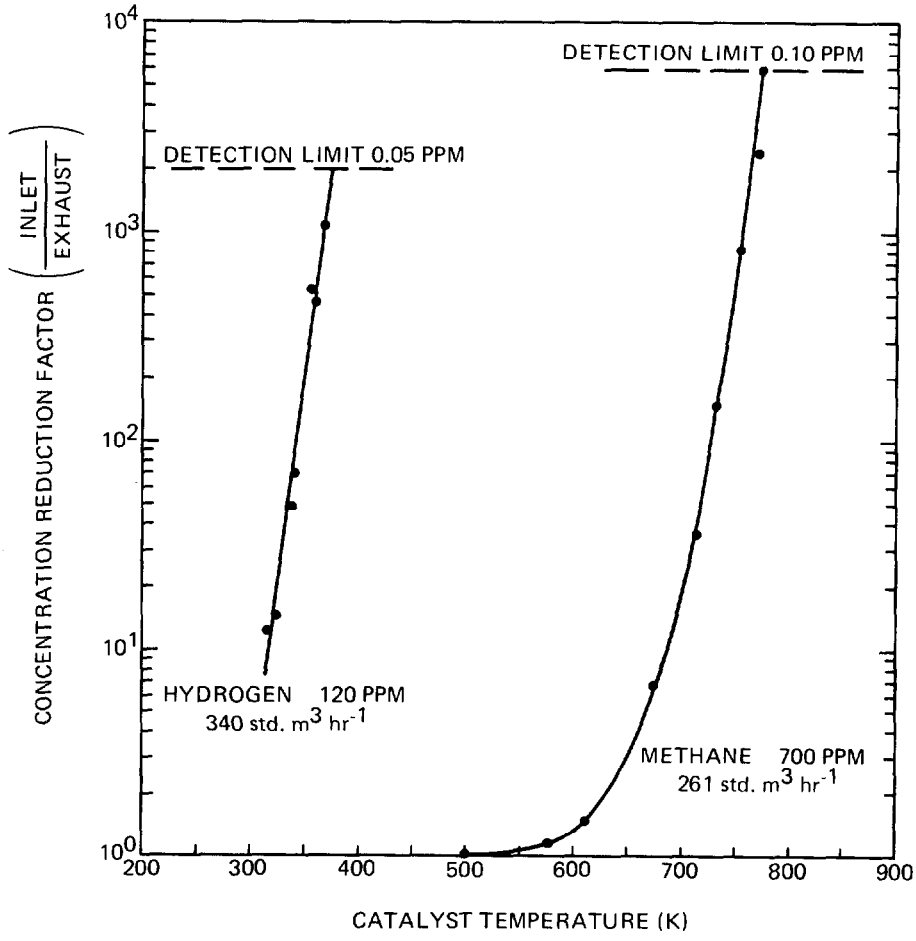

Figure 17 Effect of GPS catalyst temperature on concentration reduction factor.

A glove box cleanup test was also run with methane to determine the rate at which a contaminant could be removed from the glove box atmosphere. Methane was injected into a nitrogen filled glove box until an initial concentration of 500 ppm was achieved. The box atmosphere was then processed by the GPS. The results are presented in Figure 18.

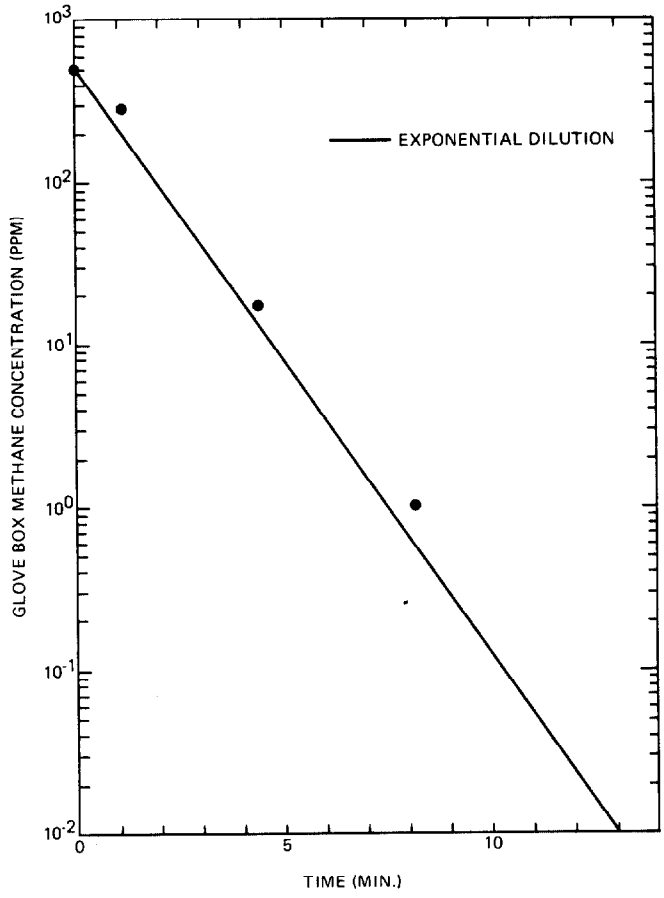

Figure 18 Glove box cleanup test results.

The VERS test results, though similar, cannot be directly compared to those for the GPS since the catalyst residence time for the VERS is approximately 2.5 times that for the GPS. At 320 K, the lowest temperature achievable, the VERS exhaust hydrogen concentration was below the detection limit of the chromatograph, 0.1 ppm. The results of the methane test were essentially the same as for the GPS (Figure 16) and show that to achieve concentration reduction factors greater than 1000, the catalyst must be operated at temperatures in excess of 750 K for methane.

GPS and VERS Tritium Tests

After the preoperational tests and GPS system modifications had been completed, both systems were tested with tritium to verify their ability to achieve concentration reduction factors of 1000 per pass at inlet concentrations of 1 ppm.

Four tritium tests were run on the GPS at a catalyst temperature of 783 K and a flow rate of 340 std m^3 hr^{-1}. Seven tests, four with tritium and three with tritiated methane, were run on the VERS at a catalyst temperature of 783 K and a flow rate of 17.0 std m^3 hr^{-1}. Hydrogen was added to some test runs to simulate tritium processing at higher concentrations. All of the tests were run without water added ahead of the second dryer. The GPS test gases were injected into a sealed glove box while the VERS test gases were injected into one of the 5.7 m^3 holding tanks and then processed through the system. The test results are summarized in Tables IV and V for the GPS and VERS, respectively. Concentration reduction factors were calculated by dividing the maximum inlet tritium concentration by the maximum exhaust tritium concentration.

Table IV GPS tritium test summary.

Test Designation	Sample Composition	Inlet Tritium Concentration Ci m^{-3}	Exhaust Tritium Concentration μCi m^{-3}	Concentration Reduction Factor
GPS T-1	T_2 in Nitrogen	0.14	2.0	7.0×10^4
GPS T-2	T_2 in Nitrogen	1.3	15.0	8.7×10^4
GPS T-3	T_2 & 2.0% H_2 in Nitrogen	9.4	1020.0	9.2×10^3
GPS T-4	T_2 in Nitrogen	115.0	250.0	4.6×10^5

Table V VERS tritium test summary.

Test Designation	Sample Composition	Inlet Tritium Concentration Ci m^{-3}	Exhaust Tritium Concentration* μCi m^{-3}	Concentration Reduction Factor
VERS T-1	T_2 in Nitrogen	0.18	$\leqq 1.0$	$\geqq 1.8 \times 10^5$
VERS T-2	T_2 in Nitrogen	0.18	$\leqq 1.0$	$\geqq 1.8 \times 10^5$
VERS CH_3 T-1	CH_3T in Nitrogen	0.18	$\leqq 1.0$	$\geqq 1.8 \times 10^5$
VERS CH_3 T-2	CH_3T in Nitrogen	1.8	$\leqq 1.0$	$\geqq 1.8 \times 10^6$
VERS CH_3 T-4	CH_3T & 0.5% H_2 in Nitrogen	7.4	$\leqq 1.0$	$\geqq 7.0 \times 10^6$
VERS T-5	T_2 & 0.5% H_2 in Nitrogen	13.2	$\leqq 1.0$	$\geqq 1.3 \times 10^7$
VERS T-6	T_2 & 2.0% H_2 in Nitrogen	132.0	$\leqq 1.0$	$\geqq 1.3 \times 10^8$

*1.0 μCi m^{-3} is the least count of the tritium monitor.

An uncertainty of approximately 30 percent should be applied to the GPS concentration reduction factors because of inaccuracies both with tritium measurements and data acquisition methods.

An uncertainty of approximately 50 percent should be applied to the VERS concentration reduction factors because of inaccuracies with tritium measurements at the 1 μCi m^{-3} level of concentration.

Summary

The concept of providing both personnel safety and environmental protection from tritium on a laboratory-wide basis by employing a secondary containment system of sealed glove boxes connected to two central decontamination systems has been implemented by Sandia Laboratories Livermore. Acceptance tests at the manufacturer's plant and preoperational tests in the Tritium Research Laboratory have demonstrated that the systems meet their design specifications and that glove box cleanup rates approaching exponential dilution can be achieved.

The tritium test program to date has demonstrated that both the Gas Purification System and Vacuum Effluent Recovery System perform 10-1000 times better than required by the design specifications, and that tritium removal systems can be designed to achieve concentration reduction factors much in excess of 1000 per pass at inlet concentrations of 1 part per million or less for tritium and for tritiated methane.

References

1. P. D. Gildea et al., "A Tritium Systems Test Facility Volume II: Appendixes," Sandia Laboratories, Livermore, SAND76-8053, October 1976, pp. 57-59.

2. P. D. Gildea, W. R. Wall, and V. P. Gede, "Results of Tritium Tests Performed on Sandia Laboratories Decontamination System," Sandia Laboratories, Livermore, SAND77-8766, May 1978.

3. J. C. Bixel and C. J. Kershner, "A Study of Catalytic Oxidation and Oxide Adsorption for the Removal of Tritium From Air," in Proceedings of the Second AEC Environmental Protection Conference, WASH-1332(74), April 16-19, 1974.

DISCUSSION

KAPASI: How was the tritiated moisture removed from the dryer beds, as liquid or solid?

GILDEA: Water is removed from the dryers in the liquid form by a regeneration system. The liquid water is collected in a room temperature separator and then drained into a mole sieve trap for disposal.

KAPASI: Was swamping used in achieving the decontamination factor you cited?

GILDEA: The equipment provides the capability for water swamping ahead of the second dryer. However, swamping was not used on the tests reported in this paper.

FREEMAN: Are your systems located in an open room with only arrangements for a glove box for removal of the heater?

GILDEA: That is essentially correct. The equipment is located in the equivalent of a walk-in hood. However, this hood does not provide for personal protection during maintenance operations. A glove box mounting arrangement is provided for heater removal/replacement since it requires opening a very large volume of the system to the room.

FREEMAN: Do you anticipate problems with contamination when performing other maintenance procedures?

GILDEA: The isolation valve-purge port arrangement is expected to minimize contamination problems for most maintenance operations.

ANON.: Will the N_2 used to regenerate the molecular sieves be reused since there will be some tritium oxide left in the gas stream even after moisture removal by condensation?

GILDEA: Yes, the nitrogen in the regeneration system is just left there until the next regeneration cycle is required. However, the majority of the moisture picked up by the nitrogen is put back on the sieve bed during the cooldown part of the cycle.

BRUGGEMAN: Please comment on the time scheme you use for the regeneration of your GPS dryers.

GILDEA: The regeneration process takes from 6-8 hours. Hot nitrogen is circulated through the sieve beds until the bed reaches 600°F, at which time the cool down cycle starts.

BRUGGEMAN: Do you have to add oxygen anywhere in your systems?

GILDEA: We add air ahead of the system blowers in order to provide oxygen for combustion of the tritium.

TRITIUM REMOVAL USING VANADIUM HYDRIDE*

F. B. Hill, Y. W. Wong, and Y. N. Chan
Department of Energy and Environment
Brookhaven National Laboratory
Upton, NY 11973

Abstract

The results of an initial examination of the feasibility of separation of tritium from gaseous protium-tritium mixtures using vanadium hydride in cyclic processes are reported. Interest was drawn to the vanadium-hydrogen system because of the so-called inverse isotope effect exhibited by this system. Thus the tritide is more stable than the protide, a fact which makes the system attractive for removal of tritium from a mixture in which the light isotope predominates. The initial results of three phases of the research program are reported, dealing with studies of the equilibrium and kinetics properties of isotope exchange, development of an equilibrium theory of isotope separation via heatless adsorption, and experiments on the performance of a single heatless adsorption stage.

In the equilibrium and kinetics studies, measurements were made of pressure-composition isotherms, the HT-H_2 separation factor and rates of HT-H_2 exchange. This information was used to evaluate constants in the theory and to understand the performance of the heatless adsorption experiments.

A recently developed equilibrium theory of heatless adsorption[17] was applied to the HT-H_2 separation using vanadium hydride. Using the theory it was predicted that no separation would occur by pressure cycling wholly within the β phase but that separation would occur by cycling between the β and γ phases and using high purge-to-feed ratios.

Heatless adsorption experiments conducted within the β phase led to inverse separations rather than no separation. A kinetic isotope effect may be responsible. Cycling between the β and γ phases led to separation but not to the predicted complete removal of HT from the product stream, possibly because of finite rates of exchange.

Further experimental and theoretical work is suggested which should ultimately make possible assessment of the feasibility and practicability of hydrogen isotope separation by this approach.

I. Introduction

Isotope effects are commonly observed in metal hydrides. The usual finding is that stability increases in the order tritide, deuteride, protide. The vanadium-hydrogen system is one of the few exceptions in that stability increases in the reverse order. An inverse isotope effect may be of value in separating mixtures of

*This work was supported by the Division of Chemical Sciences, U.S. Department of Energy, Washington, D.C., under Contract No. EY-76-C-02-0016.

hydrogen isotopes consisting mainly of protium with a trace of a heavier isotope, deuterium or tritium.

With this viewpoint in mind, an investigation of the feasibility of removal of tritium from a gaseous protium-tritium mixture using vanadium hydride has been undertaken. The investigation was formulated and is being carried out with the idea in mind of using cyclic processes such as heatless adsorption (cycling pressure) or cycling zone adsorption (cycling temperature) to carry out the separation. Heatless adsorption has been the process studied to date. Three topics have been examined and are discussed in the present paper: equilibrium and kinetics properties of isotope exchange in the vanadium-hydrogen system, the theory of isotope exchange via heatless adsorption, and the performance of a single heatless adsorption stage.

II. Equilibrium and Kinetics Studies

Experimental information needed for development of a theory of isotope separation via heatless adsorption using vanadium hydride and in general needed for the design and analysis of isotope separation processes using this system includes pressure-composition isotherms for H_2, the HT-H_2 separation factor, and information on rates of attainment of equilibrium in isotope exchange. Experimental studies to obtain this information are described briefly in this section. Details are available elsewhere.[1]

Materials

Hydrogen was obtained from the Matheson Gas Co., Rutherford, N.J., with a purity of 99.999%. Gaseous tritium was obtained from the New England Nuclear Corp., Boston, Mass., in the form of a one-curie ampoule, carrier free. A master batch of tritiated hydrogen (approximately 4×10^{-9} mole fraction HT in H_2) was prepared by diluting the tritium with $\sim 3\ m^3$ of the Matheson hydrogen. Ingots of vanadium were obtained from the Gallard-Schlesinger Chemical Manufacturing Corp., Carle Place, N.Y. The vanadium purity was 99.5% V minimum with major impurities in percent, 0.15 Si, 0.05 Fe, 0.04 N, 0.02 O, 0.03 C, 0.01 all other metals. Upon receipt the ingots were partially hydrided to facilitate crushing and sizing with standard sieves.

Pressure-Composition Isotherms

These measurements were made using the techniques and apparatus of Reilly and Wiswall.[2] Measurements were made in the $VH_{\sim 0.6}$-$VH_{\sim 1.8}$ region at temperatures from 0° to $250^{o}C$, and pressures from approximately atmospheric to 7000 kPa (1000 psi). The results are shown in Figure 1. The plateau pressures, corresponding to dihydride dissociation, were approximately twice those reported by Reilly and Wiswall[3] for hydride made from zone-refined V, thus reflecting the strong influence of impurities. Hydrogen content of hydrides made from commercial grade V was lower than that for hydrides from zone refined V. Impurities were found to exert no significant influence on the temperature dependence of the plateau pressures, confirming the earlier findings of Reilly and Wiswall.[4]

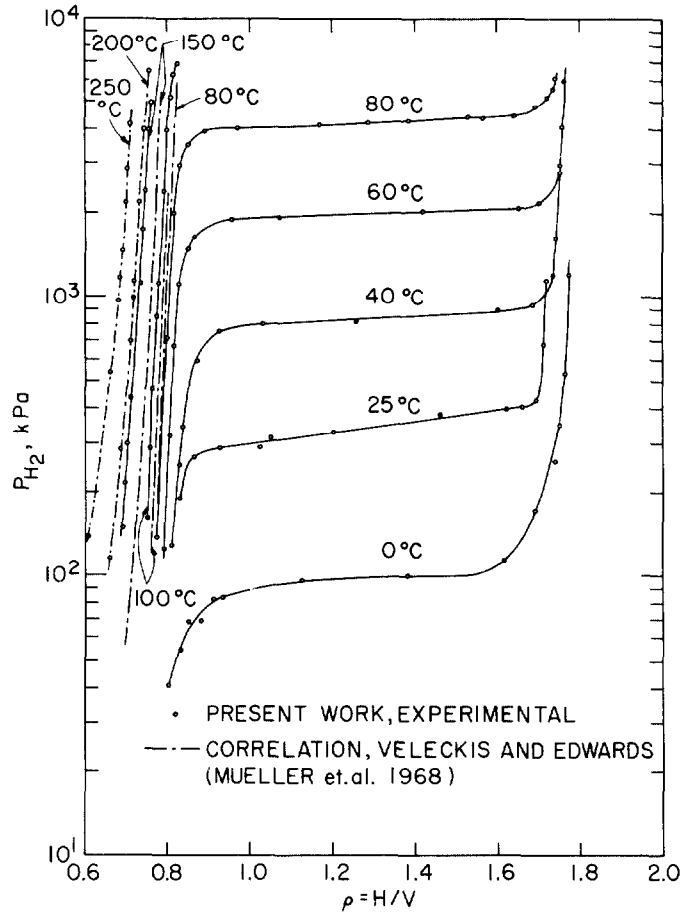

Figure 1. Pressure-composition isotherm data for the vanadium (commercial grade)-hydrogen system.

Also shown in Figure 1 is a comparison of the present data with the predictions of a semi-empirical formula due to Veleckis and Edwards:[5]

$$\ln p_{mm}^{\frac{1}{2}} = 10.283 + 1.0598 \ln \frac{\rho}{0.89-\rho} + \frac{1}{T}(-3489.2 - 3269.0\rho + 2563.0\rho^2 - 732.39\rho^3 + 4818.3\rho^4) \cdot \quad (1)$$

Agreement with this relation is good at high temperature and at pressures below the dihydride dissociation pressure. Equation (1) was developed by fitting pressure-composition data for the α phase to a model based on simple interstitial solution of hydrogen atoms in a perfect crystalline lattice. Thus this model appears to apply also to the β phase at higher temperatures.

The distribution coefficient for H_2, $K_{H_2} = C_H/C_{H_2}$, was calculated from the isotherm data as follows. From the perfect gas law,

$$C_{H_2} = \frac{P}{RT}. \tag{2}$$

The equilibrium concentration of hydrogen atoms in the solid phase is given by

$$C_H = \rho \Big/ \left[\frac{50.95 + 1.008\rho}{\rho_s} \right] \tag{3}$$

where ρ is the hydrogen-to-vanadium ratio corresponding to the pressure P on the isotherm, 50.95 and 1.008 are the atomic weights of V and H and ρ_s is the density of vanadium hydride in g/cm^3. As indicated above, the distribution coefficient is the quotient, C_H/C_{H_2}.

Chromatography Experiments

Separation factors and rate information were obtained from chromatography experiments in which pulses of tritiated hydrogen were eluted from a column packed with vanadium hydride particles. The eluted pulses were detected by means of an internal proportional counter. First and second moments of these pulses were determined in an extensive series of experiments in which particle size, temperature, pressure and hydrogen flow rate were variables.

The first and second moment data were interpreted in terms of a theoretical model of mass transfer and exchange reaction. In this model the exchange reaction occurring at the gas-solid interface is

$$HT(g) + H(s) \underset{k_r^T}{\overset{k_f^T}{\rightleftarrows}} H_2(g) + T(s) \tag{4}$$

The overall exchange process is postulated to occur in the following steps in series: diffusion of HT through a gas film surrounding a hydride particle, exchange at the gas-solid interface via reaction (4), and diffusion of T atoms into the interior of the particle. Also dispersion of HT in the gas phase occurs in the axial direction.

For this model it can be shown that the first absolute moment (elution time) and second central moment (variance) are related to equilibrium and rate constants of the constituent processes of the model by the following relations:

$$\mu_1'(h) = \left(1 + \frac{1-\varepsilon}{\varepsilon}\,\frac{\alpha}{2}\,K_{H_2}\right)\frac{h}{u} + \frac{t_0}{2} \tag{5}$$

$$\mu_2(h) = \left\{ \frac{1-\varepsilon}{\varepsilon}\,\frac{\alpha}{2}\,K_{H_2}\left[\left(\frac{\frac{\alpha}{2}K_{H_2}}{3D_{HT-H_2}} + \frac{1}{15D_s}\right)r_p^2 + \frac{\frac{\alpha}{2}K_{H_2}}{k_f^T C_H^*}\right] + E_z\left(1 + \frac{1-\varepsilon}{\varepsilon}\,\frac{\alpha}{2}\,K_{H_2}\right)^2 \frac{1}{u^2}\right\}\frac{2h}{u} + \frac{t_0^2}{12} \tag{6}$$

An assumption implicit in Equation (6) is that the flow in the column is laminar.

By inspection of Equation (5) it is apparent that by using values of $\mu_1'(h)$, K_{H_2}, h, u, and t_0 in this equation one can evaluate α, the HT-H_2 separation factor. The distribution coefficient, K_{H_2}, is obtained for this purpose from the pressure-composition isotherms as indicated in the previous section. Similarly, Equation (6) can be used to evaluate rate information. The details of this evaluation are given by Wong and Hill.[1]

The chromatography experiments were conducted over the temperature range 40° to 307°C and over the pressure range 210 to 1030 kPa (30 to 150 psi). Hydrogen flow rates were varied from 80 to 400 standard cm^3/min. Four particle sizes were used: 40/45 mesh (380 μm geometric average diameter), 30/40 (500), 20/25 (770), and 16/20 (1000). Values of the separation factor, α, determined from first moment data are plotted versus temperature in Figure 2. It may be

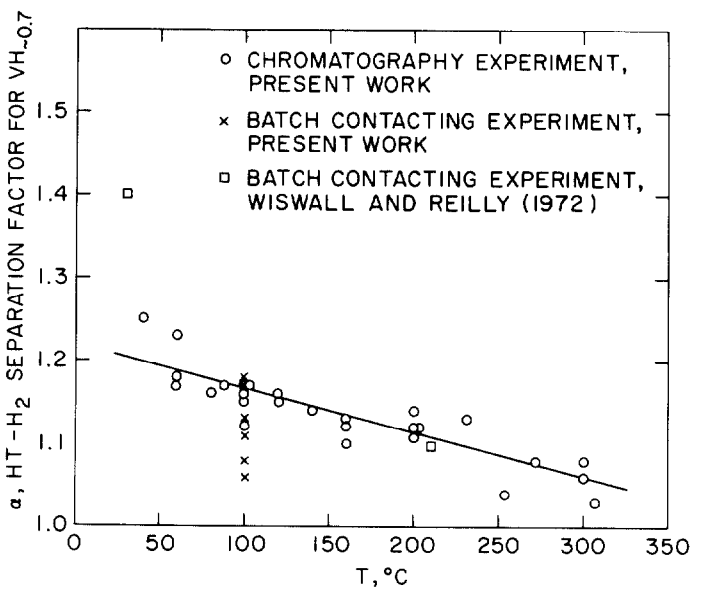

9-228-78

Figure 2. HT-H_2 separation factors for β vanadium hydride.

shown that α is not a function of pressure.[1] This behavior is expected since α is held to be related to the Einstein vibration frequencies of the isotopes in the metal lattice[6] and hence should be a function of lattice structure and temperature only. It is generally true that isotope effects disappear, i.e., $\alpha \rightarrow 1$, at high temperature.[7] As a result, the magnitude of the measured α was expected to decrease with temperature. This was found to be so experimentally. It is interesting that there is no discontinuity in the variation of α with temperature in the range 160° to 180°C where a transition from the β to the α phase occurs.[8] Also shown in Figure 2 are separation factors obtained by Wiswall and Reilly[9] and in this work using the batch contacting technique of Tanaka, Wiswall and Reilly.[10] Good agreement exists between the data for

the two types of experiments, thus demonstrating as did Schneider and Smith[11] that values of equilibrium properties can be accurately determined from kinetic measurements. Also agreement is good between data for hydrides derived from pure and commercial grade V (Wiswall and Reilly's data are for zone refined V). The presence or absence of impurities seemed to have no influence on separation factor.

By suitable representation of second moment data it was possible to show that the term in square brackets in Equation (6) did not vary with particle size and thus that this term was essentially equal to $\frac{\alpha}{2} K_{H_2}/(k_f^T C_H^*)$. This term represents the resistance due to the exchange reaction. The terms multiplied by r_p^2 represent the resistances due to external diffusion and solid phase diffusion. The implication is that the exchange reaction is controlling.

With knowledge that the first term in square brackets in Equation (6) is small compared with the second, this equation was used in combination with values of ε, α, and K_{H_2} to determine values of $k_f^T C_H^*$ for each set of temperature and pressure conditions. For purposes which will become apparent below each value of $k_f^T C_H^*$ was then multiplied by $C_{H_2}^* = P/RT$, where the values of P and T were those corresponding to the experiments from which the value of $k_f^T C_H^*$ was derived. Values of $k_f^T C_H^* C_{H_2}^*$ so determined are shown in Figure 3. The

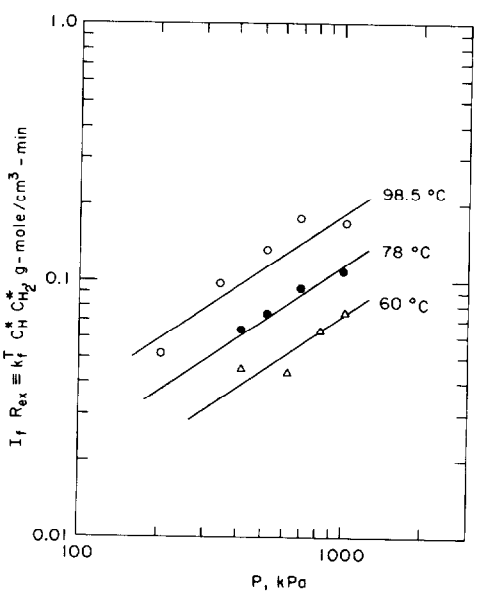

Figure 3. Pressure and temperature dependence of the exchange reaction rate.

temperature and pressure dependence of $k_f^T C_H^* C_{H_2}^*$ was found to be given by

$$k_f^T C_H^* C_{H_2}^* = 4.06\ P^{0.7} \exp\left(-\frac{24600}{RT}\right) \text{ gm mole/cm}^3\text{-min}, \tag{7}$$

where P is in kPa and the activation energy is in joule/gm-mole.

For the purpose of examining the significance of the temperature and pressure dependence of the exchange reaction rate it is convenient to proceed as follows. The rate of disappearance of HT is given by $k_f^T C_H^* C_{HT}^*$. This rate may be expressed in terms of the rate of the hydrogen exchange reaction

$$H_2(g) + H(s) \underset{k_r^H}{\overset{k_f^H}{\rightleftarrows}} H_2(g) + H(s) \tag{8}$$

as follows:

$$k_f^T C_H^* C_{HT}^* \equiv \frac{k_f^T}{k_f^H} k_f^H C_H^* C_{H_2}^* \frac{C_{HT}^*}{C_{H_2}^*} \tag{9}$$

$$= I_f\ R_{ex} \frac{C_{HT}^*}{C_{H_2}^*}$$

As one can see,the product of the hydrogen exchange rate, R_{ex}, and the forward isotope effect, I_f, is identically the left hand side of Equation (7). The forward isotope effect is independent of pressure and is a slowly varying function of temperature.[7] Hence all of the pressure dependence and substantially all of the temperature dependence of Equation (7) may be ascribed to the hydrogen exchange rate R_{ex}. The pressure dependence of the hydrogen exchange reaction rate may range from P^0 to P^1 according to the detailed nature of the mechanism of chemisorption and reaction of H_2. Three such mechanisms together with their pressure dependencies are those of Bonhoeffer and Farkas (P^0), Rideal-Eley, two site ($P^{0.5}$), and Rideal-Eley, single site (P^1). A pressure dependence given by $P^{0.7}$ can be ascribed to a mixture of contributions from all three mechanisms. Alternately, the explanation of Scholten and Konvalinka[12] may be valid. They found a pressure dependence of $P^{0.64}$ for the rate of hydrogen exchange on β palladium hydride. This pressure dependence closely approximated the variation with $P^{2/3}$ found for a mechanism based on a surface composition of Pd_3H_2 (approximately the composition of $PdH_{0.68}$ used experimentally) and the assumption that the rate of reaction was proportional to the number of H_2 collisions with the surface and the chance of encounter with a free Pd atom. The same argument would apply to the β vanadium hydride system with its approximate composition V_3H_2.

The temperature dependence of the hydrogen exchange rate is in the range expected for activated chemisorption.[13]

Also obtainable from second moment data are values of the axial dispersion coefficient, E_z. These were found to be just slightly greater than expectations based on molecular diffusion only. Thus some additional mechanism of axial mixing appeared to have been present.

III. Theory

In this section an equilibrium theory of hydrogen isotope separation via heatless adsorption using vanadium hydride is presented. First a brief description of the heatless adsorption process is given.

Heatless adsorption is a cyclic separation process involving two adsorption beds. Each cycle consists of four steps (Figure 4). In

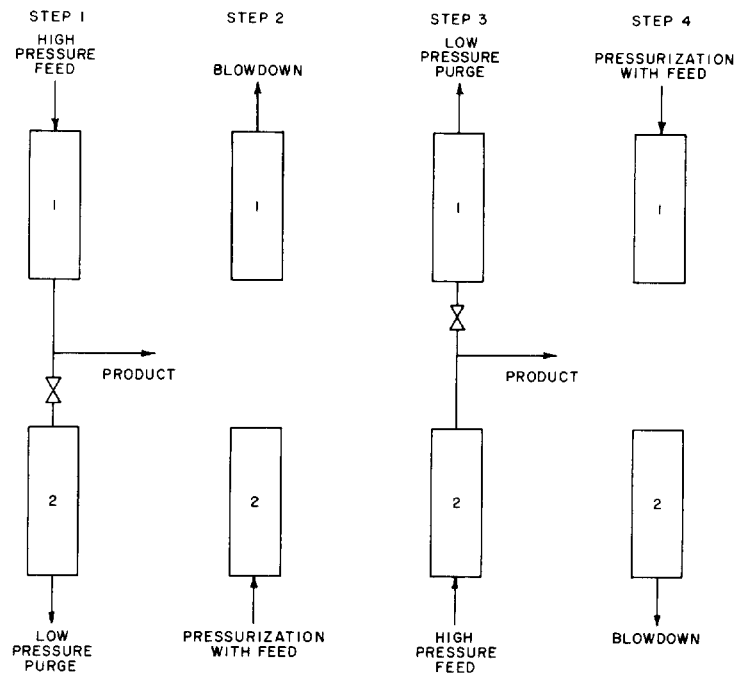

Figure 4. Steps in a cycle of heatless adsorption.

the first step, a high pressure feed mixture is continuously supplied to Bed 1, and during this step sorbable components are taken up. A portion of the purified Bed 1 effluent is taken off as product and the remainder is throttled down to a lower pressure and is supplied to Bed 2 and serves to purge previously sorbed species. In the second step Bed 2 is pressurized with the feed and Bed 1 undergoes depressurization or blowdown to the purge pressure. The third and fourth steps are the same as the first two except that the points of feed introduction and purge and blowdown removal are reversed with respect to Beds 1 and 2. Heatless adsorption has the unusual characteristic that if a sufficiently high fraction of the feed is used as purge and if the cycle time is sufficiently long then at steady state the product stream will be completely free of adsorbable or preferentially adsorbable components.

Shendalman and Mitchell[14] have presented an equilibrium theory of heatless adsorption. Their theory was based on the following assumptions.

1. The feed consists of a nonadsorbing carrier gas containing a trace amount of an adsorbing component.

2. The adsorbing component obeys a linear distribution law.

3. Equilibrium is instantaneously established between phases.

4. The system is isothermal.

5. Dispersion axially is negligible.

6. Flow and composition are uniform radially.

7. The frictional pressure drop across a bed due to flow is negligible.

8. The ideal gas law is valid.

Development of the theory proceeded along the lines of the theory of parametric pumping.[15] The penetration distance concept[16] was employed. The novel feature in heatless adsorption which it was necessary to treat was the presence of pressurization and blowdown steps.

The theory presented by Shendalman and Mitchell is conceptually valid in its prediction of the rate of movement of concentration characteristics during the feed and purge step, concentration changes occurring within the column as the result of pressure changes, and the critical purge-to-feed ratio (the minimum value required for complete column cleanup). However an error was made in the calculation of sorbing component uptake during pressurization, which can lead to significant overestimation of that quantity and consequently to incorrect values of the average blowdown and purge concentrations.

The calculation of sorbing component uptake during pressurization was recently correctly described by Chan, et al.[17] and the complete corrected theory was presented. Also the theory was extended to the case in which the carrier is also adsorbed.

In this section of the paper the theory of Chan, et al.[17] is applied to the removal of a trace level of HT from a stream of H_2 using vanadium hydride. The principal modification of the original theory required is the introduction of the proper isotherm. For the sake of brevity, the theory will be presented in outline form for a separation conducted wholly within the β phase.

In the β phase, ($VH_{\sim 0.6}$ - $VH_{\sim 0.8}$) a pressure-composition isotherm for H_2 (see Figure 1) may be represented by

$$\ln P = a\, C_H + b \qquad (10)$$

where a and b are functions of temperature.

We define the HT-H_2 separation factor as follows:

$$\alpha = \left(\frac{C_T}{C_H}\right) \Big/ \left(\frac{C_{HT}}{2C_{H_2}}\right) \tag{11}$$

where α is a function of temperature.

A balance for H_2 over a differential length of a column is

$$\varepsilon \left[\frac{\partial C_{H_2}}{\partial t} + \frac{\partial\left(uC_{H_2}\right)}{\partial z}\right] + (1-\varepsilon)\frac{1}{2}\frac{\partial C_H}{\partial t} = 0 \tag{12}$$

A similar balance for T atoms is

$$\varepsilon \left[\frac{\partial C_{HT}}{\partial t} + \frac{\partial\left(uC_{HT}\right)}{\partial z}\right] + (1-\varepsilon)\frac{\partial C_T}{\partial t} = 0 \tag{13}$$

With the use of Equations (10) and (11) and the perfect gas law, expressions for $\frac{\partial C_H}{\partial t}$ and $\frac{\partial C_T}{\partial t}$ may be derived. By using these expressions, the perfect gas law, and assumption 7 in Equations (12) and (13) the following equations may be obtained:

$$\left[\frac{\varepsilon}{RT} + \frac{(1-\varepsilon)}{2aP}\right]\frac{\partial P}{\partial t} + \frac{\varepsilon P}{RT}\frac{\partial u}{\partial z} = 0 \tag{14}$$

$$\left[\frac{\varepsilon P}{RT} + (1-\varepsilon)\frac{\alpha}{2}C_H\right]\frac{\partial y}{\partial t} + \frac{\varepsilon u P}{RT}\frac{\partial y}{\partial z} - (1-\varepsilon)\frac{1-\alpha}{2}\frac{y}{aP}\frac{\partial P}{\partial t} = 0 \tag{15}$$

The method of characteristics is applied to these equations (Shendalman and Mitchell,[14] Chan, et al.[17]) with the following results. During process steps occurring at constant pressure (feed and purge steps) the movement of characteristics is described by

$$\frac{dz}{dt} = \frac{\frac{\varepsilon P}{RT}}{\frac{\varepsilon P}{RT} + (1-\varepsilon)\frac{\alpha}{2}C_H}\,u \tag{16}$$

Let

$$B = \frac{\frac{\varepsilon P}{RT}}{\frac{\varepsilon P}{RT} + (1-\varepsilon)\frac{\alpha}{2}C_H} \tag{17}$$

Then the penetration distances for high and low pressure concentration fronts are

$$L_H = B_H u_H \Delta t \tag{18}$$

$$L_L = B_L u_L \Delta t \tag{19}$$

During pressure changes the movement of characteristics and changes in concentration are given by

$$\ln \frac{z_2}{z_1} = -\int_{P_1}^{P_2} \frac{\frac{\varepsilon}{RT} + \frac{(1-\varepsilon)}{2aP}}{\frac{\varepsilon P}{RT} + (1-\varepsilon)\frac{\alpha}{2a}(\ln p - b)} dP \tag{20}$$

$$\ln \frac{y_2}{y_1} = \int_{P_1}^{P_2} \frac{(1-\varepsilon)\frac{1-\alpha}{2aP}}{\frac{\varepsilon P}{RT} + (1-\varepsilon)\frac{\alpha}{2a}(\ln p - b)} dP \tag{21}$$

or, defining $E(P_2,P_1)$ and $F(P_2,P_1)$ as the exponentials of the right hand sides of Equations (20) and (21),

$$z_H = E(P_H,P_L)z_L \tag{22}$$

$$y_H = F(P_H,P_L)y_L \tag{23}$$

The net displacement of a concentration front during a complete cycle of operation can be shown to be

$$\Delta L = L_L - E(P_L,P_H)L_H \tag{24}$$

For $\Delta L = 0$,

$$\frac{L_L}{L_H} = E(P_H,P_L) \tag{25}$$

The fraction of the feed which is rejected as purge when $\Delta L = 0$ may be calculated from this equation by multiplying by the ratio, P_L/P_H. This fraction is called the critical purge-to-feed ratio:

$$G_{crit} = E(P_H,P_L)\frac{P_L}{P_H} \tag{26}$$

When $L_L/L_H \geq G_{crit}$ and $L_H \leq h$, it may be shown that

$$\lim_{n\to\infty} y_n^{Pr} = 0 \tag{27}$$

or that the product stream will be completely free of preferentially sorbable component at steady state.

During the pressurization step the HT contained within the column at the outset of the pressure change will move as dictated by Equation (20) and will experience concentration changes in accordance with Equation (21). In particular, HT at $z = h$ when $t = t_1$ (see Figure 5) will move to $z = A$ by the time $t = t_2$. Therefore at the end of the pressurization step the section of the column defined by

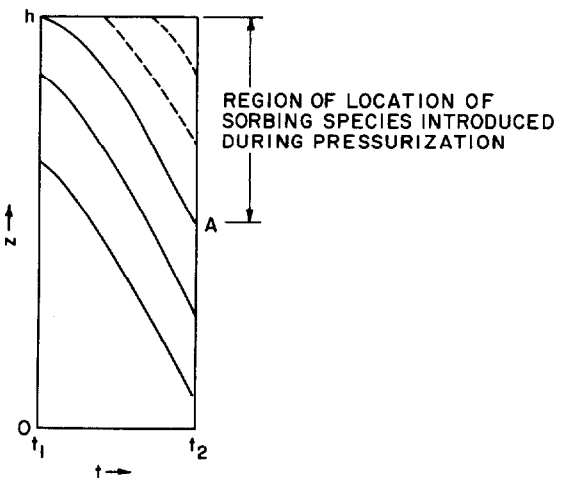

Figure 5. The pressurization step in heatless adsorption.

$A<z\leq h$ will be occupied by all of the HT which entered the column during the pressurization step. Shendalman and Mitchell assumed the gas phase mole fraction within this section would be uniformly equal to the feed mole fraction, y_F. That this cannot be so may be shown simply as follows. During pressurization as one moves from left to right along $z = h$ in Figure 5, the pressure is increasing continuously. Therefore gas introduced into the column at different times will "see" different initial pressures with the result that the lower limit on the integrals in Equations (20) and (21) changes along $z = h$. The mole fraction of HT at $t = t_2$ then varies within the section of the column of interest from a value at A resulting from a low pressure limit of P_L in Equation (21) to the value y_F at $z = h$ corresponding to $P_1 = P_H$.

In the case of a linear isotherm[17] an analytical relation defining the mole fraction distribution within $A\leq z\leq h$ can be obtained. In the present case Equations (20) and (21) are integrated numerically with $z_1 = h$ and $y_1 = y_F$ for values of P_1 between P_L and P_H. Pairs of values $\{y_i, z_i\}$ along $t = t_2$ are thereby obtained which can be fitted satisfactorily by a regression procedure. This method does lead to a good mass balance between HT introduced to the column during pressurization and the HT contained in $A\leq z\leq h$ after pressurization.

Using the relations obtained thus far a difference equation may be derived relating the purge mole fraction after n cycles of operation to the feed mole fraction, to y_{av}, the average mole fraction introduced during pressurization, and to product mole fractions of earlier cycles. The difference equation is obtained by tracing the movement of concentration fronts through the column:

$$y_n^{Pg} = \frac{\left[h - (h-L_H)\frac{1}{E(P_H,P_L)}\right]\frac{1}{F(P_H,P_L)}y_F}{L_L} + \frac{h}{L_L}\left[\frac{1}{E(P_H,P_L} - 1\right]y_{av}$$

$$+ q\,\frac{\Delta L_L}{L_L}\,y_{n-r-1}^{Pr} + (1-q)\,\frac{\Delta L_L}{L_L}\,y_{n-r}^{Pr} \qquad (28)$$

Enrichment ratios can now be found. For the blowdown, for instance, the total amount of protium and the total amount of tritium in the column before and after blowdown are calculated. From this information the average mole fraction of HT in the blowdown may be calculated. The same procedure is followed for the purge. Enrichment ratios are then the ratio of the average mole fraction of HT in the blowdown or purge to the feed mole fraction. Thus the blowdown enrichment is

$$E_b = \frac{\left\{\left[\frac{\varepsilon P_H}{RT} + (1-\varepsilon)\frac{\alpha}{2}C_H^H\right]\frac{L_H}{h} - \left[\frac{\varepsilon P_L}{RT} + (1-\varepsilon)\frac{\alpha}{2}C_H^L\right]\right\}\left[h-(h-L_H)/E(P_H,P_L)\right]\frac{1}{h}\cdot\frac{1}{F(P_H,P_L)}}{\frac{\varepsilon}{RT}(P_H-P_L) + (1-\varepsilon)\frac{1}{2}(C_H^H-C_H^L)} \qquad (29)$$

The purge enrichment is by definition

$$E_{Pg} = \frac{y_n^{Pg}}{y_F} \qquad (30)$$

For purposes of comparison with experiments to be described in the next section, calculations were made of the performance of the heatless adsorption process using equations from the above development. All of the calculations were made for apparatus having the shortest possible columns necessary for complete removal of HT from the product stream. This condition is realized when the column height is set equal to the low pressure penetration distance,

$$h = L_L \qquad (31)$$

and when at the same time the column height is equal to the pressurization displacement (h-A in Figure 5) plus the high pressure penetration distance:

$$h = h-A + L_H$$

or

$$A = L_H \qquad (32)$$

Enrichment in such a column is the maximum obtainable. Enrichment in longer columns will be the same or smaller.

Calculations were made for conditions approximating or bracketing those used in experiments to be described in the next section. For all calculations h = 45.7 cm, S = 0.472 cm^2, and ε = 0.5.

Single Phase Operating Mode

Separation experiments may be conducted wholly within the β phase by cycling the pressure at constant temperature between limits such that operation occurs along a vertical segment of a pressure-composition isotherm for which the hydride composition is in the range $VH_{\sim 0.6}$ to $VH_{\sim 0.8}$ (see Figure 1). This means, for instance, if pressures are restricted to the range, say, 100 to 1000 kPa (∿15 to ∿150 psi) that experiments may be conducted at temperatures of 60°C or higher.

Table I. Calculated performance of heatless adsorption operating in single phase mode.

T, °C	α	G_{crit}	E_{ov}
100	1.17	0.9985	1.0072
118	1.16	1.001	1.0044
150	1.14	0.9977	1.0076
200	1.12	0.9974	1.0074
250	1.09	0.9966	1.0078

Table I presents the results of calculations of performance in the single phase region. There it is seen that for temperatures ranging from 100° to 250°C the critical purge-to-feed ratios are so high that they are tantamount to total reflux. In a corresponding way the overall enrichments (average value in the combined purge and blowdown) are extremely small. Thus essentially no separation is predicted for this mode of operation. For all intents and purposes this is because the equilibrium hydrogen content of the solid in the β region varies very little with pressure and the HT-H_2 separation factor does not change at all with pressure. For example, with respect to hydrogen content, as indicated in Figure 1 for the 100°C isotherm, the hydrogen-to-vanadium ratio, ρ, increases only by 7 percent between 100 and 1000 kPa.

Two Phase Operating Mode

Significant changes in hydrogen content and separation factor are possible at lower temperatures where operation over the same pressure range involves cycling between the β and γ phases. Thus, as an example, at 40°C ρ would vary from about 0.8 at 100 kPa to approximately 1.7 at 1000 kPa, more than a factor of 2. From Wiswall and Reilly[9] the HT-H_2 separation factor in the γ phase is about 1.7 at 40°C. From Figure 2, it is 1.20 in the β phase at this temperature.

Calculations of process performance when cycling between the β and γ phases were carried out for three different temperatures: 16, 25 and 40°C. The isotherms were represented by a number of straight lines. The details of this representation were dependent on the particular low and high pressures chosen for the calculation. The lines chosen for the 40°C isotherm for instance are shown in

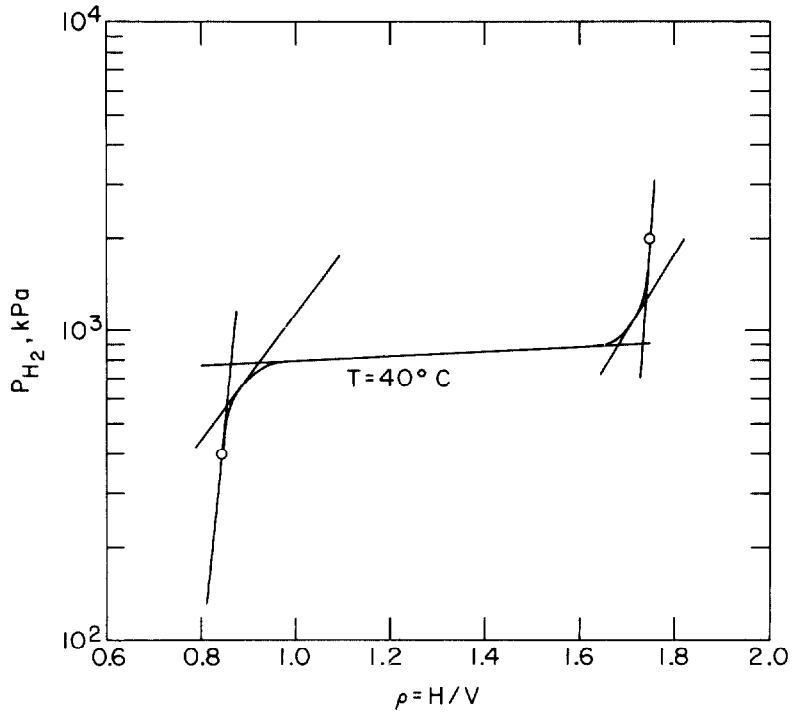

Figure 6. Representation of pressure-composition isotherms for operation in the two phase region.

Figure 6. In making the calculation it was assumed that the separation factor varied continuously in the two phase region from its value in the β phase to that in the γ phase according to the lever rule. All of the equations for process performance were modified to accommodate the two phase isotherm and the accompanying separation factor variation.

Table II. Calculated performance of heatless adsorption operating in two phase mode.

Feed flow rate = 250 sccm
Cycle time = 40 min

T, °C	P_L, kPa	α,β-phase	P_H, kPa	α,γ-phase	G_{crit}	E_{ov}
0	40	1.22	200	1.89	0.766	2.06
25	200	1.21	1000	1.75	0.819	1.41
40	400	1.20	2000	1.66	0.840	1.35

The results of the calculation are given in Table II. There it may be seen that the critical purge-to-feed ratio ranges from 0.77 to 0.84 as the temperature increases from 0° to 40°C. HT is thus completely removed from the product stream which ranges in total amount from 23 to 16 percent of the feed introduced during the high pressure continuous flow step. Overall enrichment decreases with temperature from 2.06 to 1.35.

IV. Performance of a Single Heatless Adsorption Stage

In this section experiments are described on a single heatless adsorption stage and the results are discussed in the light of predictions of the equilibrium theory and of the findings of the chromatography experiments.

Apparatus

A schematic diagram of the apparatus is shown in Figure 7. Each column was made of stainless steel, had an inside diameter of 0.775 cm, and contained 59.4 grams of vanadium hydride particles. The packed bed had a void fraction of 0.5 and a length of 45.7 cm. The bed was supported at the bottom by a stainless steel filter. Stainless steel wool was used to fill the space above the bed. The temperature of the column was maintained constant by means of a jacket and constant temperature circulating bath. Resistance heating wires wrapped around the outside of the jacket were used to raise the column temperature to levels as high as 450°C for the purpose of activating the vanadium particles. Hydrogen gas at high pressure was directed into one column and purge gas at low pressure was introduced into the other. This was achieved by a so-called feed and purge flow

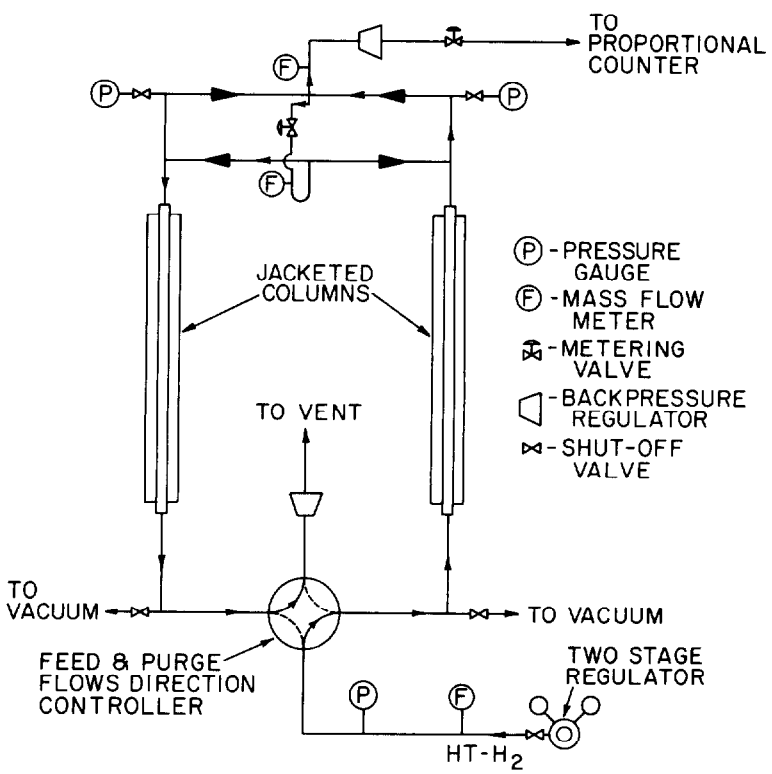

Figure 7. Schematic diagram of heatless adsorption apparatus.

direction controller on the feed side and check valves on the product side. The flow direction controller consisted of an arrangement of four air-operated valves actuated by solid state timers. The valves were operated in such a way that one column was fed while the other was purged and vice versa.

The purge was derived from the high pressure product stream Thus part of the stream emerging from the high pressure column was withdrawn as product and the rest was let down to a lower pressure and introduced into the low pressure column as purge. The lowering of the pressure was a direct result of the pressure drop across a fine metering valve. The high pressure stream was prevented from entering the low pressure column by a check valve. The pressure levels at the two columns were maintained by the feed gas regulator and the respective back pressure regulators. The column pressures and the pressure drops across the columns were measured by three high precision pressure gauges. The flow rates of the feed, the product and the purge were monitored by mass flow meters. All the valves used, except the fine metering valve, were bellows-sealed valves. A flow-through proportional counter of the kind described by Bernstein & Ballantine[18] was used to monitor the tritium level in either the product or the purge streams. The gas flowing through the counter was a mixture of the product gas and P-10 counting gas. They were combined and mixed in a gas proportioner.

Materials

The materials used were the same as those used in the equilibrium and kinetic studies described earlier, with one addition. The mixture used as feed in the present experiments was obtained by diluting 0.07 m^3 of the master batch of tritiated hydrogen with about 3 m^3 of pure hydrogen.

Procedure

The bed was activated in the following way. After charging the vanadium particles to the column, the bed was outgassed at 450°C until a vacuum better than 7×10^{-4} Pa was attained. The bed was then cooled to room temperature and pressurized with hydrogen to 1030 kPa. Hydrogen adsorption was very rapid and was accompanied by rapid heat release. A bed temperature rise of 100°C was not unusual. After carrying out this procedure twice, the bed was considered to be fully activated. Prior to each pressure cycling run, column 1 was saturated with feed gas at high pressure P_H and column 2 was saturated with the same gas at low pressure P_L. This was achieved by feeding tritiated hydrogen gas at P_H to column 1 at a rate of 200 sccm and allowing the emerging stream to bleed down to low pressure P_L and flow through column 2. The effluent of column 2 was monitored by the internal proportional counter until a steady state count rate was reached. The feed, product and purge flow rates were then adjusted to the conditions desired for the experimental run. The run was started by activating the solid state timers which controlled the switching of the air-operated valves. At half cycle intervals, this valve switching alternately directed feed into one column while allowing purge to escape from the other. The concentration of tritium in the product stream was monitored continuously during the whole run. The heatless adsorption runs were conducted over two distinct regions of the

pressure-composition diagram of the vanadium-hydrogen system, namely, the single phase β region and the two phase β-γ region. In the monohydride (β) region, the structure of the hydride phase remained the same at the two extreme pressure conditions. Also, the change in hydrogen content of the hydride was small. In the two phase region the hydride changed from a body-centered tetragonal lattice structure at low pressure to a face-centered cubic one at high pressure. The change in hydrogen content was appreciable in this case. The pressure cycling runs were carried out to study the isotope separation as a function of pressure ratio $\frac{P_H}{P_L}$, feed to purge ratio, temperature, and cycle time.

Results and Discussion

Single Phase Operating Mode. The results of the pressure cycling runs in the β phase were completely unexpected. Whereas according to equilibrium theory concepts slight depletion of tritium in the product stream would be expected to occur at small G, in fact appreciable enrichment was found. This enrichment was commonly of the order of 40 percent at steady state and reached a maximum value of 54 percent in one run. Concentration transients for runs conducted in the β phase are shown in Figures 8 to 10. The ordinate in these figures is the mole fraction in the product stream divided by the mole fraction in the feed. The abcissa is the number of cycles of operation. In all runs a steady state was reached after an initial transient period of operation. The transients remained cyclic in nature for those runs with the smaller purge-to-feed ratios, longer cycle times, and higher feed flow rates. Purge-to-feed ratio (Figure 8) is seen to have no well defined effect on enrichment. Thus the enrichment with no purge (G = 0) is little different from that with substantial purge (G = 0.85). This is advantageous, for the fraction of the feed which is enriched is greater with G = 0. At G = 0 the depleted stream consists only of the blowdown. The

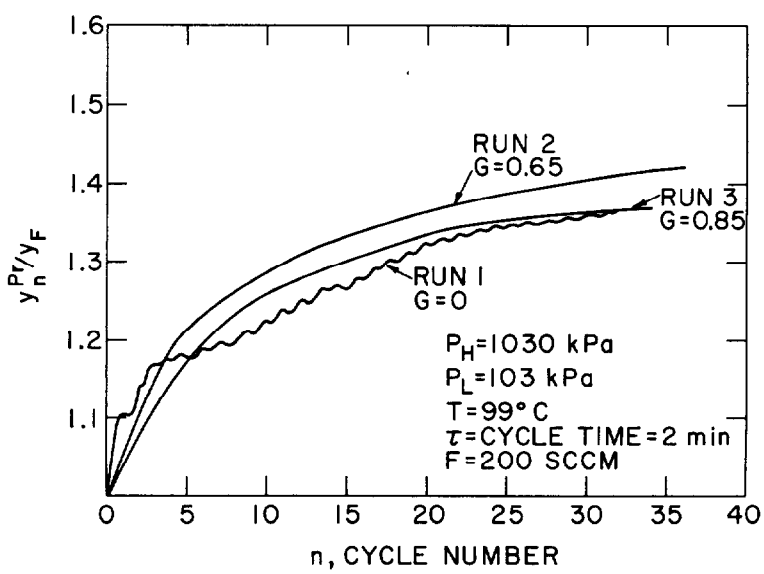

Figure 8. Transients in product concentration for heatless adsorption experiments conducted in the β phase: effect of purge-to-feed ratio.

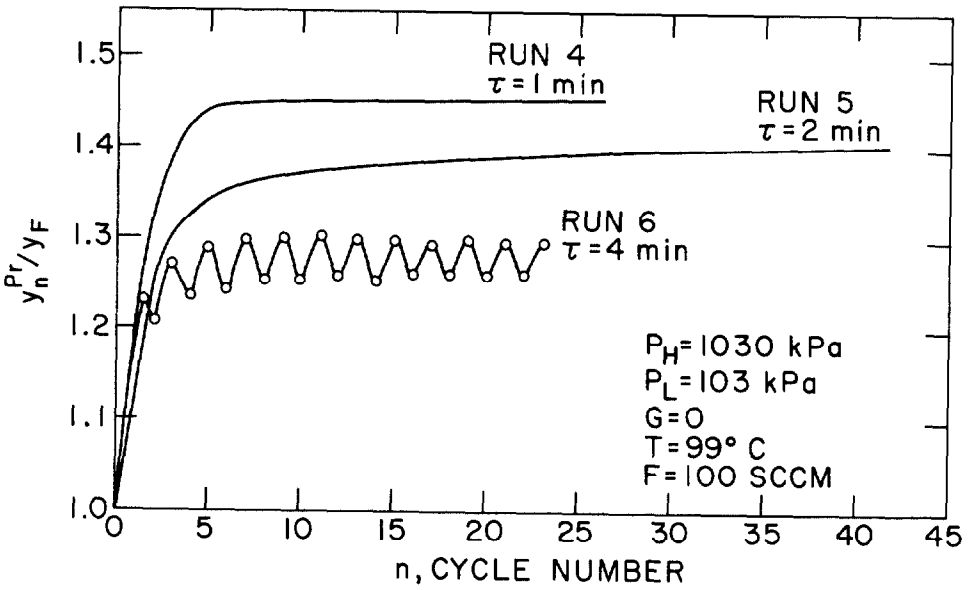

Figure 9. Transients in product concentration for heatless adsorption experiments conducted in the β phase: effect of cycle time.

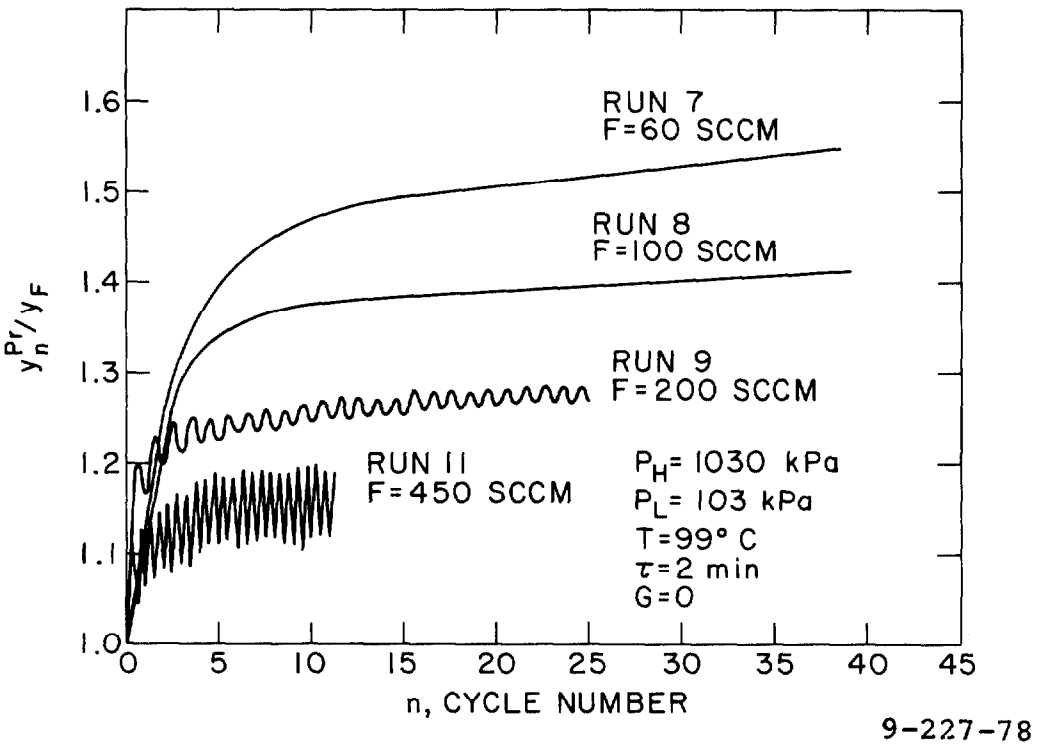

Figure 10. Transients in product concentration for heatless adsorption experiments conducted in the β phase: effect of feed flow rate.

blowdown in turn consists of the same volume of H_2 per cycle regardless of the value of G. Because of this fact the remaining experiments described for the β phase were all conducted with no purge.

Product enrichment increases as the cycle time decreases (Figure 9) and as the feed flow rate decreases (Figure 10). Data (not shown) for runs exploring the influence of variation of the high pressure and the temperature show that product enrichment increases with both variables but appears to approach a limit (∿45 percent) as the high pressure approaches 1400 kPa (∿200 psi).

The depletion in the blowdown was not measured because of experimental difficulty but the amount of the blowdown per cycle was measured. For Run 8, for instance, P_H = 1030 kPa, P_L = 103 kPa and T = 100°C, the blowdown amounted to 0.02 moles H_2, in good agreement with the value calculated from the pressure-composition isotherm. Using this value and the measured steady state enrichment in the product (1.41), we calculate the depletion of HT in the blowdown for a feed flow rate of 100 sccm to be 9 percent. The total quantity of product amounts to about 18 percent of the feed. Hydrogen and tritium balances for this run are shown in Table III. From this table it is apparent that recycle may be beneficial in increasing the amount of product enriched and in increasing the depletion in the blowdown. This possibility is being investigated.

Table III. Hydrogen and tritium balances in single phase operating mode (Run 8).

Stream		Moles H_2	Percent of feed	y/y_F
Product	$\frac{100 \text{ sccm} \times 1 \text{ min}}{22400}$	=0.0045	0.18	1.41
Purge		0.0	0.00	----
Blowdown		0.02	0.82	0.91
Total feed		0.0245	1.00	1.00

It should be noted that Runs 1 (Figure 8) and 9 (Figure 10) were conducted under nominally identical conditions and yet the ultimate enrichments obtained were noticeably different. The difference between them was that Run 1 was conducted with freshly activated beds whereas Run 9 was in fact conducted long after activation. This difference points up the fact that the beds deteriorate with use, probably as the result of introduction of impurities such as water vapor or oxygen which cause inactivation. Activation after every few runs was required to obtain good reproducibility.

Additional experiments are required to determine the origin of the inverse separation. A possible cause may be a kinetic isotope effect. Enrichment of the product stream may result if H_2 is more rapidly absorbed than HT. The inverse separation may well not be associated with the feed and purge steps in the process. This is because the time scales of the exchange reaction estimated from the chromatographic data discussed earlier are somewhat smaller than the

half-cycle times. Thus $\frac{\alpha}{2} K_{H_2}/(k_f^T C_H^*)$, the chemical reaction time in Equation (6), at 1030 kPa and 100°C is 17 s. From this result one would expect that exchange taking place during a half cycle of duration, say, 30 s or more, would be likely to take place under conditions near equilibrium. The inverse separation may therefore arise in the pressurization and blowdown steps. Those steps are known to occur very rapidly, perhaps in less than 1 s. A quantitative investigation of the rates of H_2 and HT absorption and desorption in these steps may disclose whether a kinetic isotope effect may give rise to the inverse separation. Tritium may be more slowly absorbed and desorbed than protium.

Two Phase Operating Mode. Experiments were conducted in this mode by using temperatures of 16° to 50°C and pressures in the range 100 to 1600 kPa (15 to 240 psi). Rates of absorption, desorption and exchange were known to be small in the γ phase and therefore cycle times of the order of 30 min to 1 hr were used.

This mode of operation did lead to depletion of tritium in the product stream as expected for the process and as predicted by equilibrium theory. The maximum depletion found in any run at steady state was 65 percent.

Transients in HT concentration in the product stream for runs conducted at 25°C are shown in Figures 11 and 12. The ordinate is the mole fraction ratio as before but the abscissa is the time of

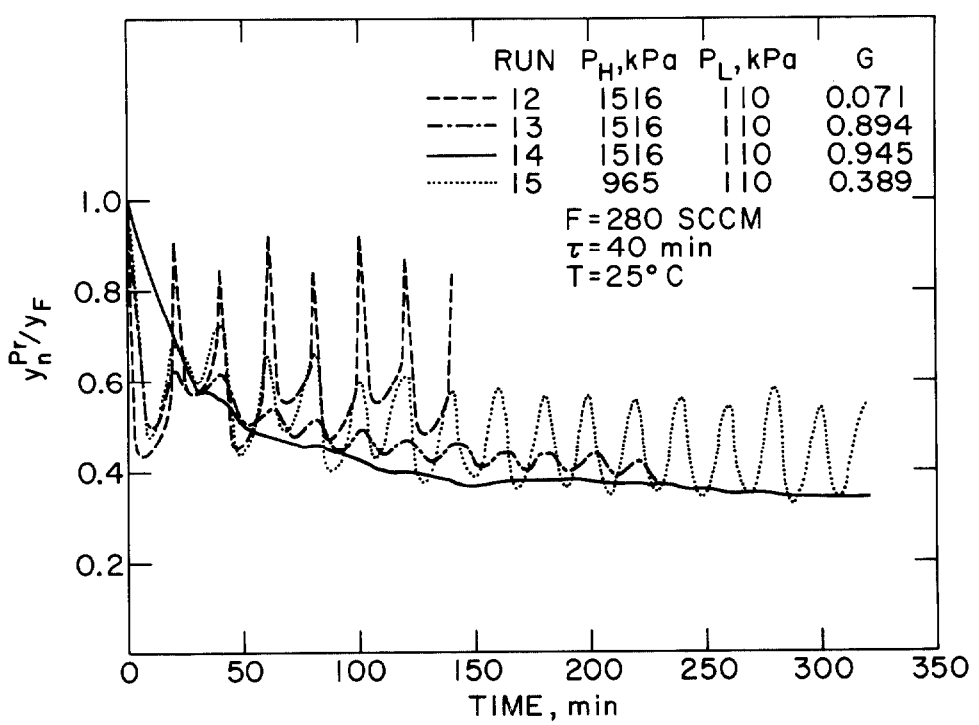

Figure 11. Transients in product concentration for heatless adsorption experiments conducted in the β and γ phases: effect of purge-to-feed ratio.

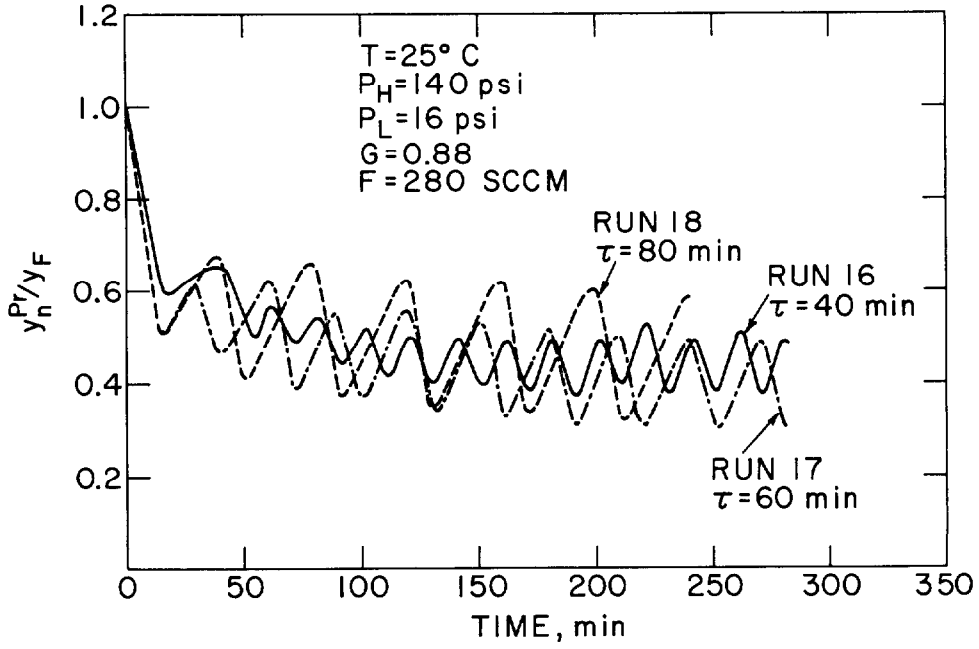

Figure 12. Transients in product concentration for heatless adsorption experiments conducted in the β and γ phases: effect of cycle time.

operation. In all cases a steady state is approached after an initial transient. In all runs but one (Figure 11, Run 14) a cyclic variation persists throughout the run. The effect of purge-to-feed ratio is shown in Figure 11. For G = 0.071 (Run 12) the sharp high peaks are regarded as indicative of incipient feed breakthrough into the product stream. Depletion in the product stream generally increases with increasing G. As indicated in the Theory section for P_H = 1000 kPa, P_L = 200 kPa, at 25°C, G_{crit} = 0.82. Therefore only for Runs 13 and 14 where G > 0.82 might complete removal of HT from the product stream have been expected. Even for these runs steady state non-zero concentrations were found. Concentration front spreading resulting from finite rates of exchange and from axial dispersion may have contributed to the failure to achieve complete HT removal.

The transients shown in Figure 12 indicate no dependence of depletion on cycle time for cycle times in the range 40 to 80 min.

Additional runs (data not shown) were made to examine the influence of temperature and high and low pressures. Little change in depletion was brought about by changes in these variables. The principal factors in these runs then were (a) cycling across the dissociation plateau and (b) purge-to-feed ratio. As long as the temperature and high and low pressures were such as to require cycling between the β and γ phases and as long as G was relatively high, significant depletion was found in the product stream.

While it was found possible to obtain depletions of HT in the product stream of up to 65 percent, at the same time the product stream represented a small fraction of the feed. Most of the feed was rejected as slightly enriched purge and blowdown gas. This circumstance may dictate as with single phase operation the use of recycle of most of the combined purge and blowdown streams, with the recycle stream being recompressed to the feed pressure. This concept is currently being explored.

As an example of the relative amounts of purified product and enriched purge and blowdown, consider Run 14, Figure 11. The amount of the blowdown gas per column per cycle calculated from the pressure-composition isotherm for the temperature and pressure conditions used and for the vanadium charge in a column is 0.536 moles H_2. A like amount of feed must be supplied during repressurization. During continous supply of feed at high pressure the amount of feed introduced per column per cycle is 280 sccm x 20 min = 5600 scc or 0.25 mole H_2. With G = 0.945 the number of moles of H_2 in the purge and product streams may be calculated. Hydrogen and tritium balances for the process are given in Table IV. The need for substantial recycle is apparent. Less recycle would be needed at smaller purge-to-feed ratios without great change in depletion.

Table IV. Hydrogen and tritium balances in two phase operating mode (Run 14).

Stream		Moles H_2	Percent of feed	y/y_F
Product	0.055 x 0.25 =	0.014	2	0.35
Purge	0.945 x 0.25 =	0.236	30	1.01
Blowdown		0.536	68	
Total feed		0.786	100	1.00

In addition to recycle another factor to be considered in the further development of a process based on the two phase operating mode is particle attrition. The large change in hydrogen content of the particles resulting from cycling between the β and γ phases can bring about substantial attrition after many cycles of operation. Indeed such attrition was found in the columns used in the present work. Attrition is commonly found in the cyclic operations employed in the use of metal hydrides in hydrogen storage. Much effort is currently being expended to overcome this problem.[19] Continued attrition in cyclic processes can lead to excessive pressure drop and to deformation of confining vessels if vessel design and operation do not properly allow for this phenomenon.

V. Summary and Concluding Remarks

1. An experimental study of the equilibrium and kinetics properties of hydrogen isotope exchange on vanadium hydride has been conducted. For hydrides made from commercial grade V, pressure-composition isotherms for the β and γ phases, HT-H_2 separation factors for the β phase, rates of HT-H_2 exchange for the β phase, and

axial dispersion coefficients have been determined.

2. An equilibrium theory of hydrogen isotope separation via heatless adsorption using vanadium hydride has been developed. Constants in the derived theoretical expressions were evaluated using the pressure-composition and separation factor data obtained as indicated above. The theory was then used to calculate process performance for HT-H_2 separation in two operating modes. In the single (β) phase mode, it was predicted that over a wide temperature range (100° to 250^oC) essentially no separation would be obtained. For the two (β-γ) phase mode, complete removal of HT from the product stream was predicted for purge-to-feed ratios ranging from 0.77 to 0.84 as the temperature increased from 0° to 40^oC. Overall enrichment in the combined purge and blowdown decreased from 2.06 to 1.34 for the same temperature range.

3. Experiments were conducted on the performance of heatless adsorption apparatus in separating HT-H_2 mixtures using vanadium hydride. In the single phase mode, enrichment in the product (up to 54 percent) was found whereas no change was expected. A kinetic isotope effect may be responsible for the inverse separation. Depletion in the product (up to 65 percent) was found as expected when operating in the two phase mode. For both modes of operation, performance may be enhanced by recycle of the combined purge and blowdown.

4. Future experimental work will involve study of rates of HT and H_2 absorption and desorption during blowdown and repressurization, investigation of the use of recycle, and examination of the efficacy of temperature cycling. Theoretical effort will be concentrated on the performance of temperature cycling processes and on the effect of finite rates of exchange. Completion of this work will make possible a conclusive assessment of the usefulness of hydrogen isotope separation via cyclic processes based on the use of vanadium hydride.

Notation

a	=	empirical constant in Equation (10)
A	=	z-coordinate of maximum penetration of fresh feed during pressurization
b	=	empirical constant in Equation (10)
B	=	fraction of tritium in gas phase
C_i	=	concentration of species i
C_H^H, C_H^L	=	concentration of hydrogen atoms in hydride particles at high and low pressures, respectively
D_{HT-H_2}	=	diffusion coefficient of HT in H_2
D_p	=	particle diameter
D_s	=	diffusion coefficient of tritium atoms in hydride particles

E_i = enrichment in stream i

$E(P_2,P_1)$ = exponential of right hand side of Equation (20)

E_z = axial dispersion coefficient

F = feed flow rates

$F(P_2,P_1)$ = exponential of right hand side of Equation (21)

G = fraction of feed introduced during high pressure flow step which is rejected as purge

h = packed height of column

I_f = forward kinetic isotope effect

k_f^H, k_r^H = forward and reverse rate constants for reaction (8)

k_f^T, k_r^T = forward and reverse reaction rate constants for reaction (4)

k_g = gas phase mass transfer coefficient

K_{H_2} = hydrogen distribution coefficient

L = penetration distance of HT concentration front

n = number of cycles of heatless adsorption process

r = the minimum non-negative number such that $(1+r)L_L - rE(P_H,P_L)L_H \geq h$

p_{mm} = hydrogen pressure, mm Hg

P = hydrogen pressure

q = a number such that $(r+q)[L_L - E(P_H,P_L)L_H] = h - E(P_H,P_L)L_H$

r_p = particle radius

R = gas constant

R_{ex} = rate of reaction (8)

S = column cross sectional area

t = time

t_0 = pulse duration

T = temperature

Δt = half cycle duration

u = superficial gas velocity

y = mole fraction of HT in H_2

z = axial distance coordinate

Greek Letters

α = HT-H_2 separation factor

ε = bed void fraction

θ = h/u, bed residence time

μ_1' = first absolute moment (mean)

μ_2 = second central moment (variance)

ρ = hydrogen-to-vanadium atom ratio

ρ_s = density of vanadium hydride

τ = cycle time

Superscripts

* = pertains to surface

Pr = product

Pg = purge

Subscripts

b = blowdown

crit = critical

F = feed

H = high

L = low

n = pertains to n-th cycle

ov = overall

Pg = purge

References

1. Wong, Y. W. and F. B. Hill, "Equilibrium and kinetics studies of hydrogen isotope exchange on vanadium hydride," submitted to A.I.Ch.E. Journal.

2. Reilly, J. J. and R. H. Wiswall, Jr., "The reaction of hydrogen with alloys of magnesium and copper," Inorg. Chem. 6, 2220 (1967).

3. Reilly, J. J. and R. H. Wiswall, Jr., "The higher hydrides of vanadium and niobium," Inorg. Chem. 9, 1678 (1970).

4. Reilly, J. J. and R. H. Wiswall, Jr., "The effect of minor constituents on the properties of vanadium and niobium hydrides," Brookhaven National Laboratory Report BNL 16546 (1972).

5. Mueller, W. M., J. P. Blackledge, and G. G. Libowitz, "Metal hydrides," Academic Press, New York, p. 601 (1968)

6. Ebisuzaki, Y. and M. O'Keeffe, "The solubility of hydrogen in transition metals and alloys," Prog. Solid State Chem. 4, 187 (1967).

7. Melander, L., "Isotope effects on reaction rates," The Ronald Press Company, New York (1960).

8. Schober, T. and H. Wenzl, "Structures, phase diagrams, phase morphologies and preparation methods of V-, Nb-, and Ta-hydrogen systems," in Alefeld, G., ed., "Hydrogen in metals," to be published by Springer-Verlag, Berlin.

9. Wiswall, Jr., R. H. and J. J. Reilly, "Inverse hydrogen isotope effects in some metal hydride systems," Inorg. Chem. 11, 1691 (1972).

10. Tanaka, J., R. H. Wiswall, and J. J. Reilly, "Hydrogen isotope effects in titanium alloy hydrides," Inorg. Chem. 17, 498 (1978).

11. Schneider, P. and J. M. Smith, "Adsorption rate constants from chromatography," A.I.Ch.E. Journal 14, 762 (1968).

12. Scholten, J. J. F. and J. A. Konvalinka, "Hydrogen-deuterium equilibrium and parahydrogen and orthodeuterium conversion over palladium: kinetics and mechanism," J. Catalysis 5, 1 (1966).

13. Flanagan, T. B., "Kinetics of hydrogen absorption and desorption," presented at the International Symposium on Hydrides for Energy Storage, Norway (1977).

14. Shendalman, L. H. and J. E. Mitchell, "A study of heatless adsorption in the model system CO_2 in He, I," Chem. Eng. Sci. 27, 1449 (1972).

15. Pigford, R. L., B. Baker, III, and D. E. Blum, "An equilibrium theory of the parametric pump," Ind. Eng. Chem. Fundamentals 8, 144 (1969).

16. Chen, H. T. and F. B. Hill, "Characteristics of batch, semi-continuous and continuous parametric pumps," Separation Sci. 6, 411 (1971).

17. Chan, Y. N. I., F. B. Hill, and Y. W. P. Wong, "Equilibrium theory of heatless adsorption," in preparation.

18. Bernstein, W. and R. Ballantine, "Gas phase counting of low energy betz-emitters," Rev. Sci. Instr. 21, 158 (1950).

19. Strickland, G., T. Milau, and Wen-Shi Yu, "The behavior of iron titanium hydride: long term effects, heat transfer and modeling," Brookhaven National Laboratory Report BNL 20876.

DISCUSSION

CHOI: This process can be best used in detritiating reactor water which usually has tritium oxide in parts per million range; is there any variation in the separation (decontamination) factor with the inlet concentration in that range?

WONG: The concentration level of tritium used in our elution chromatography experiment was $\sim 10^{-6}$ Ci/cm^3. The separation factors obtained agreed quite well with those obtained in a batch reactor in which the tritium level was about one order of magnitude higher. However, it is a good idea to investigate further the concentration effect on the separation factor.

KNECHT: What do you see as a commercial application of this method? An estimate of the scale required for a D_2O reactor or reprocessing plant water clean-up system would be useful.

WONG: This process has the potential to recover deuterium or tritium from a hydrogen stream with the protium being used in an ammonia synthesis process to make the economics of one process more attractive. This process is useful in decontaminating tritiated water from nuclear reactors. First, the water has to be split into hydrogen and oxygen by an electrolytic process. The hydrogen then can be separated by this process. Finally, the concentrated tritium can be stored as stable tritides for safe disposal. We are now working on a single stage process. Multiple-stage processes will be investigated in the future. At that time, scale of operation and economic feasibility will be looked at.

STUDY ON THE TRITIUM REMOVAL FROM THE SODIUM IN LMFBR

K. Hata, Y. Nishizawa, Y. Osawa
Mitsubishi Atomic Power Industries, Inc.
Omiya, Japan

Abstract

Removal of tritium in the sodium coolant of LMFBR, is important for achieving the release of radioactivities as low as reasonably achievable. It is well known that cold trap should be an effective method for controlling tritium in sodium. To develop an effective tritium trapping system with "reactive getter (chemical trap)", in-sodium hydrogen absorption behavior has been studied.

The absorption experiment was conducted by dipping some test materials into sodium on which cover gas was composed of an $Ar-H_2$ mixture. Hydrogen analysis and metallographic examination for the test materials were made after the experiment.

From these experiments, it was concluded that Yttrium canned with Nickel or Niobium was the most suitable as "reactive getter". Further investigation to develop the "chemical trap" made from these materials for practical application has been in progress.

I. Introduction

Tritium is produced in LMFBR core by three primary mechanisms; (1) ternary fission of the fuel, (2) activation of boron in the B_4C control rods, and (3) activation of boron and lithium impurities presented in the fuel and sodium. Most of the tritium generated in the reactor core, is expected to be released into the coolant sodium. For achieving the release of radioactivities to the environment as low as reasonably achievable, tritium is one of the most difficult radioactive isotopes to control in LMFBR. Because, as an isotope of hydrogen, it diffuses easily through the structural materials at the LMFBR temperatures.

Cold trap is well known to be an effective method in containing tritium and preventing its release. Although this method is employed efficiently, however, it is estimated that a considerable amount of tritium would be released[1].

For the purpose of developing a tritium trapping method with "reactive getter", which should be more effective than the usual cold trap method, the screening test of the materials which might be suitable as the getter, has been performed.

This paper discribes the results of the test for some materials, with respect to their in-sodium hydrogen absorption behavior and their feasibility as the getter.

II. Principle of Chemical-Trapping Method

In the sodium-hydrogen system, the solubility of hydrogen in sodium has been recently reported by D. R. Vissers et al.[2], as follows.

$$S = 1.0 \times 10^{-3} \exp\left(-\frac{6550}{T} + 61.52\right) \quad \{\text{atoms-H/g-Na}\} \qquad (1)$$

Subsitution of a cold trap temperatures (°K) for T in equation (1) gives the minimum hydrogen concentrations in sodium that can be attained by the cold trap method. For example, it is shown in FIG.2 that they come to $\sim 1 \times 10^{17}$ (atoms-H/g-Na) when cold trap is controlled at 150 °C.

In the unsaturated solution ranges of the Na-H system, equilibrium would be established between hydrogen in gas phase and hydrogen in solution;

$$\frac{1}{2} H_2 \text{ (gas)} \rightleftarrows \underline{H} \text{ (in solution in Na)} \qquad (2)$$

The equilibrium can be expressed by the following equation;

$$C = K \cdot P^{\frac{1}{2}} \qquad (3)$$

where C: concentration of hydrogen in the solution
K: Sievert's constant
P: hydrogen pressure

Equation (3) is known as Sievert's law which states that the solubility of hydrogen in sodium is proportional to the square root of the hydrogen pressure. The Sievert's constant for the sodium-hydrogen system was reported as follows, and to be unsensitive to small variation in temperature[3].

$$K = 8.3 \times 10^{19} \quad \{(\text{atoms-H/g-Na})/(\text{atm})^{\frac{1}{2}}\} \text{ at } 450°C \qquad (4)$$

In a metal-hydrogen system, if the system forms hydride phase, pressure-composition isotherms such as those shown in FIG. 1 are generally obtained.

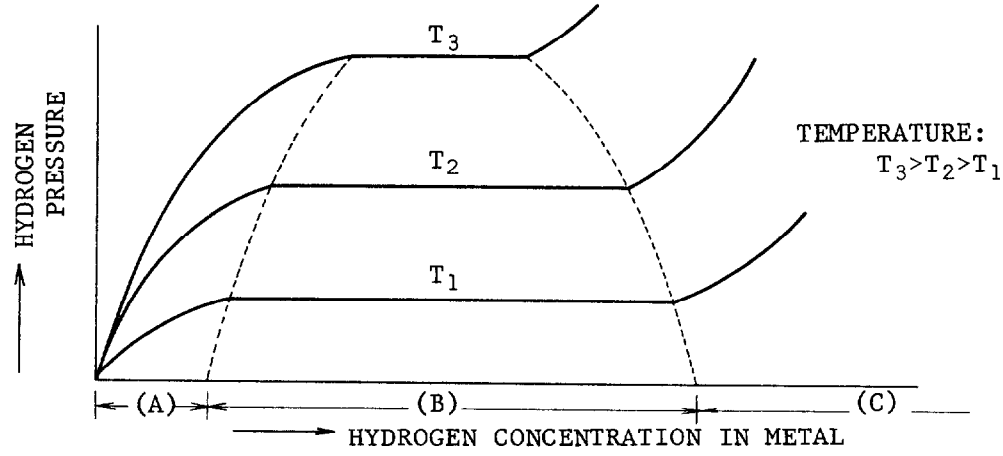

FIGURE 1 GENERAL PRESSURE - COMPOSITION ISOTHERMS FOR AN M-H SYSTEM

In FIG. 1 the region (A) shows solid solution of hydrogen in a metal, and the region (B) shows 2-phase coexistence of saturated solid solution and a hydride. In the plateau-pressure region (B), log P vs. 1/T can be expressed in the following equation which is sometimes called Van't Hoff isochore.

$$\log P = -\frac{A}{T} + B \tag{5}$$

where P: hydrogen dissociation pressure
T: temperature (°K)
A, B: constants
A and B in equation (5) have been reported in many metal-hydrogen system[4].

If a metal, which has a strong tendency to combine with hydrogen and accordingly exibits a low hydrogen plateau-pressure, were sufficiently added to the sodium-hydrogen system at temperature T_1, some hydrogen in solution in sodium would be removed into the metal to form the hydride. Finally, equilibrated hydrogen concentration in the sodium can be calculated from equation (3), (4), (5), as follows.

$$C_1 = K \cdot 10^{\frac{1}{2}(-\frac{A}{T_1} + B)} \tag{6}$$

This is the principle which chemical trap method is based on. The graphs, log C vs. 1/T for some metals, which form stable hydribes, are shown in FIG. 2 together with the hydrogen solubility curve of equation (1).

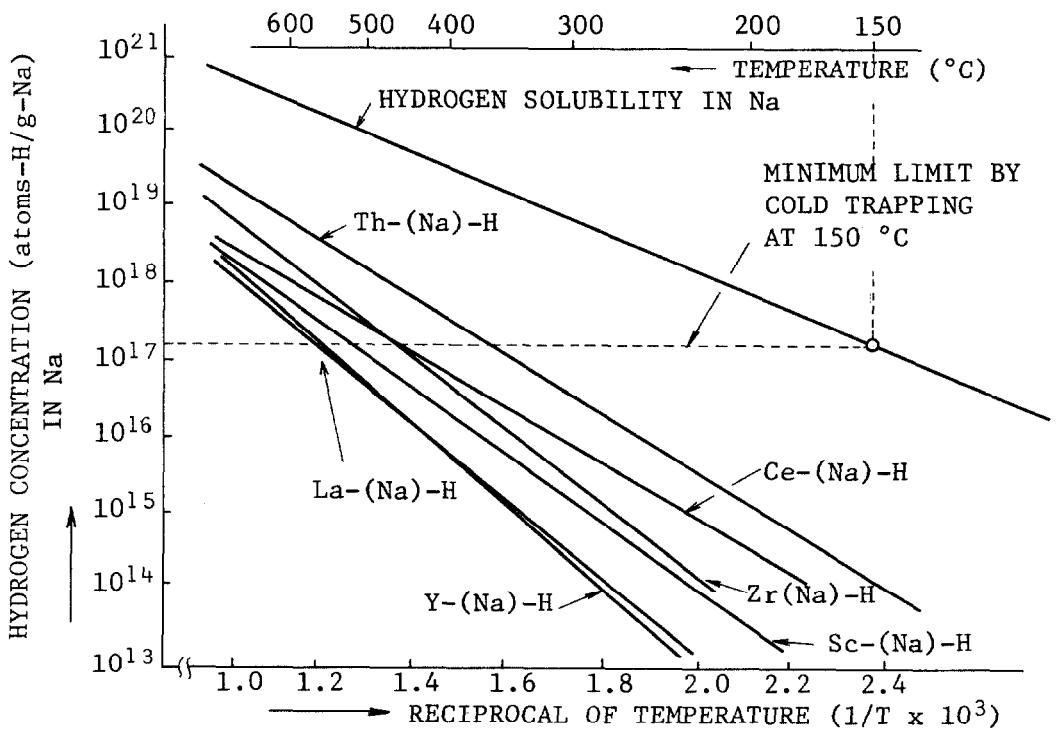

FIGURE 2
CALCULATED HYDROGEN CONCENTRATION vs. RECIPROCAL OF TEMPERATURE FOR SOME HYPOTHETICAL M-Na-H EQUILIBRIUM SYSTEM

III. Experimental

Apparatus

The apparatus for the in-sodium hydrogen absorption experiment is shown in FIG. 3. The main constituents were a charge tank (160 dia. x 230 height), a test tank (160 dia. x 230 height) and piping/valves (21.7 dia.). The electric heating system and the cover-gas supply/evacuate system were also attached. The apparatus was composed entirely of 304 stainless steel except for zirconium-foil arranged in the charge tank.

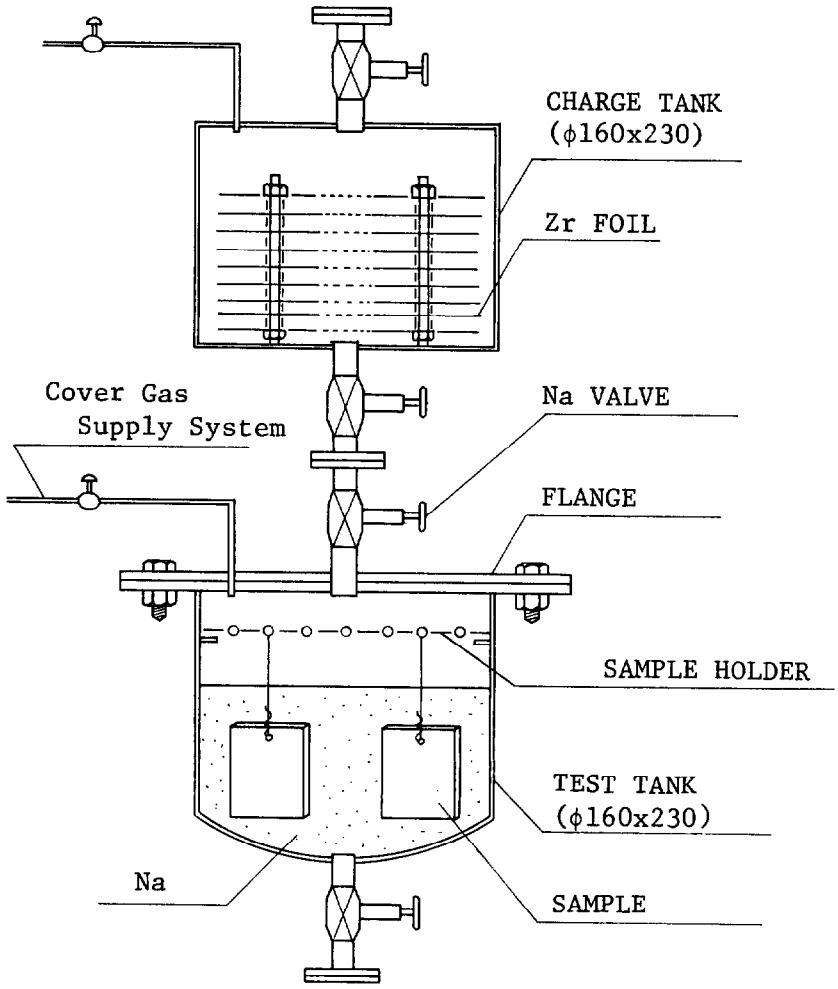

FIGURE 3
EXPERIMENTAL APPARATUS

Sample Preparation

Test materials for the experiment were selected in consideration of their hydrogen affinity, their compatibility with hot sodium, and their availability.

Titanium (Ti) exhibits a wide solid solution region (∿ 10 at %H, at 300 ∿ 600 °C), and is often used as good hydrogen absorbent. Zirconium (Zr) is a stable hydride former. (See FIG. 2) Ti and Zr are commonly available and compatible with hot sodium. Ti and Zr have a tendency to be oxidized in sodium which contains some oxygen. Generally surface oxide film is known to sometimes interfere, and/or reduce the permeation of hydrogen. Therefore, to examine an effect of surface oxide film on hydrogen absorption, we prepared, as test samles, Ti/Zr with and without surface oxide film, respectively.

Yttrium (Y) and cerium (Ce) as well as other rare earth metals, although they have attractive property of forming very stable hydrides (see FIG. 2), are hardly compatible with hot sodium. By this reason, they can't be used in direct contact with hot sodium. Modifying this poor compatibility by the methods of alloying or canning, we prepared the test samples of Ti-5 % Ce alloy and of Y canned with Ni. Ni is compatible with hot sodium and through Ni, hydrogen can easily permeate at high temperature. The test samples prepared for the experiment are summarized as follows and are also shown in FIG. 4.

(Test Samples)
(1) Ti
(2) Ti with oxide film (0.3μ thickness)
(3) Zr
(4) Zr with oxide film (0.2μ thickness)
(5) Ti-5 % Ce alloy
(6) Y canned with Ni

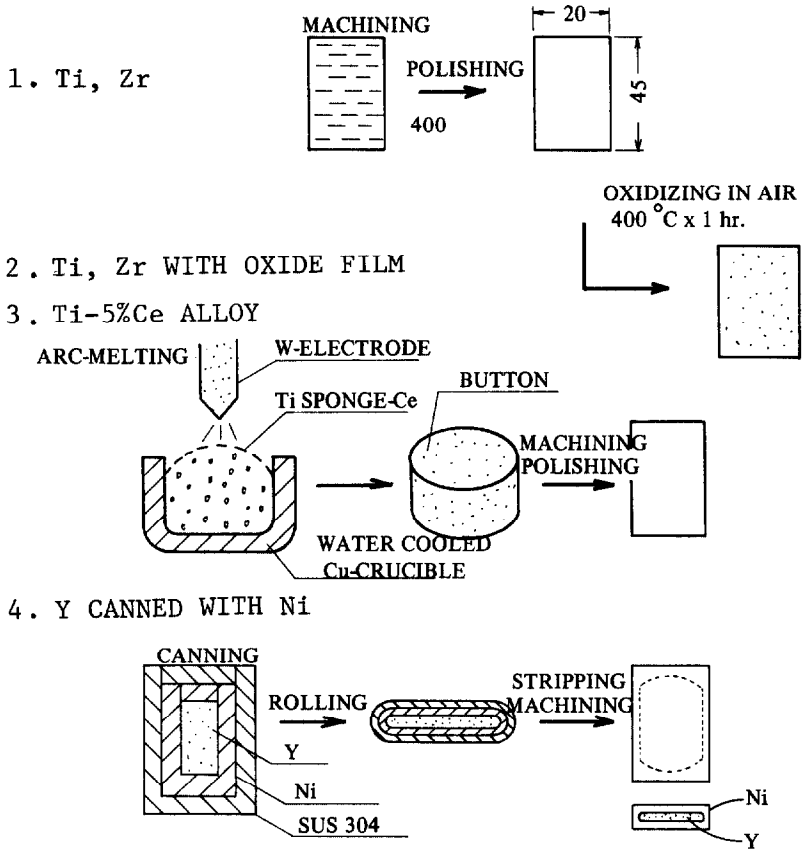

FIGURE 4
TEST SAMPLES PREPARATION

From the results of those experiments, Y canned with Ni was expected to be very attractive as getter materials. To accumulate more data on the hydrogen absorption behavior of these canning materials, additional in-sodium hydrogen absorption experiments of which test samples were composed of Ce or Y for meat and Ni or Nb for cladding has been performed. Test sample for the additional experiments is shown in FIG. 5.

i.	Y	Canned with	Ni
ii.	Ce	"	Ni
iii.	Y	"	Nb

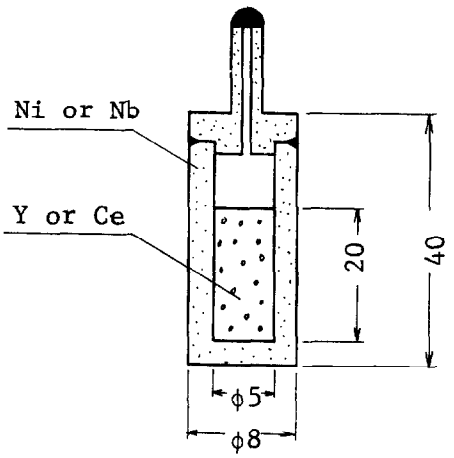

FIGURE 5
TEST SAMPLE FOR ADDITIONAL EXPERIMENTS

In-sodium Hydrogen Absorption

Test samples were hanged with small wire (SUS 304) from the holder in the test tank. (see FIG. 3) Sodium was poured from the charge tank into the test tank. Then cover-gas was replaced from a pure Ar to an Ar-H_2 mixture gas. Then, in-sodium hydrogen absorption experiments were conducted at constant temperature.

The experimental parameters were summarized in Table I.

Table I Experimental parameters

Dipping Temperature (°C) \ Dipping Time (Hr.)	100	200	400
350	*	*	*
450	*	*	*
550	*	-	-

*: conducted
-: not conducted

(Additional experiments)
° Dipping Temperature (°C): 500
° Dipping Time (hr): 74, 170, 510, 820

Sodium. Prior to the in-sodium hydrogen absorption experiment, the sodium was purified at 600 °C for 100 hr in the charge tank, where zirconium-foil was arranged as getter. The sodium inventory was 2.5 Kg and the surface area of the foil was 7×10^3 cm^2. By this purification treatment, most impurities contained in the sodium (such as O, N, C, H) have been removed.

Cover-gas. $Ar-H_2$ mixture gas was used for the in-sodium experiment, so as to keep the hydrogen concentrations in sodium at constant values. The compositions of the $Ar-H_2$ mixture gas were shown in Table II. The pressure of cover gas was kept at 0.1 (Kg/cm^2. gauge) thoughout the experimental periods. Therefore, hydrogen concentrations in the sodium were supposed to be as follows for all the experimental periods.

$$C = K \cdot P^{\frac{1}{2}} \simeq 4 \times 10^{17} \qquad \{\text{atom-H/g-Na}\}$$

Table II Ar-H_2 mixture gas composition

Argon	99.9 % up
Hydrogen	$23.9^{\pm 1}$ p.p.m. (for additional experiments) $19.3^{\pm 1}$ p.p.m.
Oxygen	<1 p.p.m.
Moisture	<1 p.p.m.

Examination

After the experiments, sodium in the test tank was drained off and the samples were drawn up from the tank. They were completely washed by ethylalchol and demineralized water to remove the stuck sodium. Then, the samples were examined as follows.

(1) surface observation and weight change measurement
(2) metallographic examination
(3) hydrogen analysis

IV. Results

Surface observation

Throughout the experiments, the samples of Ti, Zr, and Ti-Ce Alloy considerably reduced their initial metallic luster, respectively. The samples of Ti/Zr with oxide film also reduced their luster of light-brownish color. Ni had essentially no changes in its aspect. By additional experiments, Nb turned its surface color from metallic gray to blackish gray, perhaps by oxidation.

The weight changes of test samples were plotted as the function of dipping time and temperature, shown in FIG. 6, 7, 8. From these figures and surface observation mentioned above, it was concluded that the compatibility of all tested materials with hot sodium

(350 ∿ 550 °C) seemed to be good. Nb exhibited a relatively high weight gains, perhaps through its oxidation, but as the oxide film formation rate was about 10μ/200 hr. for initial period and seemed to obey in parabolic law (see FIG. 8), therefore Nb might be also feasible in hot sodium (500 °C) for this application.

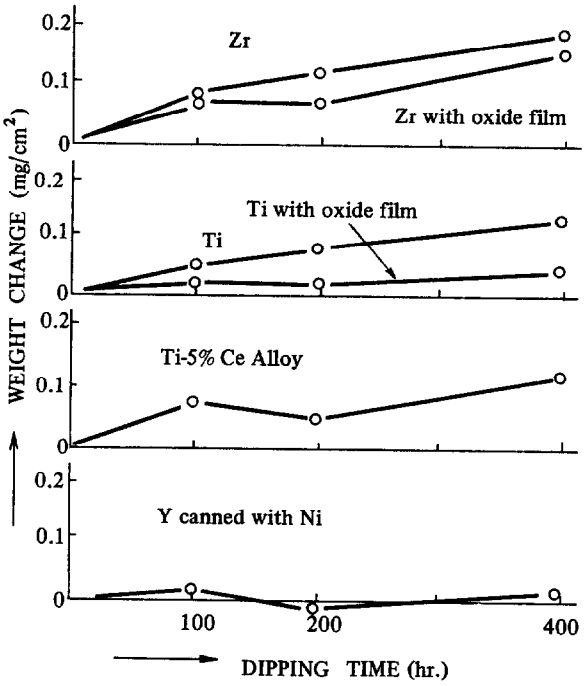

FIGURE 6
WEIGHT CHANGE
(Sodium Temp. = 450 °C)

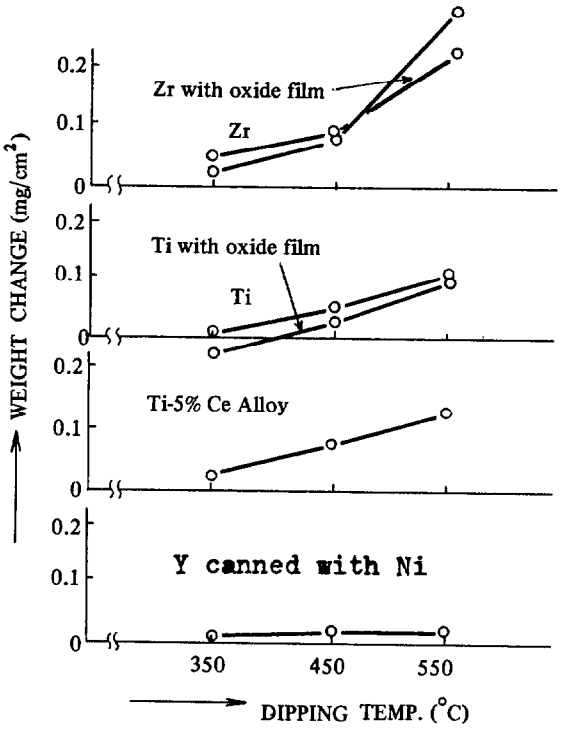

FIGURE 7
WEIGHT CHANGE
(Dipping Time = 100 hr.)

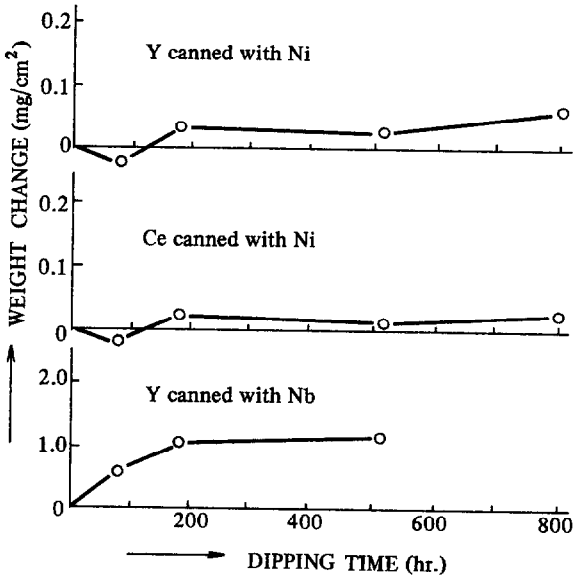

FIGURE 8
WEIGHT CHANGE
(Sodium Temp. = 500 °C)

Metallography

For those samples of Ti, Zr with/without an oxide film on the surface, and of Ti-Ce Alloy, there were little changes in their microstructures throughout the in-sodium hydrogen absorption experiments. As for Ni, there were no changes in its microstructure.

In additional experiment, at the outer surface of the samples (Na-Ni or Na-Nb interfaces), there were no changes in their microstructures. On the other hand, at the inner surface of the samples composed of Y (Y-Ni or Y-Nb interfaces), there were little changes in their microstructures of Ni and Nb, but at the inner surface of the samples of Ni-Ce couple there exhibited a considerable interation between Ce and Ni. This is shown in PHOTO.1. It can be seen that Ce was aggressive upon Ni at tested temperature (500 °C), causing a matrix attack and an intergranular attack.

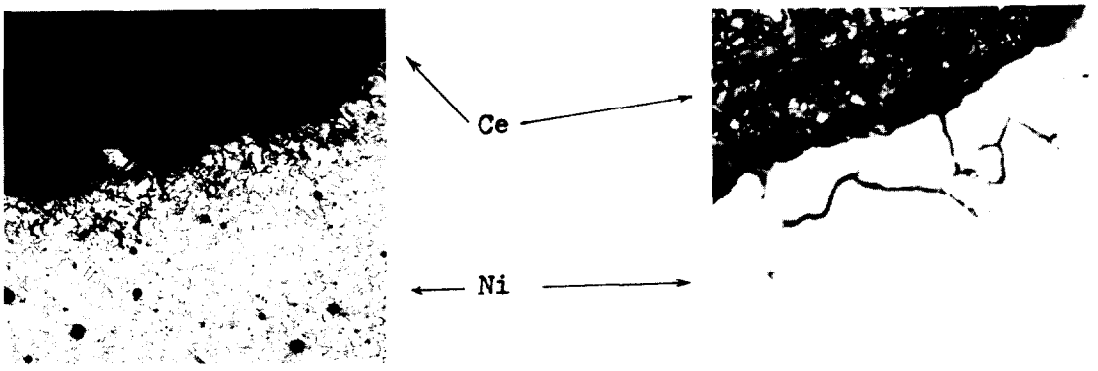

(x75) (x600)

PHOTO. 1
MICROSTRUCTURE OF Ni CONTACTED WITH Ce

This result is also supported by the phase diagram of Ni-Ce, in FIG. 9 which shows that Ni-Ce system forms an eutectic compound with low melting points (455 °C). The same behavior would be also shown between Ni and the other lanthanide elements which form the stable hydrides.

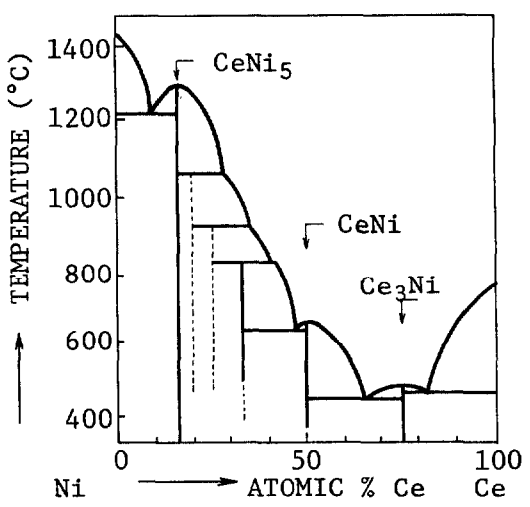

FIGURE 9
Phase Diagram for Ni-Ce

Through the experiments, Y and Ce had a tendency to be pulverized, perhaps forming a hydride phase.

From these results of metallographic examination together with those results of weight change measurements, it was concluded that Ti, Zr, Ti-Ce Alloy and canning materials which were composed of Y or Ce (also other lanthanide elements) for meat and Ni or Nb for cladding were all excellent in the view point of compatibilities, except for Ni-Lanthanide couples.

Hydrogen Analysis

Hydrogen analyses were conducted on the samples of pre-, and post-,in-sodium hydrogen absorption experiments by using the vacuum-outgassing technique.

Those results were plotted versus dipping time and dipping temperature, shown in FIG. 10, 11. The results of Ti-Ce Alloy sample were not included there, because they were so scattered perhaps due to its high initially absorbed gas contents.

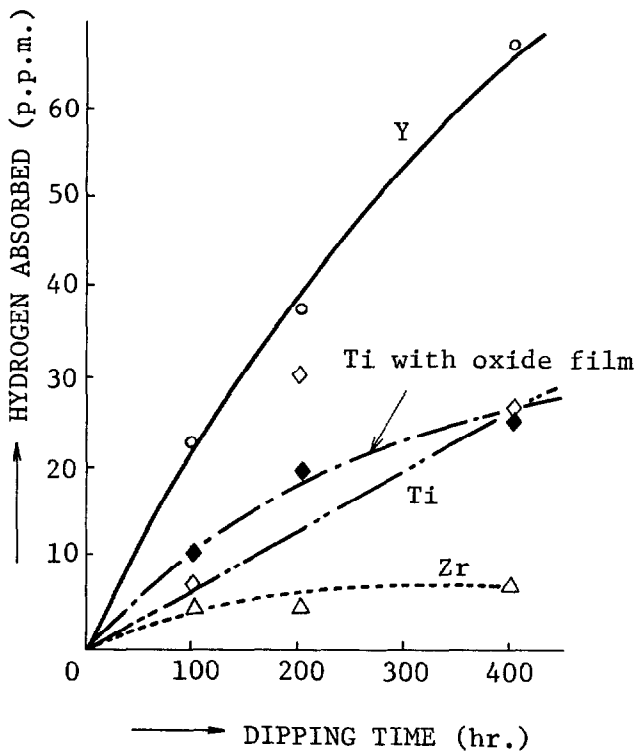

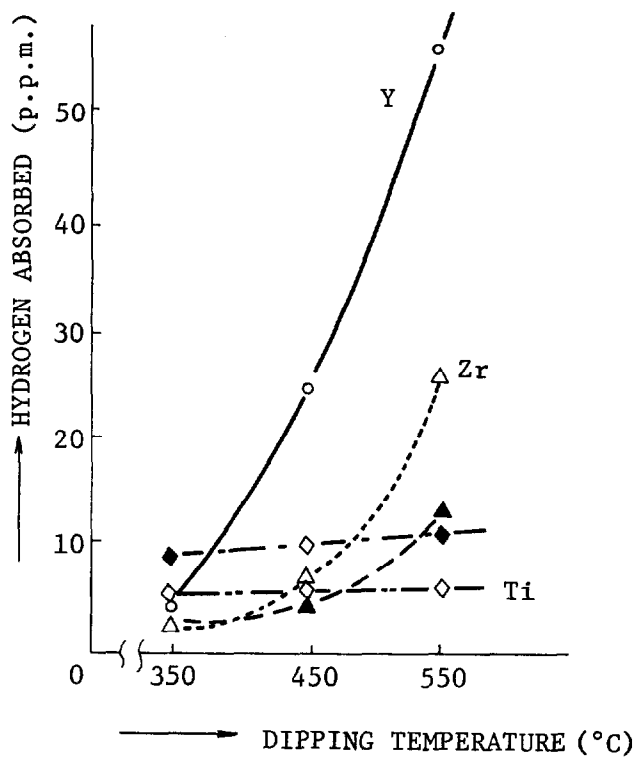

LEGNED
- ○ ..... Y canned with Ni
- △ ..... Zr
- ▲ ..... Zr with oxide film
- ◇ ..... Ti
- ◆ ..... Ti with oxide film

FIGURE 10
HYDROGEN ABSORPTION BEHAVIOR
(Dipping Temp. = 450 °C)

FIGURE 11
HYDROGEN ABSORPTION BEHAVIOR
(Dipping Time = 100 hr.)

As can be seen from FIG. 10, 11, Y canned with Ni is expected to be very attractive as "hydrogen getter". Although Zr absorbed a considerable amount of hydrogen at 550 °C, but as shown in FIG. 2, minimum attainable hydrogen concentration in sodium is nearly equal both in case of using the Zr getter (550 °C) and the cold trap (150 °C). Accordingly Zr seemed to be not so attractive as "hydrogen getter".

Hydrogen contents were also analyzed of the additional experiments which have been conducted on the materials of Y-Ni, Y-Nb, and Ce-Ni couples at temperature 500 °C. The results are shown in FIG. 12.

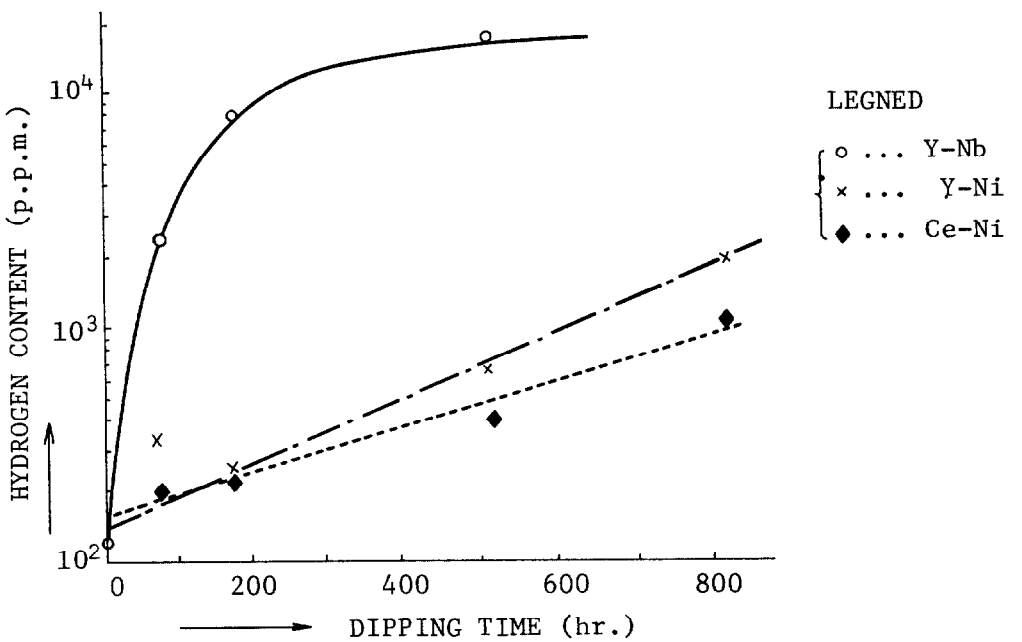

FIGURE 12
HYDROGEN ABSORPTION BEHAVIOR
(Sodium Temp. = 500 °C)

From FIG. 12, it can be seen that: Hydrogen absorption rates of Y and Ce are not decreased with increases of hydrogen contents by absorption. Y canned with Nb is shown to be saturated at the value of 2 x 10^4 p.p.m. hydrogen. This is nearly coincident with $YH_{1.9}$ which is yttrium dihidride exhibited by Y-H phase diagram, shown in FIG. 13.

The difference of hydrogen absorption rate between Y-Nb and Y-Ni would be due to the hydrogen permeation rates though Nb and Ni. i.e., through Nb, it is much higher than through Ni by 1 ∿ 2 order of magnitude at those temperatures.

From these experiments, it was concluded that Y canned with Ni or Nb would be the most suitable as "hydrogen (tritium) getter" in sodium.

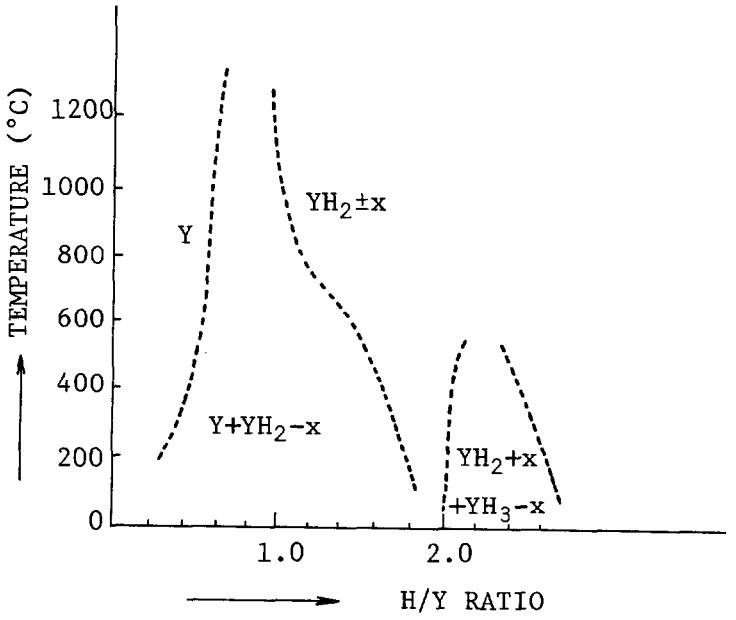

FIGURE 13
PHASE DIAGRAM FOR Y-H

V. Conclusion

(1) Chemical trap with reactive getter was found to be a promising method for the tritium removal in sodium coolant of LMFBR.

(2) Chemical trap with Y is expected to reduce the tritium concentration in sodium to more than one order of magnitude lower, as compared with cold trap. This means that tritium releases from the primary sodium coolant would be also lowered by more than one order of magnitude. Y getter has a so much capacity as absorbing hydrogen to about 2 wt. % of the Y. Further it would be more safe and easy to manage the "spent chemical trap", compared with that of cold trap.

(3) Chemical trap is also applicable for hydrogen removal in sodium of secondary coolant of LMFBR and for tritium removal in lithium coolant of CTR.

(4) For Nb, as canning material, indeed it is superior in hydrogen permeation, but it is necessary to be more investigated in compatibility study because it has a tendency to be oxidized in sodium solving some oxygen.

Developing the chemical trap for practical application, more quantitative informations are necessary. Further developments are in progress to accumulate the more quantitative data and informations on practical application of the tritium trapping system.

Acknowledgment

This work was performed under contract with Power Reactor and Nuclear Fuel Development Corp. (PNC).

The authors wish to express their appreciations to Dr. K. Mochizuki, senior engineer, FBR Development Project (PNC), and Mr. K. Akagane, assistant senior engineer, FBR Development Project (PNC), for their valuable suggestions. Technical contritutions from K. Kasahara, T. Kamei, H. Taki are gratefully acknowledged.

References

1. Erdman C.A., "Radionuclide production, transport, and release from normal operation of LMFBRs" EPA-520/3-75-019, November 1975

2. D. R. Vissers, J. T. Holmes, L. G. Bartholme and P. N. Nelson, J. Nuclear Technology Vol. 21, March 1974

3. R. Kumar, "Tritium transport in an LMFBR" ANL-8089, August 1974

4. W. H. Meuller, J. P. Blackledge, G. G. Libowitz, "Metal Hydrides" 1968

MONITORING AND REMOVAL OF GASEOUS CARBON-14 SPECIES

M.J. Kabat
Ontario Hydro
Health Physics Department
Toronto, Ontario

Abstract

A simple and efficient method was developed for the monitoring of low level carbon-14 in nuclear power station areas and gaseous effluent. Gaseous carbon compounds (hydrocarbons and CO) are catalytically oxidized to CO_2, which is then absorbed on solid $Ca(OH)_2$ at elevated temperatures. The ^{14}C collected is quantitatively liberated by thermal decomposition of $CaCO_3$ as CO_2, which is either measured directly by flow-through detectors or absorbed in alkali hydroxide followed by liquid scintillation counting.

The method can also be used for the removal of gaseous ^{14}C. The $Ca^{14}CO_3$ can be immobilized in concrete for long term disposal. $Ca(OH)_2$ is an inexpensive absorber. It is selective for CO_2 and has high capacity and efficiency for its absorption and retention.

A theoretical evaluation of the optimum conditions for CO_2 absorption and liberation is discussed and experimental investigations are described. There is good agreement between theoretical predictions and experimental findings.

I. Introduction

With the growth of the nuclear industry throughout the world, there is increasing concern with the global and regional impact associated with the discharge of long-lived radionuclides. Carbon-14 is one of the most significant radionuclides in this group. Considerable efforts have been made in industrial countries in the last decade to determine its global impact, emission standards, monitoring and control techniques and adequate long term disposal. In CANDU, power stations nitrogen gas has been removed from the annulus between pressure and calandria tubes in all recently built reactors, but a significant amount of ^{14}C is still produced in moderator systems. Therefore, a project is currently in progress in the Ontario Hydro Health Physics Department to develop adequate techniques for monitoring and control of ^{14}C in power station systems, areas and effluents with the prospect of its safe long term disposal.

II. Carbon-14 Production and Releases from Nuclear Facilities

Production Rates

Carbon-14 is produced in nuclear reactors by neutron activation of N, O and C in the coolant and moderator and impurities in reactor systems and components. The basic reactions are:

$$^{17}O\ (n,\alpha)\ ^{14}C$$
$$^{14}N\ (n,p)\ ^{14}C$$
$$^{13}C\ (n,\gamma)\ ^{14}C$$

The yield of ^{14}C from other reactions is negligible.

Major sources of ^{14}C in CANDU reactors are the moderator system (large quantity of D_2O) and the nitrogen filled annulus gas systems. Carbon-14 production rates calculated for two operating CANDU power reactors, 540 MWe units at the Pickering NGS and 750 MWe units at the Bruce NGS are listed in Table I with data on ^{14}C production in other reactors derived by W. Davis Jr. in publication (1). The CANDU production rates were calculated from core-averaged Westcott fluxes and 200 m/s cross-sections of 0.235 b, 1.81 b, and 0.9 mb respectively for the above reactions.

Table I
Estimated Production Rates of ^{14}C in Various Reactor Types

Reactor	Carbon-14 Production Rates - Ci/GWe-yr			
	Coolant	Other Systems - Ci/GWe-yr		Fuel (Average Values)
CANDU - 540 MWe	9	Moderator D_2O	440	15
		N_2 Annulus System	430	
750 MWe	10	Moderator D_2O	547	20
		CO_2 Annulus System	0.02	
BWR	4.7	Cladding & Struct. Mater.	43.3-60.4	17.6
PWR	5.0	Cladding & Struct. Mater.	30.5-41.6	18.8
LMFBR	nil	Cladding & Struct. Mater.	12.8	6.3
HTGR	nil	Cladding & Struct. Mater.	< 190	12

Chemical Forms

Reactor Systems. Carbon-14 was identified in reactor systems as a mixture of CO_2, CO and hydrocarbons. Their ratio depends on the chemistry of the respective reactor system. C.O. Kunz et. al. reported in publication (2) that a major portion of ^{14}C measured in PWR systems was present as hydrocarbons and only small amounts as carbon oxides because D_2 is maintained in the primary coolant as a cover gas. The above authors also reported in publication (3) that in BWR

station more than 90% of ^{14}C was present as CO_2. It was also suggested that the predominant mechanism appears to be oxidation of carbon to CO_2 and CO by oxygen radicals formed from radiolytic decomposition of the coolant water.

An annulus gas sample (N_2) from a CANDU reactor was analyzed in the NY State Department of Health Laboratory. In this sample > 75% of ^{14}C was present as hydrocarbons, as expected, because of the presence of D_2 in the annulus gas (from the coolant). Samples of primary coolant off-gas (D_2) and moderator cover gas (He) have not yet been analyzed but from chemical conditions it can be assumed that hydrocarbons are the major ^{14}C compounds in the primary coolant and significant portions of ^{14}C in the moderator system are in oxide forms.

Fuel. It was suggested in publication (1) that ^{14}C produced in UO_2 fuel might become bound to uranium as carbide, remain as impurity atoms, or be converted to carbon monoxide or dioxide. It was also assumed that major portion of ^{14}C in the fuel will be converted to CO_2 in dissolving operations at the fuel reprocessing plant.

Carbon-14 Releases

It was reported in publication (2) that combined gaseous ^{14}C effluent from a 1000 MWe PWR would be approximately 6 Ci/year. The BWR release rate of approximately 8 Ci/GWe-year was estimated from measurements, described in publication (3). No other experimental data on ^{14}C effluents is available at present. The magnitude of ^{14}C releases through all potential pathways from PWR and BWR stations was estimated in publication (9) and ^{14}C release from the HTGR reprocessing facility evaluated in publication (10). Measurements of ^{14}C release from CANDU reactors are in progress and will be reported in the near future.

Carbon-14 production can be greatly reduced by avoiding the presence of nitrogen in high neutron flux systems and areas. Releases of ^{14}C can be further reduced by removing it from power station and fuel reprocessing plant systems and effluents, transferring it to a solid form, chemically stable, and for permanent disposal.

III. Present Status in Monitoring and Control of Gaseous Carbon-14 Releases

Monitoring and Control Requirements

No regulatory requirements have yet been issued on monitoring and control of ^{14}C effluents. However, from the carbon-14 environmental impact analysis performed by the Commission of the European Communities (4), US-EPA (5), and several authors (6,7,8) it is evident that the requirements on the control and monitoring of ^{14}C release will be formulated in the near future. Also in Ontario Hydro, work is in progress on deriving ^{14}C release limits.

Carbon-14 Monitoring Methods

Several methods were developed for "carbon dating" which are not directly applicable for ^{14}C monitoring in nuclear facilities. However, the practice of CO_2 purification with heated CaO, applied in some ^{14}C dating procedures, was further developed for direct collection of gaseous ^{14}C in nuclear facilities as described later in this paper. The well known method of CO_2 collection in alkaline solutions was used on several occasions for $^{14}CO_2$ sampling. However, this method is not selective for CO_2 since other carbon compounds can be partially

absorbed and other radionuclides can interfere with ^{14}C measurement. A heated catalyst must be added when "total ^{14}C" is to be collected and evaporation or spills of alkaline solution can introduce significant experimental errors.

A sophisticated laboratory method was developed in the NY State Department of Health Laboratory (11) for ^{14}C analysis. Carbon-14 gaseous compounds are separated with a gas chromotograph and radiometrically evaluated. This method was successfully applied in PWR and BWR effluents and also a CANDU sample evaluation. Unfortunately, it is too complex for routine monitoring of ^{14}C in nuclear facilities operational field.

Carbon-14 Removal Methods

All proposed methods for ^{14}C removal are based on converting it to CO_2 and solidification as $CaCO_3$ for disposal. In publication (12) a detailed evaluation was made on $^{14}CO_2$ fixation methods and available options for $CaCO_3$ disposal. The dry CO_2-CaO process for CO_2 fixation was rejected and the following aqueous processes were considered.

1. The direct reaction of CO_2 with a slaked lime slurry.
2. A double alkali process where CO_2 is absorbed in NaOH solution and then transferred to $CaCO_3$ by reaction of Na_2CO_3 with slaked lime slurry.

The simpler direct CO_2 fixation process was recommended. It was suggested that ^{85}Kr was the controlling radiation hazard in the ^{14}C fixation and disposal processes. It was also concluded that shallow land burial of $CaCO_3$ appears to be the optimal disposal method available.

In publication (9) all available techniques with the potential for ^{14}C removal were reviewed. A system for ^{14}C removal from LWR effluents was proposed and the cost of fixation and disposal processes evaluated. The assumption was also made in this report that direct reaction of CO_2 with solid CaO is not practical for this purpose.

It was recognized from operational experience with similar systems in the chemical industry that a number of technical difficulties must also be expected in operating the systems for absorption of CO_2 in alkaline liquids, i.e. complexity and size of the equipment, possibility of contamination from leaking liquids, foaming of liquids, plugging the column with $CaCO_3$, presence of gamma emitting radionuclides causing building of radiation fields on $Ca^{14}CO_3$ containers, etc.

Chemistry of $CaO/Ca(OH)_2$ Reactions with CO_2

The methods referred to in Carbon-14 Removal Methods are based on reactions of disassociated forms of $Ca(OH)_2$ or NaOH with CO_2 in aqueous solutions. The direct reaction of solid CaO with CO_2, which is much slower under normal temperature and pressure conditions, was not considered for CO_2 fixation on an industrial scale.

From some "carbon dating" procedures and data from chemical publications and physico-chemical considerations it is evident that the rate of the direct reaction of gaseous CO_2 with solid CaO and $Ca(OH)_2$ significantly increases with temperature. Therefore, in publication (13), a proposal was made to fix $^{14}CO_2$ on solid CaO at a higher temperature.

The following reactions are involved in the process of CO_2 fixation on solid CaO and $Ca(OH)_2$:

$$CaO + CO_2 \rightleftharpoons CaCO_3 \qquad \text{I}$$

$$Ca(OH)_2 + CO_2 \longrightarrow CaCO_3 + H_2O \qquad \text{II}$$

$$CaO + CO_2 \longleftarrow \qquad Kp = 1.6 \times 10^{-23}/25°C \qquad \text{III}$$

$$Ca(OH)_2 \rightleftharpoons CaO + H_2O \qquad \text{IV}$$

Reactions I and II are practically irreversible at temperature up to 300°C because in reaction III the thermal dissociation of $CaCO_3$ can be neglected at this temperature. Reaction III was discussed in detail in several publications while very little data on the kinetics of reactions I and II have been found in chemical literature. In publication (14) the equilibrium constant of reaction III ($Kp = 1.6 \times 10^{-23}$) was given and it was suggested that "metal oxide (solid) carbon dioxide (gas) reactions, which might in theory yield the carbonate, are often too slow in practice, possibly because of inactivity of the oxide surface."

J. Johnson in publication (15) derived an equation for CO_2 pressure above $CaCO_3$ which was well in agreement with experimental findings:

$$\log p = -9340\ T^{-1} + 1.1 \log T + 0.0012\ T + 8.882$$

The temperature dependence of both CO_2 pressure above $CaCO_3$, calculated from the above equation, and water vapour pressure above $Ca(OH)_2$ from data in publication (16) are illustrated in Figure 1.

Rapid absorption of CO_2 with moist $Ca(OH)_2$ and no CO_2 absorption with dry CaO at normal temperature when moisture was excluded, was reported in publication (17). According to several authors, referred to in this publication, "dry calcium oxide absorbs no CO_2 in the cold, but a reaction occurs when the temperature is raised to 420°C". Also that "crystaline CaO combines with CO_2 very slowly while the porous variety combines rapidly with the same gas." Also, "no absorption of nitric oxide on CaO" is reported in publication (19).

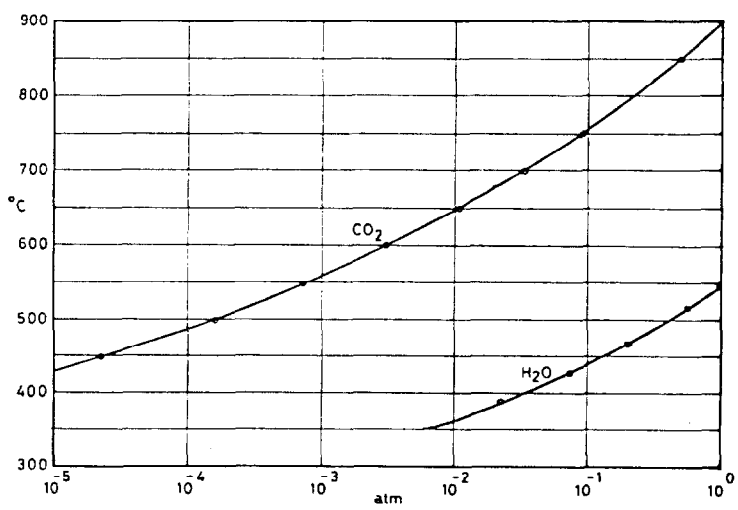

Figure 1

It was deduced from the above information that the direct reaction of solid $Ca(OH)_2$ (rather than CaO) with gaseous CO_2 could be sufficiently fast at increased temperatures for efficient absorption of CO_2 for both ^{14}C monitoring and removal at nuclear facilities.

V. Proposal for CO_2 Absorbent

Performance Requirements

Sampling of $^{14}CO_2$:

- Collection efficiency for CO_2 of $\geq$ 99% at reasonably low residence time, < 500°C temperature and CO_2 concentration range of 0.1 - 1000 ppm.
- Sufficient capacity for sampling air, with 350 ppm CO_2, for a one week period.
- Simple equipment and procedure involving minimal sampling error in the field.
- High collection selectivity for CO_2, minimum retention of noble gas radionuclides.
- Quantitative desorption of ^{14}C in a form suitable for its radiometric evaluation.
- Minimum release of other radionuclides in the process of ^{14}C desorption.

Removal of $^{14}CO_2$:

- Collection efficiency for CO_2 of > 90% at temperatures < 500°C, and CO_2 concentrations of 0.1 - 1000 ppm.
- Large volume reduction factors for CO_2.
- Operationally simple collection process.
- Minimal possibility of radioactive contamination arising from processing the used absorbent for disposal.
- Minimal radiation field at the disposal containers surface.
- Negligible release of radionuclides from the containers during long term storage.

Proposal for CO_2 Collection Method

From the above requirements, the absorption of gaseous CO_2 on solid $Ca(OH)_2$ was the logical choice for both ^{14}C sampling and removal.

The proposal for the CO_2 collector was based on the following considerations:

1. In order to obtain both adequate absorption velocity and maximum capacity:
   - The operating temperature was to be > 300°C but should not exceed approximately 500°C when significant decomposition of $Ca(OH)_2$ occurs.

- The $Ca(OH)_2$ absorbent must have a large absorption surface.
- Reasonable residence time (0.1 - 1 s) should be allowed for the chemical reaction to be efficient.

2. The selectivity of CO_2 adsorption results from the specific affinity of $Ca(OH)_2$ for CO_2. No noble gas retention can occur at increased temperature. Tritiated water vapour present in the gas sample could be partially absorbed in $Ca(OH)_2$ through isotopic exchange process. However, tritium can be separated later by fractional desorption; it desorbs from the absorbent at < 600°C temperature, at which no significant $CaCO_3$ decomposition occurs.

3. Carbon-14 can be selectively desorbed as CO_2 at approximately 900°C. A low purge of inert gas accelerates the process of $CaCO_3$ decomposition by continuously removing the gaseous reaction product (CO_2). Coincidently, the purge provides a gas carrier for transferring $^{14}CO_2$ for radiometric evaluation.

4. The spent absorbent, a solid mixture of $CaCO_3$ + $Ca(OH)_2$ can be easily sealed without any handling of loose contaminated material. Negligible amounts of other radionuclides would be present with ^{14}C in the disposal containers and negligible leaching of ^{14}C from containers would occur during their long term storage.

To evaluate the above concept, a laboratory system was built and the absorption of CO_2 tested, with both CaO and $Ca(OH)_2$ as described in the next section.

VI. Experimental Studies on Carbon-14 Monitoring

Process Description

In most field applications, gaseous organic compounds and CO are first oxydized to CO_2 by catalytic combustion. Carbon dioxide absorption on CaO and $Ca(OH)_2$ was evaluated by injecting $^{14}CO_2$ into an air stream containing approximately 330 ppm of nonradioactive CO_2 and passing the air through test columns containing the absorbents. From the measured $^{14}CO_2$ concentration upstream and downstream of the column the efficiency and capacity of both CaO and $Ca(OH)_2$ for CO_2 absorption was evaluated within a wide range of experimental conditions. The temperature and gas purging effects on $Ca\text{-}CO_3$ dissociation were then evaluated by continuous measurement of $^{14}CO_2$ concentrations in the purge gas downstream of the column and also by collecting CO_2 in NaOH solution followed by liquid scintillation counting of ^{14}C.

Equipment Description

The experimental system in shown in Figures 2 and 3. It contains the following components.

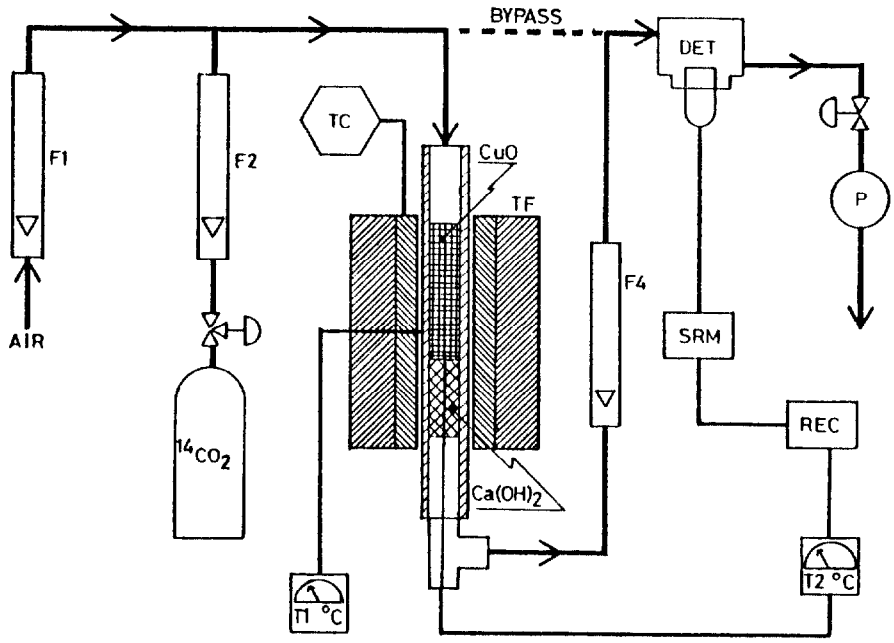

Figure 2

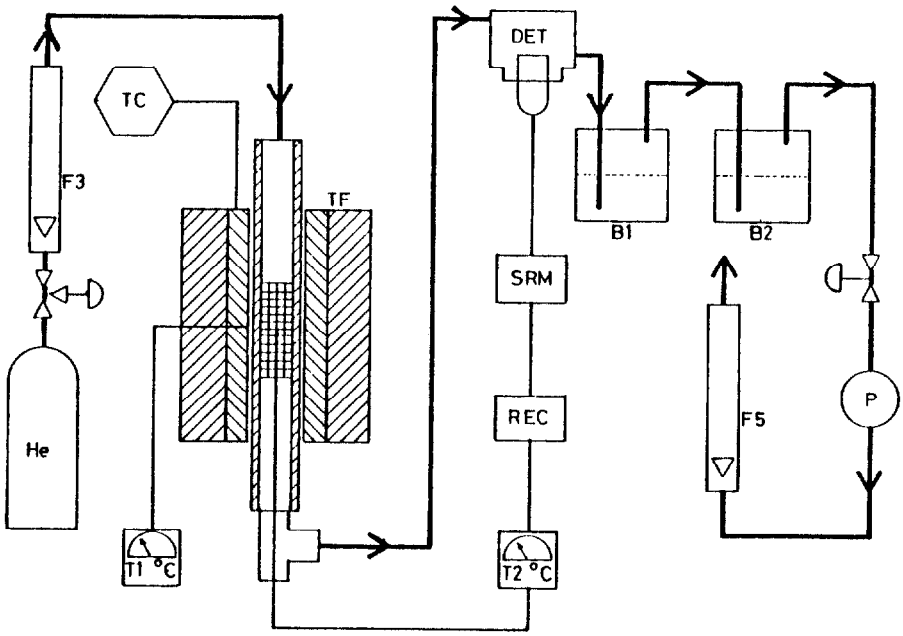

Figure 3

- Carbon-14 and purge gas supply.
- Systems for measurement and control of operational parameters (flow, temperature).

- Catalyst for combustion of ^{14}C species and CO_2 absorber.
- ^{14}C monitors (upstream and downstream of the CO_2 absorber).

Carbon-14 and Purging Gas. The carbon dioxide ($^{14}CO_2$) used for CaO testing was generated from the Pickering NGS annulus gas as follows:

A stream of N_2 from the annulus gas system containing ^{14}C (mostly as CH_4) was passed through CuO at approximately 400°C and the resulting $^{14}CO_2$ was then absorbed on $Ca(OH)_2$ at the same temperature. When approximately 20 mCi of ^{14}C was accumulated as $Ca^{14}CO_3$, the temperature of the column was increased to 900°C and the $^{14}CO_2$ produced from $CaCO_3$ thermal dissociation was transferred into an evacuated stainless steel bomb which was then filled with N_2 to approximately 7 MPa (1000psi) pressure.

Nitrogen from the bomb, containing 10 - 100 μCI of $^{14}CO_2$/L was then injected into air or other gas stream and carried into the tested column.

Helium, nitrogen or air were used for purging desorbed CO_2 from the absorber column in testing the process of $CaCO_3$ thermal decomposition.

Measurement and Control of Operational Parameters. In most experiments, laboratory air containing 330 ± 15 ppm of CO_2 was drawn through the tested column with the pump P at the flow rate of 5 Lpm. Carbon-14 ($^{14}CO_2$ in nitrogen) was injected into the air stream from the pressurized stainless steel bomb at the rate of 10 - 30 mL/m.

The gas flows and the column temperatures were continuously measured and controlled for both the CO_2 absorption and the $CaCO_3$ dissociation.

Calibrated flow meters F_1, F_2 and F_3 measured gas flow rates at the inlet and F_4, F_5 installed downstream of the columns, was used to monitor system leaks.

Thermocouple T_1 detected the temperature of the tubular furnace TF equipped with the temperature controller TC.

The temperature inside the absorbent was detected with the thermocouple T_2 installed axially of the absorption column and recorded.

The Catalyst and Absorbent Columns. Cupric oxide, prepared in our laboratory, was used in our experiments. In the experimental setup, both the catalyst column (CuO) and the absorbent column [CaO or $Ca(OH)_2$] were contained in a quartz tube, 25 mm diameter and separated with a stainless steel screen. The column length was: 50-100 mm of CuO and 30-50 mm of CaO. The grain size of CuO was 10-40, while two size ranges of CaO and $Ca(OH)_2$, 10-20 and 20-40, were tested separately.

Carbon-14 Monitors. Continuous on line measurement of ^{14}C concentration was performed with a thin wall (< 2 mg/cm^2) GM detector D installed in through-flow chambers (50 and 1000 mL volume) installed upstream and downstream of the absorber column. Both the count rate and accumulated counts were measured with an NE-SR5 scaler/rate meter (SRM) and the ^{14}C count rate was recorded. In desorption experiments, $^{14}CO_2$ was also absorbed in NaOH solution and measured with a liquid scintillation counter.

Materials. Most of the system was assembled of quartz and glass tubing. Plastic tygon tubing was only used for connecting system components. Thermocouple sheath and the screens separating the catalyst and the absorbent columns were made of stainless steel. A polyethylene flow chamber was used for monitoring low concentrations of ^{14}C in the collection process and a glass chamber for counting high concentrations of ^{14}C in the desorption process.

Catalytic Oxidation of ^{14}C Species

Catalyst Performance Requirements. The basic requirements on the catalysts performance for hydrocarbons and CO oxidation are as follows:

1. For ^{14}C sampling:
   a) Combustion efficiency of > 97% for hydrocarbons at 0.1 - 1000 ppm concentrations and temperature range 350-450°C.
   b) No significant retention of any chemical form of carbon.
   c) At least one week lifetime for hydrocarbons oxidation from air under typical sampling conditions.
   d) At least 24 hours capacity for hydrocarbons oxidation from gas containing no oxygen (which requires CuO type catalyst).
2. For ^{14}C removal:
   a) Combustion efficiency > 90% in oxygen free gas within 350-450°C and CH_4 concentration 0.1-500 ppm.
   b) Capacity for > one week of continuous oxidation of methane at an average concentration of 10 ppm, from gas containing no oxygen.
   c) Regeneration capability (when applied for ^{14}C removal from gas containing no oxygen).

Testing of Catalysts. The GM-AC converter catalyst type number 78925 and two Hopcalite samples (from MSA and Safety Supply), which were tested in our laboratory with a gas chromatograph did not comply with the requirements 1b, 1d, 2a, 2b, and 2c. Also, CuO from Fisher Scientific, prepared by the oxidation of Cu wire, was not adequately efficient.

Development of the catalyst was not originally intended in this project. However, when no commercially available catalyst was found to perform as needed for the quantitative sampling of ^{14}C, cupric oxide was prepared in our laboratory by precipitation from hot $CuSO_4$ solution, ground and tested with a gas chromatograph under the assumed sampling conditions. This material satisfied all the above requirements for ^{14}C sampling and removal, except its regeneration capability.

The measured performance of this catalyst for methane combustion was as follows:

1. The minimum temperature for efficient combustion of methane in air is 270°C at the residence time of 3 seconds. A slightly higher temperature - approximately 300°C - is needed for complete CH_4 combustion from oxygen free gas.
2. The measured efficiency values for combusting CH_4 (1000 ppm) over a one week period in air at 310°C were:

> 99.5% at > 3 second residence time
> 99% at > 2 second residence time
> 97% at > 1 second residence time

The total volume of air, with 1000 ppm of CH_4 was > 10^5 volumes of the catalyst. It is expected that the catalyst lifetime is significantly longer than one week under the above conditions.

3. For combustion of methane in nitrogen, the available oxygen from one volume of CuO oxidized 5000 volumes of 0.1% CH_4 in N_2. The efficiency was > 97% at the residence time of approximately six seconds and temperature of 320°C.

4. At low methane concentrations (< 1 ppm), its combustion was still improved and also the catalyst's lifetime proportionally increased.

5. The catalyst, in agreement with experimental data in publication (18), was more efficient for CO than for CH_4 combustion at the same temperature and residence time.

6. The combustion efficiency increases with the catalyst temperature (measured up to 600°C) but temperature cycling has a detrimental effect on the catalyst.

7. Carbon-14 retention of < 0.1% was measured on the precipitated CuO catalyst after passing large volumes of gas containing a mixture of $^{14}CO_2$, ^{14}CO and ^{14}C hydrocarbons.

8. Once the catalyst was exhausted it cannot be reoxidized to regain its original efficiency for methane combustion, probably because of its restructured surface.

Testing Of $^{14}CO_2$ Absorption on CaO and $Ca(OH)_2$

Materials Tested. Three grades of commercially available CaO were tested in the original CaO form and also as $Ca(OH)_2$ prepared in our laboratory.

The technical quality and purified CaO lumps from Fisher Scientific were ground and two grain sizes, 10-20 and 20-40 mesh, selected for our measurements.

The analytical grade CaO was not tested in its original powdered form.

Further, both the purified and analytical CaO were converted to solid, granulated $Ca(OH)_2$ by slaking CaO with distilled water, drying the sludge, grinding and selecting 10-20 and 20-40 mesh sizes. In this process, BaO, SrO and solid impurities were further removed from the "purified" CaO. From the measured weight loss of the "reprocessed CaO" after heating to 600°C, it was evident that the original CaO was quantitatively converted to $Ca(OH)_2$ through the above process. Also, the specific weight of this material was reduced. The average specific weight values of the tested absorbents are listed in Table II.

Table II

Absorbent Type	Mesh Size	Specific Weight g/cm^3
CaO - technical	20-40	0.87
CaO - purified	20-40	0.85
CaO - purified	10-20	0.8
$Ca(OH)_2$ - from both purified and analytical CaO	20-40	0.4
$Ca(OH)_2$ - from both purified and analytical CaO	10-20	0.35

Testing Conditions. Experimental conditions applied in the evaluation of CaO and $Ca(OH)_2$ absorbents were as follows:

The efficiency and capacity for CO_2 absorption was tested within the temperature range of 20°C to 550°C.

Laboratory air (approximately 50% RH) containing 330 ± 15 ppm of CO_2, with the addition of approximately 0.1 ppm of $^{14}CO_2$ was applied in most measurements. At a flow rate of 5 Lpm and absorbent volume of 30-50 cm^3 the "residence time" was 0.36 - 0.6 seconds. To confirm references to the slow reaction of dry CaO with CO_2, the efficiency of both $Ca(OH)_2$ and dry CaO for absorption of CO_2 from dry nitrogen was evaluated.

The collection capacity was calculated from the total amount of air passed through the absorber until its efficiency for CO_2 removal was reduced to approximately 95%. From air volume, CO_2 concentration and absorbent weight, the portion of CaO or $Ca(OH)_2$ converted to $CaCO_3$ was calculated.

The penetration of 5% $^{14}CO_2$ was radiometrically monitored with better than ± 10% accuracy at the 95% confidence level.

Absorption of CO_2. Results of absorbers' efficiency and capacity testing with air containing 330 ± 15 ppm of CO_2 are summarized in Table III.

Results of $Ca(OH)_2$ and dry CaO efficiency testing with CO_2 in dry nitrogen are given in Table IV.

The time dependence of CO_2 penetration through absorber containing 30 mL (approximately 11 g) $Ca(OH)_2$ is illustrated in Figure 4.

The efficiency of powdered, analytical grade CaO could not be evaluated because under typical experimental conditions its flow resistance was too high and it developed channelling of the sample which caused erroneous results.

Table III

Absorbent	Mesh Size	Temp. (°C)	Residence Time (Sec.)	Total Air Volume at 5% Penetr. (m^3)	Collect Capacity (%* at 98% eff.)	Average Collect Capacity (%* at 95% eff.)
1. CaO - technical	10-20	400	0.6	0.23		0.5
2. CaO - purified	10-20	20-200	2.0	0.14		0.3
3. CaO - purified	10-20	400	0.6	0.9		2.0
4. CaO - purified	20-40	400	0.6	2.2		4.8
5. $Ca(OH)_2$ from purified CaO	10-20	300	0.6	0.7	5.5	7.0
6. $Ca(OH)^2$ from purified CaO dried out 700°C	10-20	300	0.6	0.35	3.0	3.5
7. $Ca(OH)_2$ from purified CaO	10-20	400	0.6	4.2	42	43
8. $Ca(OH)_2$ repeated use (after $CaCO_3$) thermal dissociation.	10-20	400	0.6	1.2	10	12
9. $Ca(OH)_2$ from purified CaO	20-40	400	0.6	4.4	44	45
10. $Ca(OH)_2$ from analytical CaO	20-40	400	0.6	4.4	44	45
11. $Ca(OH)_2$ from purified CaO	10-20	20-250	0.36	0.4	3.0	4.0
12. $Ca(OH)_2$ from purified CaO	10-20	350	0.36	2.6	25	27
13. $Ca(OH)_2$ from purified CaO	10-20	400	0.36	3.7	37	38
14. $Ca(OH)_2$ from purified CaO	10-20	450	0.36	5.9	58	60
15. $Ca(OH)_2$ from purified CaO dried out 650°C	10-20	450	0.36	1.1	10	11

* Percent of the theoretical capacity calculated from stochiometric ratio.

Table IV

Absorbent	Size	Concentration of CO_2 in N_2 (ppm)	Residence Time (Sec.)	Temperature (°C)	CO_2 Absorption Efficiency (%)
$Ca(OH)_2$ from purified CaO	10-20	1	0.6	360 - 380	$\geq$ 99.7
				400	99.5
				450	99
				550	< 90
CaO from $Ca(OH)_2$ dried at 700°C	10-20	330	0.6	400	nil
				500	nil
				600	nil

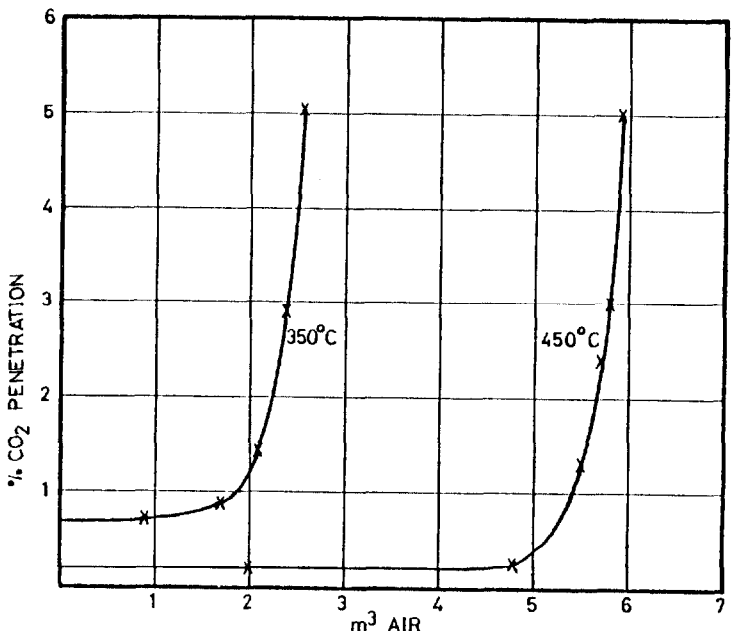

Figure 4

Thermal Dissociation of $CaCO_3$

The graph on Figure 1 shows that the equilibrium CO_2 pressure above $CaCO_3$ reaches 1 atm at a temperature of approximately 900°C. Therefore, the rate of $Ca^{14}CO_3$ dissociation was experimentally evaluated within 700-950°C.

After CO_2 penetration exceeded 5% in the absorption period, $^{14}CO_2$ flow was terminated, a low purge flow (50-100 mL/m) of inert gas was maintained and the column temperature continuously increased. In the temperature range 500-650°C water was released from the column due to decomposition of remaining $Ca(OH)_2$. With further column temperature increase noticeable decomposition of $CaCO_3$ started at $\geq$ 700°C and rapid and complete decomposition of $CaCO_3$ occurred at 900°C.

No significant effect of the purge gas quality was found in our experiments. Helium was used in most experiments, but using N_2, dry or humidified air did not cause any significant difference in the CO_2 desorption from the column.

CO_2 Absorption on System Components

It was found from the experiments that $^{14}CO_2$ reacts with plastic materials and metals used in the experimental setup. It can be assumed that physical absorption, chemisorption and isotopic exchange are involved.

Any ^{14}C hold-up on the system components is undesirable in the sampling process. Therefore, $^{14}CO_2$ sorption on stainless steel was investigated. Slugs of stainless steel wire were exposed to $^{14}CO_2/N_2$ at a residence time of approximately 0.5 minutes, for 30 minutes at temperatures of 20°C and 400°C. The system was then purged with pure He and the temperature increased to 900°C. The amount of ^{14}C, desorbed from the stainless steel wire, was then measured. Results are summarized in Table V.

It was also determined that $^{14}CO_2$ from the gaseous sample was partially sorbed on the mylar foil covering the GM detector and subsequently desorbed using a pure gas purge, with a half-life of approximately 15 minutes.

Significant sorption of both $^{14}CO_2$ and $^{14}CH_4$ on PVC tygon tubing was also observed.

As expected, no measureable ^{14}C sorption occurred on quartz, Vycor glass and pyrex glass components.

Radiometric Determination of ^{14}C Gaseous Species

Both direct and indirect counting methods were applied in our laboratory for ^{14}C measurement.

Table V

Absorption Temperature (°C)	$^{14}CO_2$ Through The S.S. Slug (μCi)	Desorption Temperature (°C)	^{14}C Desorbed (% of CO_2 Passed)	Total $^{14}CO_2$ Desorbed (%)
20	67.6	20 - 400	3.7	
		400 - 950	2.6	6.65
		1000	0.35	
400	338	400	0.76	
		400 - 950	1.2	2.25
		1000	0.29	

Plastic scintillation cell NE802 with a photomultiplier or a thin wall (< 2 mg/cm^2) GM detector installed in flow-through chambers, 50 mL and 1 L volume were applied for direct counting of gaseous forms of ^{14}C.

When a low activity of ^{14}C in a small volume of gaseous sample was to be measured, the sample was transferred into the cell and the detector counts were integrated with a scaler for the time period required for adequately low

statiscal error.

The GM chambers were applied in most "continuous flow" measurements, particularly in CO_2 absorption/desorption experiments. Specific activity of ^{14}C was evaluated from the detector count rate and the "total ^{14}C" from integration of detector counts.

Tritium or other radionuclides did not interfere with ^{14}C measurements.

A liquid scintillation counting method was used in cases when very low activity of ^{14}C was to be measured, the water condensate from $Ca(OH)_2$ decomposition was to be included in the ^{14}C evaluation or when tritium was present in the sample. Carbon dioxide and water desorbed from $Ca(OH)_2$ was absorbed in 0.5 N NaOH solution which was then mixed with Aquasol 2 scintillator and measured with a three-channel liquid scintillation counter.

Detection efficiencies of our counting cells for ^{14}C are listed in Table VI.

Table VI

Detector	Cell Volume cm^3	Net cpm From 1 μCi ^{14}C/L cpm	Detection Efficiency For ^{14}C %
GM Detector	50	3670	3.3
GM Detector	1000	5560	0.25
NE802	11	4320	17.8
Liquid Scintillation Counter	5 mL NaOH Solution + 15 mL Aquasol 2	--	85

VII. Discussion of Results

Oxidation of ^{14}C Compounds

The results of our experiments show that the efficiency of precipitated CuO for oxidation of carbon monoxide and hydrocarbons is sufficient for both ^{14}C sampling and its removal. It also has an adequate lifetime for combustion of hydrocarbons and CO from gas containing oxygen. The capacity for combusting hydrocarbons from oxygen free gas is at least 20 Ci of pure $^{14}CH_4$/kg of CuO or a proportional quantity of high hydrocarbons. No significant retention of ^{14}C on the CuO was measured under typical sampling conditions.

This catalyst is particulary suitable for ^{14}C sampling. It can be also used in ^{14}C removal from gas containing at least an equivalent concentration of oxygen.

Use of another catalyst, with a regeneration capability, would be more economical in industrial application where hydrocarbons are to be combusted from oxygen free gas and carbon retention does not cause any difficulties.

Absorption of CO_2

From the results of CaO and $Ca(OH)_2$ testing, the following conclusions have been drawn:

1. Only $Ca(OH)_2$ has a high efficiency and capacity for absorption of gaseous CO_2 within the temperature range 350-450°C. Practically no CO_2 can be absorbed from a dry carrier gas on dry CaO within the above temperature range and residence time of $\leq$ 1 second.

2. There is no difference in the efficiency and capacity between $Ca(OH)_2$ made of purified or analytical grade CaO.

3. Calcium hydroxide, 10-20 mesh, is more suitable for field application than the 20-40 mesh which has much higher flow resistance and is only slightly more efficient for CO_2 absorption.

4. The optimum temperature range for CO_2 collection is 350-450°C. Lower temperatures(360-400°C) are more suitable for CO_2 at < 1 ppm concentration. The absorbent lifetime increases almost proportionally to reduced CO_2 concentration. A temperature of 450°C is more practical when the CO_2 concentration exceeds 100 ppm.

5. At 550°C, a significant portion of $Ca(OH)_2$ is dehydrated to an inactive CaO. At this temperature, the efficiency of the absorbent is less than 90% at the beginning of the collection period.

6. It is evident from Table III and Figure 4 that within the recommended temperature range, $Ca(OH)_2$ maintains its high collection efficiency until a rapid CO_2 breakthrough occurs.

Decomposition of $CaCO_3$

In our experiments, the course of $CaCO_3$ thermal decomposition was well in agreement with that theoretically predicted.

The optimum parameters for desorption of CO_2 are 900-950°C column temperature and 50-100 mL/m gas purge (N_2 or He). Under these conditions, the process of $CaCO_3$ decomposition can be completed in less than 15 minutes.

If tritium was absorbed (through an isotopic exchange with OH^1) on $Ca(OH)_2$ in the sampling process, it can be selectively desorbed by increasing the absorbent temperature to 600°C for approximately 15 minutes and purged off with N_2 or He. No loss of CO_2 occurs at this temperature. Then CO_2 is desorbed from the absorbent with the second increase of column temperature to > 900°C.

For radiometric evaluation of ^{14}C the previously described direct counting method with a GM detector in continuous flow regime is suitable for measurement of medium activity ^{14}C.

A plastic scintillator and GM low volume cells in the scaler counting mode are more convenient for measurement of medium to low activity of ^{14}C in small volumes.

Absorption of $^{14}CO_2$ in NaOH solution and liquid scintillation counting gives the best results for measuring large volume samples with a wide range of ^{14}C

concentrations and $^{14}CO_2$ samples containing a water condensate.

VIII. Field Applications

Theoretical considerations and the experimental work on this project were oriented toward demonstration of the potential of this method for both sampling and removal of ^{14}C in nuclear field operations.

From the results discussed above, the following proposals were made:

Carbon-14 Sampler

1. The proposed field sampler for "total ^{14}C" is illustrated in Figure 5.

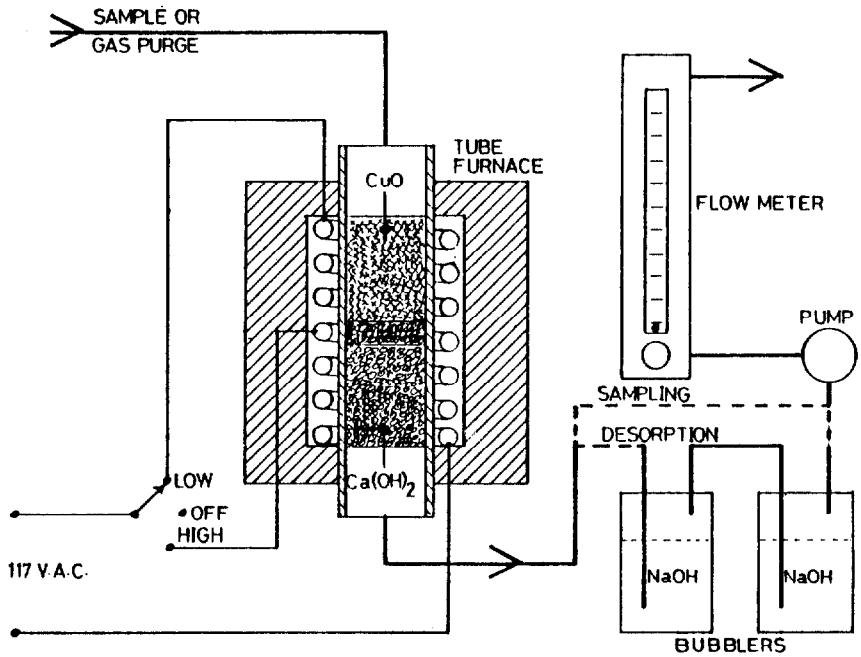

Figure 5

Both the catalyst (CuO) and the absorbent [$Ca(OH)_2$] are loaded in the quartz or Vycor tube QT, separated with quartz fibre or stainless steel screen and surrounded with the heating element H. The element is assembled of two parts, heating the CuO and $Ca(OH)_2$ columns separately. The resistance of the heaters is selected in such a way that in the sampling process they are in series (the switch S is in the position a) and both columns are heated to 400°C.

For CO_2 desorption, the switch is in position b, and full power is applied to heat only the absorbent column to 950°C.

In the collection period, the sampling pump P is connected to the outlet of the $Ca(OH)_2$ and the sample flow is measured with the flowmeter F. For CO_2 desorption, the first bubbler inlet I is connected downstream of the absorbent and the pump inlet to the outlet O of the second bubbler.

An identical assembly, but without the catalyst (CuO) can be used for selective sampling of $^{14}CO_2$ from other gaseous ^{14}C compounds.

Several different alternatives of this sampler can be built for specific needs, containing separate catalyst and absorbent columns, automatic control and readout of column temperature, constant flow controller, particulate filter at the sampler inlet, direct $^{14}CO_2$ detection in the desorption process, etc. For best performance, the size of the sampler should be optimized for both the sampling flow and period required. The optimum sampling parameters and column loads are recommended in Table VII.

Procedure for ^{14}C Sampling and $^{14}CO_2$ Desorption

After filling columns with appropriate amounts of catalyst and absorbent, a flow meter is connected to the CuO column inlet and a pump to the outlet of the absorber. Heaters on both columns are switched on and the system left for an adequate time period (depending on type of heaters and size of the column) to equilibriate the catalyst and absorbent temperature. Then sample flow is initiated and maintained for the selected time period.

When ^{14}C sampling is completed, two bubblers filled with 100 mL of 0.5 N NaOH each, are connected in series between the absorbent column and sampling pump. A purge gas flow of 100 mL/m is established and temperature of the absorber increased to 950°C. This temperature is then maintained for 15-20 minutes while continuing to purge at 100 mL/m. When CO_2 desorption is completed, the ^{14}C in the solutions is evaluated by liquid scintillation counting.

Carbon-14 Removal System

The removal system principle is identical to that of the above sampler. The material choice is not critical in this application. The whole system can be made of carbon steel because its operational temperature does not exceed 450°C and retention of ^{14}C on system components does not have any negative effect.

The catalyst choice depends on the character of both the carrier gas and ^{14}C compounds to be removed. Commercially available catalyst which can be regenerated is preferable for systems removing ^{14}C components from oxygen free gas.

Only a heated cartridge with an adequate quantity of $Ca(OH)_2$ is required when $^{14}CO_2$ is to be removed from systems or gaseous effluents at a nuclear facility. The recommended loads and temperatures of the absorbent are given in Table VIII.

The recommended purification flow limit is 10 L/s (~ 20 cfm) per kilogram of $Ca(OH)_2$. This value is independent of CO_2 concentration and gives $\geq$ 99% efficiency for CO_2 removal throughout the operational period as calculated from Table VIII.

The principle of the removal process is very simple. The process does not form by-products or involve handling loose contamination. Carbon dioxide can be removed from high pressure gaseous systems, its adsorption is very selective, therefore the used absorbent cartridges will cause negligible gamma fields. No handling of loose $Ca^{14}CO_3$ is necessary, the absorber cartridges can be disposed directly or fixed in concrete for disposal. The high capacity of $Ca(OH)_2$ for CO_2 results in low volume waste to be disposed. The remaining $Ca(OH)_2$ in the disposed cartridge will absorb CO_2 eventually penetrating into the container and

reduce the possibility of ^{14}C leak.

Table VII

Sample	Carbon Compounds		Flow	Total Sample Volume	Recommended Loads*		Column Temp.
	CO_2 (ppm)	Hydrocarb. + CO (ppm)	(Lpm)	(m^3)	CuO (g)	$Ca(OH)_2$ (g)	(°C)
Air (or gas containing O_2)	330	300 - 1000	1	≤ 1.5	50	15	450
			5	≤ 1.5	150	15	450
Air (or gas containing O_2)	330	0 - 300	1	≤ 3.0	50	15	450
			5	≤ 3.0	150	15	450
Air (or gas containing O_2)	330	0 - 300	1	< 0.5	50	5	450
			5	< 0.5	150	10	450
Oxygen free gas	50-500	50 - 500	1	≤ 1.5	100	15	450
			5	≤ 1.5	300	15	450
Oxygen free gas	1-50	1 - 50	1	≤ 5.0	70	10	400
			5	≤ 5.0	300	10	400
Oxygen free gas	< 1	< 1	1	≤ 5.0	70	5	380
			5	≤ 5.0	300	7	380
Oxygen free gas	0-500	0 - 500	1	< 0.5	100	5	400
			5	< 0.5	300	5	400

* A smaller load than recommended can cause inadequate sampling efficiency and capacity.

A significantly larger load of the absorbent column can slow down the process of desorption.

Table VIII

CO_2 Concentration (ppm)	Absorbent Temperature (°C)	Absorbent Load [kg $Ca(OH)_2$ Per kg CO_2 Removed]
> 100	450	3.5
1 - 100	400	4.5
< 1	370	5.0

IX. Conclusions

The method described for CO_2 collection on solid $Ca(OH)_2$ is applicable in two ways:

1. For ^{14}C monitoring purposes for selective $^{14}CO_2$ or "total ^{14}C" sampling in nuclear facilities and their environment. At present, systematic investigations of ^{14}C levels in CANDU station systems, areas and effluents are in progress, applying the above described techniques. The sampling equipment will be further simplified as operating experience is obtained.

2. This method has good potential for ^{14}C removal. Large amounts of ^{14}C can be solidified directly during collection. The highly concentrated ^{14}C as $CaCO_3$ can be hermetically sealed and easily disposed of. A purification loop prototype will be tested in the field and possibly used in the future for ^{14}C control in CANDU reactor moderator systems.

Acknowledgments

The author wishes to acknowledge the assistance of co-workers J.L. Hartwell on carrying the absorbents testing and B.C. Neil and G. McCann on catalysts testing.

References

1. W. Davis Jr.
"Carbon-14 Production in Nuclear Reactors"
ORNL/NUREG/TM-12, February 1977

2. C. Kunz, W.E. Mahoney, T.W. Miller
"C-14 Gaseous Effluents from Pressurized Water Reactors"
Health Physics Society, Symposium on Population Exposures,
Knoxville, October 1974

3. C. Kunz, W.E. Mahoney, T.W. Miller
"^{14}C Gaseous Effluents from Boiling Water Reactors"
Annual Meeting of the American Nuclear Society, New Orleans,
June 1975

4. G.N. Kelly, J.A. Jones, Pamela M. Bryant and F. Morley
"The Predicted Radiation Exposure of the Population of the European Community Resulting from Discharges of Krypton-85, Tritium, Carbon-14 and Iodine-129 from the Nuclear Power Industry to the Year 2000"
V/2676/75 Commission of the European Communities, Luxemburg,
September 1975

5. T.W. Fowler, R.L. Clark, J.M. Gruhlke, J.L. Russell
"Public Health Considerations of Carbon-14 Discharges from the Light Water-Cooled Nuclear Power Reactor Industry"
ORP/Tad-76-3, U.S. Environmental Protection Agency, July 1976

6. R.O. Pohl
"Nuclear Energy: Health Impact of Carbon-14"
Rad. and Environmental Biophys. 13, 315-237 (1976)

7. H. Bonka, K. Brusserman, G. Schwartz, V. Willrodt
"Production and Emmission of Carbon-14 from Nuclear Power Stations and Reprocessing Plants and its Radiological Significance"
Paper No. 281, The Fourth International Congress of the IRPA, Paris, April 1977

8. P.J. Magno, C.B. Nelson, W.H. Ellett
"A Consideration of the Significance of Carbon-14 Discharges from the Nuclear Power Industry"
13th AEC Air Cleaning Conference, San Francisco, August 1974

9. G.R. Bray, Ch. L. Miller, T.D. Nguyen, J.W. Rieke
"Assessment of Carbon-14 Control Technology and Cost for the LWR Fuel Cycle"
Rep. EPA 520/4-77-013, September 1977

10. J.W. Snider, S.V. Kaye
"Process Behaviour and Environmental Assessments of ^{14}C Releases from an HTGR Fuel Reprocessing Facility"
Controlling Airborne Effluents from Fuel Cycle Plants,
ANS-AIChE Meeting, Sun Valley, August 1976

11. C. Kunz, N.Y. State Department of Health Laboratory,
Private Communication

12. A.G. Croft
"An Evaluation of Options Relative to the Fixation and Disposal of ^{14}C--Contaminated CO_2 as $CaCO_3$"
ORNL/TM-5171, UC-77, April 1976

13. M.J. Kabat
Consideration on Control of Tritium and Carbon-14 in Nuclear Power Stations
Rep. Air Cont. 3.1/75, October 1975

14. Comprehensive Inorganic Chemistry
Vol. 1, pg. 1235, Pergamon Press

15. J. Johnston
"The Thermal Dissociation of Calcium Carbonate"
Journ. Amer. Chem. Soc., 32, 938-946, 1910

16. J. Johnston
"The Free Energy Changes Attending the Formation of Certain Carbonates and Hydroxides"
Journ. Amer. Chem. Soc., 30, 1357-1365, 1908

17. Mellor
A Comprehensive Treatise on Inorganic and Theoretical Chemistry
Vol. 3, pg. 664

DISCUSSION

COLLINS: Do you intend to install this in all effluent release points in your CANDU reactors?

KABAT: Carbon-14 purification is being considered for reactor systems in which a major quantity of ^{14}C is generated, i.e. moderator cover gas and some annulus gas systems in CANDU reactors.

COLLINS: Is AECL doing anything about establishing limits for ^{14}C in reactor effluent?

KABAT: The work on establishing ^{14}C release limits is in progress in the Health Physics and the Radiation Monitoring and Environmental Protection Departments of Ontario Hydro.

HAAG: My question is directed toward the role of relative humidity with respect to CO_2 fixation and the effect of pressure drop problems when scaling up.

KABAT: A detailed explanation has been given in this paper of the negligible humidity effect on CO_2 fixation by Ca $(OH)_2$ at temperatures up to 450°C. Moderately large mesh absorbent can be used in scaling up the absorder bed to reduce pressure drop. It can be assumed from the results of comparing 20-40 mesh with 10-20 mesh that no significant loss in efficiency will result from increasing the absorbent particle size.

ON THE CATALYTIC REMOVAL OF OZONE PRODUCED IN RADIOACTIVE MEDIA

R.-D. Penzhorn, K. Günther and P. Schuster

Kernforschungszentrum Karlsruhe, Institut für Radiochemie,
7500 Karlsruhe, Postfach 3640, Federal Republic of Germany

Abstract

Eighteen materials and catalysts were tested for their catalytic efficiency in decomposing ozone. The best results at 80°C and linear flow velocities of O_2/O_3 mixtures between 0 and 0.9 (m/s) were obtained with catalysts containing silver or palladium. Catalysts containing platinum proved to be particularly inactive. A Ag on Al_2O_3 catalyst removed ozone with 100 % efficiency from a 700 l/h gas stream carrying aprox. 35 g O_3/l even at temperatures as low as -80°C. For several catalysts a further decrease in temperature, i.e.: below -60°C, was accompanied by an increase in the rate of ozone removal. The highest efficiency at cryogenic temperatures was obtained with a silver catalyst.

From a systematic investigation of the inhibiting effect of nitrogen oxides on the catalytic ozone destruction, it was concluded that catalysts containing palladium are most resistant to N_xO_y poisoning.

Ozone and oxygen can be eliminated simultaneously, down to the ppm range, from a process gas with a previously reduced copper catalyst. For this purpose Al_2O_3 is a better metal carrier than SiO_2, the specific area providing a good criterion for catalyst selection. N_xO_y poisoning of Cu catalysts is reversible and comparatively insignificant.

I Introduction

Beams of fast electrons as well as powerfull γ-sources in air are known to generate ozone and nitrogen oxides in quantities that may represent health hazards 1/. Explosions have often resulted from experiments that involve the irradiation of liquid air or liquid nitrogen containing oxygen as an impurity. The usual cause of an explosion in a closed system is the evaporation of nitrogen which permits the accumulation of ozone, oxygen and oxides of nitrogen due to differences in their boiling points. In open systems oxygen accumulates in liquid nitrogen due to lique-

faction of oxygen from the air 2,3/. Very high concentrations of ozone were also reported during cryogenic recovery and purification of fission noble gases 4/.

The G values for ozone formation from oxygen have been widely investigated. They varie from 2-5 at 4 K in the solid phase 5/, 6-12 at 77 K in the liquid phase 5-8/ and 7-17 at room temperature in the gas phase 6,8,9/, depending mainly upon the total dose and dose rate 9/. To account for the dependancy on the dose rate, a detailed mechanism has been proposed that is based on reactions of ionic and neutral oxygen species 6/. The ozone yields in mixtures of oxygen with N_2 or noble gases, in which most of the energy is absorbed by the diluents, are considerably higher than those expected from a mechanism involving only oxygen species. This observation is particularly true at high oxygen dilutions. Obviously, radiation induced excited and ionic species of the diluents are formed which in turn are capable of generating, via energy transfer reactions, ozon precursors such as O_2^+ and O.

From spark initiated measurments of explosion limits it has been found that, at room temperature and pressure, concentrations below 9-12 mol % O_3 in O_2 are not explosive 10-14/. These values increase to 14.3 and 35 mol % ozone at 200 and 100 K respectively and decrease to 8.8 mol % O_3 when argon is used instead of O_2 14,15/. Out of safety considerations the ozone concentration should however be kept well below these limits, because of the unknown effects of chemical explosion inciting agents like for instance N_2O_5, Cl_2, H_2O_2, unsaturated hydrocarbons, etc. 16,17/. It is in this context that we examined the catalytic decomposition of ozone over a variety of catalysts and experimental parameters.

II Catalytic ozone decomposition at or above room temperature

After preliminary tests on the ozone destruction efficiency with a variety of catalysts, a selection of the more promising was investigated in greater detail. These catalysts, whose characteristics have been summarized in Table 1, were either directly purchased from the manufactors or kindly made on request by the indicated firms.

Several conventional stainless steel gas flow apparatuses were build to carry out the experiments. Depending upon the desired concentration, the ozon was generated, either with a Fischer Model 504 (max. 1 m^3/h and 35 g O_3/h) or a Model 501 (max. 0.1 m^3/h and 3 g O_3/h) silent discharge ozon generator. Ozon analysis was carried out directly in the gas flow - before and after the catalyst bed - either by UV absorption with a Cary 15 spectrophotometer or with a home made chemiluminiscence

Tab. 1: Characteristics of investigated catalysts.

Identification code	Origin	Support material	Active metal	Surface area (m^2/g) new	Surface area (m^2/g) after treatment with O_3	Pellet dimension Ø x length (mm)
AG-RKO-1	Merck	none	Ag	---	---	0.06 wire
AG-MKO-12	Heraeus	Al_2O_3	Ag	99.8	98.3	3.2 x 3.4
PD-MKO-4	Fluka	Asbest	Pd	10.2	n.d.	fibers
PD-MKO-9	Degussa	Al_2O_3	Pd	263	268.9	3.7 - 2.8*
PD-RKO-11	Fluka	none	Pd	---	---	sponge
MO-MKO-7	Degussa	none	Metalloxides	114.9	n.d.	3.8 x ∿ 4.3
PT-MKO-8	Heraeus	Al_2O_3	Pt	114	112	3.2 x 3.4
CU-MKO-3	Merck	none	Cu	---	---	wire
BTS	Fluka	Al_2O_3	Cu	202	113	4.3 x 1.0
R-3-11	BASF	Al_2O_3	Cu	181.6	108.2	4.8 x 2.8
Actimet-13	Doduco	Al_2O_3	Cu	56.0	65.3	5.0 x 5.1
Cu MKO-30	Degussa	SiO_2	Cu	258.1	n.d.	irregular ≈ 4

* spheres

n.d. = not determined

detector coupled via a 4-way valve and a sample loop to the gas stream. The determination of oxygen was accomplished with a Magnos 2T as well as with a D5/2000 Simec oxygen analyser. By using reactors of several dimensions - all provided with numerous thermocouples, a cooling mantle and T01 mini heating lines - it was possible to vary the flow dynamics within a wide range.

The efficiency of ozone removal with 2 g of various catalysts at 80°C as a function of the linear flow velocity (0-0.9 (m/s)) of a oxygen gas stream containing 22.3 g O_3/l is shown in Fig. 1.

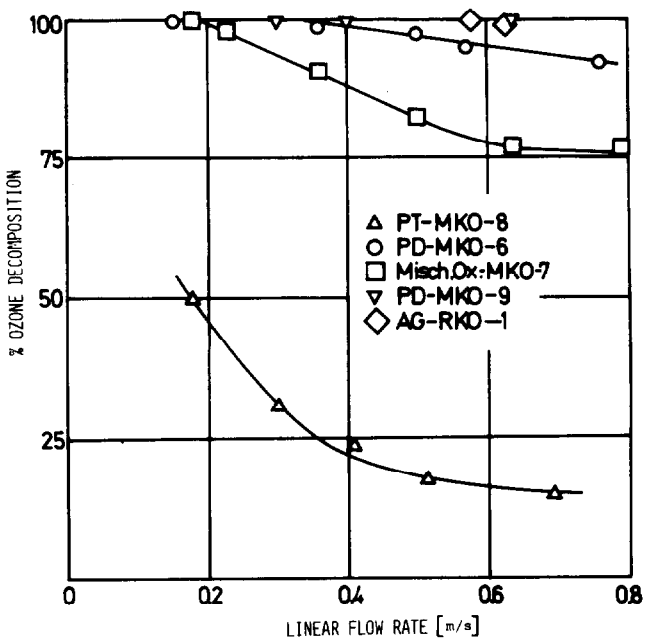

OZONE DECOMPOSITION AS A FUNCTION OF FLOW RATE.

Fig. 1

It is seen that catalysts having Ag or Pd as the active metal are much more efficient than those having Pt.

Silver can be employed either as a film on a long glas spiral (silver mirror), as a wire (AG-MKO-1) or on a support material such as Al_2O_3 (AG-MKO-12). The first two are convenient when high stream velocities are required. The catalytic nature of the ozone destruction on silver is apparent from the fact that 1.15 mol ozone were decomposed on $9 \cdot 10^{-2}$ mol Ag at room temperature without significant loss in efficiency. Confirming the earlier observation of Schwab and Hartmann 18/ that the oxides of silver are at least as effective as the pure metal, we also observe that after an initial induction period a black oxide is formed (Ag_2O and or AgO) that in turn exhibits strong catalytic activity. From several runs at 25 and 80°C on 0.7-8.4 g AG-MKO-1 and linear flow velocities up to 0.9 (m/s) it could be shown that the min. weight m_{Ag} in (g) of catalyst that is necessary to destroy 100 % of the ozone can be estimated from the following relationship

$$f = \frac{k \cdot v}{m_{Ag}}$$

where v is the flow rate in (1/h) and k is a proportionality constant having values of 2.6 ± 0.9 and 1.4 ± 0.4 (g·h/l) at 25 and 80°C respectively.

III Catalyst poisoning by nitrogen oxides

Since nitrogen oxides are usually formed together with ozone during the radiolysis of N_2-O_2 mixtures, the inhibiting effect of N_xO_y on the catalytic ozone destruction was more closely examined. The N_xO_y partial pressure was determined by ozone titration. In excess ozone the following reactions can take place

$$O_3 + NO \rightarrow O_2 + NO_2$$
$$O_3 + NO_2 \rightarrow O_2 + NO_3$$
$$NO_2 + NO_3 \rightleftharpoons N_2O_5 \ .$$

In view that neither NO nor NO_2 could be detected by Second Derivative UV-Spectroscopy in the gas stream we conclude that nitrogen pentoxide is the only nitrogen species present. The results of the effect of the fraction

$$f = \frac{N_2O_5}{N_2O_5 + O_3}$$

on the ozone breakdown efficiency of the AG-MKO-1 catalyst are shown in Fig. 2.

Relatively low partial pressures of N_xO_y ($f \cong 0.09$) are sufficient to stop the catalytic activity. It was observed however that whereas the AG-MKO-1 catalyst is irreversibly poisoned at 20°C, it completely recovers at 80°C. A systematic investigation on the influence of the linear flow velocity (0-0.7 m/s) on the heterogeneous O_3 decomposition efficiency at 80°C and f = 0.05 showed that all the tested catalysts are sensitive to the presence of N_xO_y, the least affected being those

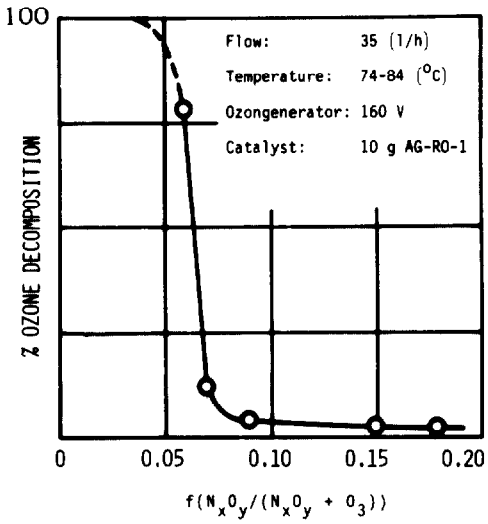

CATALYST POISONING BY N_xO_y.

Fig. 2

containing Pd (see Fig. 3).

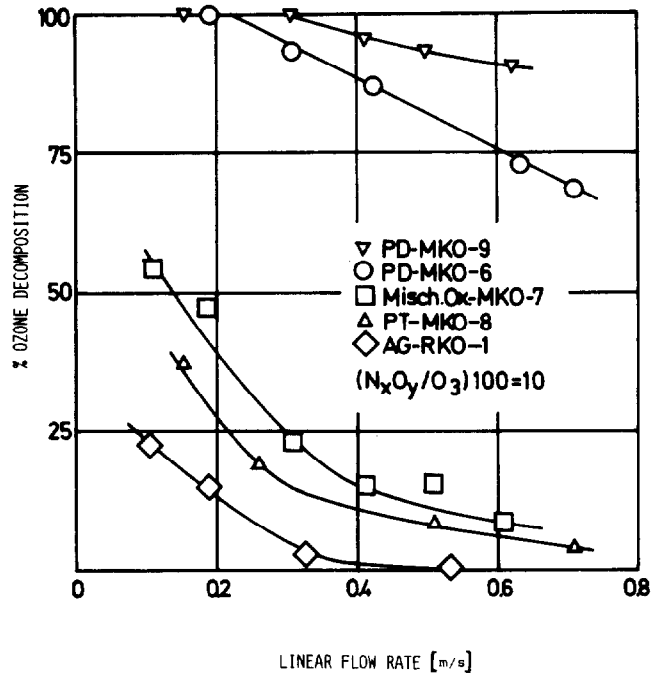

OZONE DECOMPOSITION AS A FUNCTION OF FLOW RATE AND N_xO_y

Fig. 3

IV Activation energies

The temperature dependency of the percent ozone decomposition on several catalysts in the temperature range from -70 up to 80°C is shown in Fig. 4. In this temperature range the thermal contribution to the ozone decomposition rate is negligible. As expected, most catalyst show a low temperature activity limit, the limit (as opposed to the activation energy) being strongly dependent upon the structure of the catalyst. Only the PD-MKO-9 catalyst seemed to reach a plateau value of 10 % at T < -50°C.

Since the rate of ozone decomposition over the catalysts AG-MKO-1, AG-MKO-12, BTS, PT-MKO-8 and PD-MKO-9 was found to be, at several temperatures, directly proportional to the ozone partial pressure in the gas stream it is concluded that the overall kinetics is first order, i.e.:

$$-\frac{d\,O_3}{dt} = k \cdot O_3 \quad . \qquad \text{(I)}$$

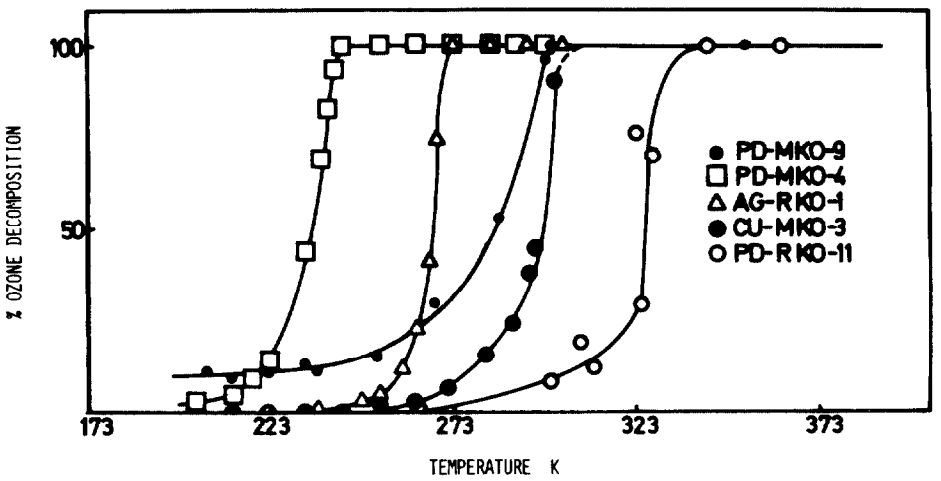

OZONE DECOMPOSITION ON VARIOUS CATALYSTS AS A FUNCTION OF TEMPERATURE

Fig. 4

The following reaction mechanism adequately describes the catalytic ozone removal

$$O_3 + \text{cat.} \rightleftarrows O_3 \cdot \text{cat.} \qquad (1), (2)$$

$$O_3 + \text{cat.} \rightarrow O \cdot \text{cat.} + O_2 \qquad (3)$$

$$O_3 \cdot \text{cat.} + O_3 \rightarrow 3\ O_2 + \text{cat.} \qquad (4)$$

$$O \cdot \text{cat.} + O_3 \rightarrow 2\ O_2 + \text{cat.} \qquad (5)$$

From steady state considerations the rate equation

$$-\frac{d\ O_3}{dt} = 2\ k_1 \cdot O_3 \left(1 - \frac{k_2}{k_2 + k_3 + k_4 \cdot O_3}\right) \qquad \text{(II)}$$

can be derived. At low ozone partial pressures $k_2 + k_3 >> k_4 \cdot O_3$ and equation (II) reduces to

$$-\frac{d\ O_3}{dt} \approx 2\ k_2 \left(1 - \frac{k_2}{k_2 + k_3}\right) \cdot O_3 \qquad \text{(III)}$$

in accordance with the experimentally observed reaction order. Arrhenius plots for the AG-MKO-1, AG-MKO-12, PD-MKO-9 catalysts in the temperature range 280-370 K yielded good straight lines. The estimated overall activation energies have been compiled in Tab. 2 together with some values found in the literature.

Tab. 2: Activation energies

Catalyst	Temp. range (K)	Apparent ΔE (kcal/mol)	Reference
Pt black	77.4 - 90	0.5	20
	77.4 - 90	1.0	19
	310 - 380	3.8	18
PT-MKO-8	280 - 370	4.4 ±	this work
	210 - 260	0	this work
Pd black	77.4 - 90	active, n.d.	20
PD-MKO-9	280 - 330	4.7	this work
	225 - 250	0	this work
Ag black	77.4 - 90	active, n.d.	20
AG-MKO-1	280 - 370	1.1	this work
AG-MKO-12	280 - 370	1.6	this work
Ag O	290 - 360	2.2	18
Cu_2O	>353	active	
Cu, CuO	77.4 - 90	inactive	20
CuO	290 - 370	2.2	18
BTS	280 - 330	3.8	this work
	210 - 250	0	this work

V Ozone decomposition at cryogenic temperatures

In view that frequently high level irradiation experiments are carried out at cryogenic temperatures and that there the explosion danger is greatest, it seemed of interest to examine the catalytic ozone decomposition at low temperature. To avoid the danger of ozone accumulation, temperatures below -135°C were avoided in these experiments+. Several catalysts, i.e.: PD-MKO-9, AG-MKO-12 and PT-MKO-8 efficiently decomposed ozone at these temperatures. Fig. 5 shows the temperature profil, due to the exothermicity of the O_3 decomposition, within a AG-MKO-12 catalyst bed when up

+ The O_3/O_2 phase diagram at 1 atm. indicates that a gaseous mixture containing 3 mol% will coexist at -145°C with a 98 % ozone liquid phase 21,22/.

to 27 g O_3/h at a flow rate of up to 0.5 m^3/h are passed over 35 g of pellets at -80°C. The effluent gas contains no ozon and reaches a temperature that is lower than that of the feed gas. The other catalysts showed simular profiles, also when cooling to much lower temperatures i.e.: -135°C. Surprisingly, with the exception of the AG-MKO-12 catalyst (not jet measured), the reaction rate increases at temperatures below -60°C with decreasing temperature. Apparently, whereas at cryogenic temperatures van der Waals adsorption requiring practically no activation energy predominates, at the higher temperatures chemisorption involving a definite activation energy is primaraly responsible for the catalytic activity. In accordance with this assumption the k-T data could be fitted with an equation of the form

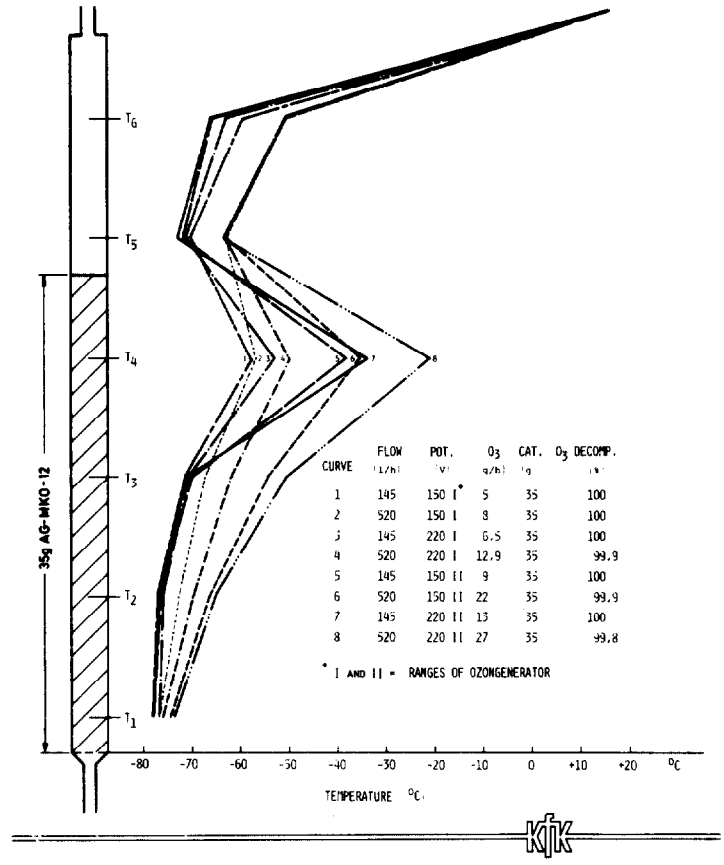

CATALYTIC DECOMPOSITION OF OZONE AT LOW TEMPERATURES.

Fig. 5

$$k = \frac{A}{T} e^{-\Delta E'/RT} \qquad (IV)$$

where $\Delta E'$ equals ΔE and 0 (kcal/mol) (see Tab. II) at temperatures above and below ~ -60°C respectively.

VI Oxygen and Ozone removal

In some applications it is of interest to remove simultaneously ozone and oxygen. An area of concern is for instance the enhancement of alkali metal corrosion by O_3/O_2 during long term storage of Kr-85.

From the literature it is well known that reduced copper catalysts remove O_2 from a process gas down to the ppm range. The oxygen absorption capacity M_{O_2} in STP l/kg varies linearly with the residence time s according to

$$M_{O_2} = A + B \cdot s \tag{5}$$

where A and B are catalyst specific constants having units of (1/kg·sec) and (1/kg) respectively (Fig. 6 shows data obtained with 50-150 g catalyst).

The results shown in Table 3, were obtained at 250°C, using input flow rates between 0.08 and 0.5 m^3/h, a 26.3 % O_2 in He feed gas and 0.05-0.15 kg of catalyst. The various investigated Cu catalysts were in their reduced form, obtained by passing CO over the catalyst bed at 150°C until the gas chromatografically measured CO_2/CO peak ratio in the effluent gas droped to zero. From Table 3 it is apparent that Al_2O_3 is a better catalyst carrier than SiO_2 and that the specific surface area (see also Tab. 1) is directly proportional to $A_{S \to O}$. Thus, for a particular catalyst carrier the specific area provides a good criterion for catalyst selection.

Tab. 3: Comparison of the O_2 absorption capacity of various catalysts

Catalyst	B (1/kg sec)	A (1/kg)
Actimet 13	2.7	10
Degussa	2.6	15
R-3-11	5.9	27
BTS	4.8	33

When the feed gas contained up to 0.4 % O_3 only a slight temperature increase in the catalyst bed was noticed and the same total amount of O_2 was adsorbed (see Fig. 6). No O_3 could be detected by UV absorption in the effluent gas. The presence of up to 5 % NO in the previously described feed gas reduced the amount of adsorbed O_2 by only a few percent. Since furthermore this poisoning is reversible, it is of little concern.

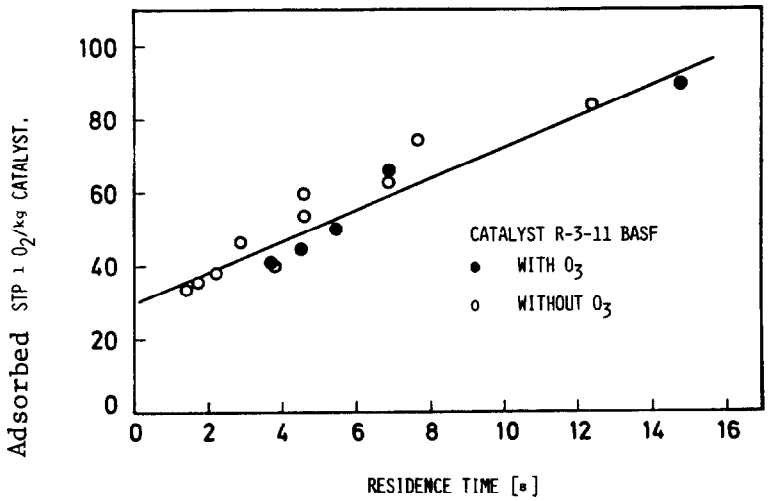

REMOVAL OF O_2 AND O_3.

Fig. 6

1/ M.T. Dmitriev, O.P. Yurasova
Gigiena i Sanitariya 32, 112, (1967)

2/ P.T. Perdue
Health Physics 21, 116, (1972)

3/ J.D. Gault, K.W. Logan, H.R. Danner
Nuclear Safety, 14, 446, (1973)

4/ C.L. Bendixsen, F.O. German, R.R. Hammer
ICP-1023, (1973)

5/ D.B. Brown, L.A. Wall
J. Phys. Chem. 65, 915, (1961)

6/ C. Willis, A.W. Boyd, M.J. Young, D.A. Armstrong
Can. J. Chem. 48, 1505, (1970)

7/ J.F. Riley
ORNL 3488, 42, (1963)

8/ M.T. Dimitriev
Zhurnal Prikladnoi Khimii 41, 39, (1968)

9/ J.F. Kircher, J.S. McNulty, J.L. McFarling, A. Levy
Rad. Research, 13, 452, (1960)

10/ E.H. Riesenfeld
Z. Elektrochemie 29, 119, (1923)

11/ H.T. Schumacher
An. Asoc. Quim. Arg. 41, 230, (1953)

12/ G.A. Cook, E. Spadinger, A.D. Kiffer, C.V. Klumpp
Ind. Eng. Chem. 48, 736, (1956)

13/ G.M. Platz, C.K. Hersh
Ind. Eng. Chem. 48, 742, (1956)

14/ V.V. Yastrebov, N.I. Kobozev
Russian J. Phys. Chem. 33, 118, (1959)

15/ R.O. Miller
J. Phys. Chem. 63, 1054, (1959)

16/ S.W. Benson, A.E. Axworthy
J. Chem. Phys. 26, 1718, (1956)

17/ J.E. Douglas, L.C. Bratt, E.M. Kinderman
J. Chem. Phys. 31, 1416, (1959)

18/ G.M. Schwab, G. Hartmann
Z. Phys. Chem. (Neue Folge) 6, 72, (1956)

19/ G.J. Emel'yanova, V.P. Lebedev, N.I. Kobozev
Kataliticheskie reaksii v zhidkoi faze Trudy Vsesoyvznoi konferentsii, Alma-Ata (1962)

20/ G.J. Emel'yanova, V.P. Lebedev, N.I. Kobozev
Vestnik Moskovkogo Universiteta, ser II, khimiya 4, 31, (1961)

21/ A.C. Jenkins, F.S. DiPaolo, C.M. Birdsall
J. Chem. Phys. 23, 2049, (1955)

22/ C. Brown, A.W. Berger, C.K. Hersh
J. Chem. Phys. 23, 1340, (1955)

DISCUSSION

CHENG: It has been known for quite some time that commercially available synthetic zeolites, such as molecular sieve 10X, can serve effectively as a catalyst for ozone destruction. Do you have any comment on that?

PENZHORN: Although I am aware that zeolites have been reported to be good catalysts, we have not investigated them so far. Our present work has been limited to metal-based catalysts.

VON AMMON: Catalysts which are active for the decomposition of ozone at the low temperatures you mentioned have a tremendous potential for application in a cryogenic krypton separation system for the offgases from reprocessing plants. It is not possible to imagine such a system without ozone formation because O_2 will always be present, even in case of O_2 separation prior to the cryogenic part. Traces of O_2 in the ppm-range will always pass the reduction catalyst during normal operation (not to speak of malfunctions). The question, whether or not such a step is necessary, cannot be answered conclusively at the moment. I wonder if some of the catalysts are active enough to be used in the liquid phase of a Kr-Xe mixture (at 180-200 K, or so) in a cryogenic column? In this case, evaporation of the gas mixture for the ozone decomposition could be avoided.

PENZHORN: Our results indicate that ozone can be destroyed efficiently even at temperatures as low as 130 K. In our experiments we have observed that at this temperature the gas flow suddenly becomes highly unsteady. From the ozone-oxygen phase diagram, we know that at temperatures in the region of 130 K a liquid, whose composition is almost 100% ozone, will condense. Since in these experiments no ozone could be detected in the effluent gas--a sign of 100% ozone decomposition--I believe that there are good chances for the catalytic removal of ozone from Kr/Xe/O_2/O_3 liquid mixtures at the temperatures you mention.

BRUGGEMAN: Considering an integrated dissolver offgas purification system, would it be necessary to remove nitrogen oxides and oxygen before the cryogenic separation of the noble gases, or would it be sufficient to remove only the nitrogen oxides in combination with catalytic ozone removal anywhere in the cryogenic installation?

PENZHORN: This question goes somewhat beyond the scope of my talk and would perhaps be better asked again this afternoon during the presentation of Dr. v. Ammon. However, it certainly is the aim of our work to develop a process whereby ozone can be continuously eliminated from cryogenic liquids. If this can be demonstrated successfully, your alternative process becomes more feasible.